SPECTRAL REFLECTANCE ANALYSIS FOR GENOME-WIDE ASSOCIATION OF THAI RICE

Oryza sativa L. UNDER PHOSPHORUS-DEFICIENT CONDITION

Mr. Sompop Pinit

จุฬาลงกรณ์มหาวิทยาลัย
CHULALONGKORN UNIVERSITY

A Dissertation Submitted in Partial Fulfillment of the Requirements

for the Degree of Doctor of Philosophy in Biotechnology

Common Course

FACULTY OF SCIENCE

Chulalongkorn University

Academic Year 2020

การวิเคราะห์ความสะท้อนเชิงสเปกตรัมเพื่อการเชื่อมโยงทั่วจีโนมของข้าวไทย *Oryza sativa* L.
ภายใต้ภาวะขาดฟอสฟอรัส

นายสมภพ พินิจ

วิทยานิพนธ์นี้เป็นส่วนหนึ่งของการศึกษาตามหลักสูตรปริญญาวิทยาศาสตรดุษฎีบัณฑิต
สาขาวิชาเทคโนโลยีชีวภาพ ไม่สังกัดภาควิชา/เทียบเท่า
คณะวิทยาศาสตร์ จุฬาลงกรณ์มหาวิทยาลัย
ปีการศึกษา 2563

Thesis Title	SPECTRAL REFLECTANCE ANALYSIS FOR GENOME-WIDE ASSOCIATION OF THAI RICE *Oryza sativa* L. UNDER PHOSPHORUS-DEFICIENT CONDITION
By	Mr. Sompop Pinit
Field of Study	Biotechnology
Thesis Advisor	Professor SUPACHITRA CHADCHAWAN, Ph.D.
Thesis Co Advisor	Assistant Professor JUTHAMAS CHAIWANON, Ph.D.

Accepted by the FACULTY OF SCIENCE, Chulalongkorn University in Partial Fulfillment of the Requirement for the Doctor of Philosophy

-- Dean of the FACULTY OF SCIENCE

(Professor POLKIT SANGVANICH, Ph.D.)

DISSERTATION COMMITTEE

-- Chairman

(Associate Professor SEHANAT PRASONGSUK, Ph.D.)

-- Thesis Advisor

(Professor SUPACHITRA CHADCHAWAN, Ph.D.)

-- Thesis Co-Advisor

(Assistant Professor JUTHAMAS CHAIWANON, Ph.D.)

-- Examiner

(SARISA NA POMBEJRA, Ph.D.)

-- Examiner

(Associate Professor KUAKARUN KRUSONG, Ph.D.)

-- External Examiner

(Somsong Chotechuen, Ph.D.)

-- External Examiner

(Duangjai Suriyaarunroj, Ph.D.)

สมภพ พินิจ : การวิเคราะห์ความสะท้อนเชิงสเปกตรัมเพื่อการเชื่อมโยงทั่วจีโนมของข้าวไทย *Oryza sativa* L. ภายใต้ภาวะขาดฟอสฟอรัส. (SPECTRAL REFLECTANCE ANALYSIS FOR GENOME-WIDE ASSOCIATION OF THAI RICE *Oryza sativa* L. UNDER PHOSPHORUS-DEFICIENT CONDITION) อ.ที่ปรึกษาหลัก : ศ. ดร.ศุภจิตรา ชัชวาลย์, อ.ที่ปรึกษาร่วม : ผศ. ดร.จุฑามาศ ชัยวนนท์

งานวิจัยฉบับนี้มีวัตถุประสงค์หลักสามประเด็น ประเด็นแรกคือ พัฒนาวิธีการตรวจวิเคราะห์ปริมาณธาตุฟอสฟอรัสอนินทรีย์ที่สามารถตรวจวัดได้อย่างรวดเร็วยิ่งขึ้น ประเด็นที่สองคือ ศึกษาดัชนีการสะท้อนเชิงสเปกตรัมที่เป็นตัวแทนการขาดธาตุฟอสฟอรัสในข้าว และประเด็นที่สามคือ เพื่อตรวจหาสนิปส์ที่มีความสัมพันธ์กับการทนทานการขาดธาตุฟอสฟอรัสในข้าวไทยด้วยเทคนิคการเชื่อมโยงทั่วจีโนม

วิธีการวิเคราะห์ธาตุฟอสฟอรัสโดยการเจาะใบถูกพัฒนาขึ้นเพื่อเพิ่มขีดความสามารถในการวิเคราะห์ธาตุฟอสฟอรัสในตัวอย่างพืชจำนวนมากให้กับการสกัดแบบปกติที่ทำร่วมกับการวิเคราะห์ด้วยปฏิกิริยา Molybdate blue ซึ่งสามารถทำได้โดยการเจาะใบให้มีขนาดเท่ากันโดยไม่จำเป็นต้องบดตัวอย่าง ชั่งน้ำหนัก และลดการเปลี่ยนถ่ายสารสกัดในหลายๆขั้นตอน จากการทดสอบเปรียบเทียบระหว่างวิธีสกัดแบบเจาะใบและวิธีการสกัดแบบปกติพบว่า ให้ผลที่สามารถเปรียบเทียบกันได้ด้วยระดับความเชื่อมั่นสูง ทั้งในพืชที่มีความสามารถในการกักเก็บธาตุฟอสฟอรัสในปริมาณที่ต่ำและสูงภายใต้สภาวะขาดธาตุฟอสฟอรัส วิธีการวิเคราะห์แบบเจาะใบนี้สามารถตรวจวิเคราะห์ธาตุฟอสฟอรัสได้ครั้งละหลายพันตัวอย่างภายในระยะเวลาเพียงไม่กี่ชั่วโมง ซึ่งเหมาะสมต่อการประยุกต์ใช้ในการทดลองที่มีความจำเป็นต้องทำงานกับตัวอย่างพืชจำนวนมาก การวิเคราะห์ธาตุฟอสฟอรัสและการตรวจวัดความสะท้อนเชิงสเปกตรัมของข้าวไทย (*Oryza sativa* L.) จำนวน 172 พันธุ์ที่ทำการปลูกในสารละลายที่มีความเข้มข้นของธาตุฟอสฟอรัสแตกต่างกัน 3 ระดับ ด้วยวิธีสกัดธาตุฟอสฟอรัสแบบเจาะใบและวิธีการตรวจวัดความสะท้อนเชิงสเปกตรัมด้วยเครื่องมือ ตามลำดับ พบว่าปริมาณธาตุฟอสฟอรัสแสดงความไวในการตรวจวัดที่สามารถระบุระดับของการขาดธาตุฟอสฟอรัสได้อย่างชัดเจน สำหรับการตรวจวัดความสะท้อนเชิงสเปกตรัมพบว่าอัตราส่วนระหว่างช่วงคลื่นย่านใกล้อินฟาเรดและช่วงคลื่นที่มองเห็นได้มีความสัมพันธ์กับระดับปริมาณฟอสฟอรัสในพืช การเชื่อมโยงทั่วจีโนมของสนิปส์จำนวน 113,114 สนิปส์ร่วมกับตัวชี้วัดความสะท้อนเชิงสเปกตรัม 127 ตัวชี้วัด สามารถทำนาย สนิปส์ที่มีความน่าจะเป็นสูงได้ถึง 48 สนิปส์ โดยเฉพาะตัวชี้วัด R_{750}/R_{700} และ R_{740}/R_{560} ในขณะที่การเชื่อมโยงทั่วจีโนมร่วมกับค่าปริมาณฟอสฟอรัสสามารถทำนายสนิปส์ที่มีความน่าจะเป็นสูงได้เพียง 15 สนิปส์ ซึ่งในจำนวนนี้มี 3 สนิปส์ที่พบได้ในทั้งสองการเชื่อมโยง ในการเชื่อมโยงทั่วจีโนมนี้สามารถระบุยีนควบคุมการตอบสนองต่อการขาดธาตุฟอสฟอรัส ซึ่งช่วยยืนยันว่าตัวชี้วัดที่พบเป็นตัวแทนการแสดงออกของพืชต่อการขาดธาตุฟอสฟอรัสได้อย่างมีประสิทธิภาพ และจากการพิจารณาจากการศึกษาการแสดงออกของยีน การระบุตำแหน่ง QTL และการพิจารณาหน้าที่ของยีนที่เคยมีการศึกษาก่อนหน้ามาแล้ว พบว่ามียีนที่ถูกทำนายหลายยีนที่มีความน่าจะเป็นสูงในการทำหน้าที่ควบคุมการตอบสนองของพืชต่อการขาดธาตุฟอสฟอรัสในข้าวไทย

สาขาวิชา	เทคโนโลยีชีวภาพ	ลายมือชื่อนิสิต ....
ปีการศึกษา	2563	ลายมือชื่อ อ.ที่ปรึกษาหลัก ....
		ลายมือชื่อ อ.ที่ปรึกษาร่วม ....

5972840923 : MAJOR BIOTECHNOLOGY

KEYWORD: Rice, Phosphorus deficiency, Spectral reflectance, Genome-wide association

Sompop Pinit : SPECTRAL REFLECTANCE ANALYSIS FOR GENOME-WIDE ASSOCIATION OF THAI RICE *Oryza sativa* L. UNDER PHOSPHORUS-DEFICIENT CONDITION. Advisor: Prof. SUPACHITRA CHADCHAWAN, Ph.D. Co-advisor: Asst. Prof. JUTHAMAS CHAIWANON, Ph.D.

The goals of this research have three main points: (i) to develop a rapid method for inorganic phosphorus quantification, (ii) to investigate spectral reflectance indices representing phosphorus deficiency in rice, and (iii) to determine SNPs associated with phosphorus deficiency tolerance in Thai rice via genome-wide association study (GWAS).

The punching method was developed to enhance the high throughput performance of the conventional Pi extraction and molybdate blue assay. Pi content can be extracted using equally small leaf areas without leaf grinding, balancing, and tedious transferring steps. The punching method provided comparable results to the conventional grinding method with a strong correlation in high and low accumulation rice cultivars under a phosphorus supplement series. Thousands' Pi content of rice samples can be quantified within a few hours, exactly suited for large-scale phenotyping or screening experiments. P deficiency response of 172 Thai rice (*Oryza sativa* L.) accessions grown in three different P concentrations. I detected Pi content and spectral reflectance data by using the punching method and hyperspectral measurement, respectively. Pi content showed sensitive evaluation results to identify P deficient level in each different treatment. For hyperspectral analysis, ratio indices between NIR and VIS wavelength showed a strong correlation with Pi content without spectral interference. The 217 ratio indices and Pi content were associated with 113,114 SNPs derived from the whole-exome sequence. The 48 significant SNPs with low *P-value* were predicted from both R_{750}/R_{700} and R_{740}/R_{560}. At the same time, Pi content association served 15 significant SNPs, which 3 SNPs of these superimposed from the index association. Interestingly, several known genes involving in P deficiency regulation were found that confirmed correct association affected by the performance of the novel phenotypic traits. Overall, the numerous candidate genes exposed their possibility in P deficiency modulation by considering previous gene expression, QTL mapping, and reported function.

Field of Study:	Biotechnology	Student's Signature ....
Academic Year:	2020	Advisor's Signature ....
		Co-advisor's Signature ....

ACKNOWLEDGEMENTS

Sompop Pinit

TABLE OF CONTENTS

LIST OF TABLES

LIST OF FIGURES

LIST OF ABBREVIATIONS

1DL_DGVI	First-order derivative green vegetation index derived using local baseline
1DZ_DGVI	First-order derivative green vegetation index derived using zero baseline
3D-DCNN	3D deep convolutional neural network
ACI	Anthocyanin content index
Al	Aluminum
ANOVA	Analysis of variance
ARI1	Anthocyanin reflectance index 1
ARI2	Anthocyanin reflectance index 2
ARVI	Atmospherically resistant vegetation index
Ca	Calcium
CARI	Chlorophyll absorption in reflectance index
CG	Conventional grinding
CI $_{red\ edge}$	Chlorophyll red edge index
CRD	Completely randomized design
CRI1	Carotenoid reflectance index 1
CRI2	Carotenoid reflectance index 2
Ctr1	Carter index 1
Ctr2	Carter indices 2
DMRT	Duncan's multiple range test

EVI	Enhanced vegetation index
Fe	Iron
FW	Fresh weight
G	Greenness index
GM1	Gitelson and Merzlyak indices 1
GM2	Gitelson and Merzlyak indices 2
GWAS	Genome-wide association study
ICP	Inductively coupled plasma
IRECI	Inverted red edge chlorophyll index
K	Potassium
LAI	Leaf area index
LD	Linkage disequilibrium
Lic1	Lichtenthaler indices 1
Lic2	Lichtenthaler indices 2
MAF	Minor allele frequency
mARI	Modified anthocyanin reflectance index
MCARI	Modified chlorophyll absorption ratio index
MD	Mildly deficient
MSI	Moisture stress index
N	Nitrogen
NDII	Normalized difference infrared index

NDVI	Normalized difference vegetation index
NDWI	Normalized difference water index
NGS	Next-generation sequencing
NIR	Near infrared
NMR	Nuclear magnetic resonance
NPCI	Normalized pigment chlorophyll index
NPQI	Normalized phaeophytinization index
NSR	New spectral reflectance
OSAVI	Optimized soil-adjusted vegetation index
P	Phosphorus
PCA	Principal component analysis
Pi	Inorganic phosphorus
PRI	Photochemical reflectance index
PSI	Phosphate starvation-induced
PSND	Pigment sensitive normalized difference
PSRI	Plant senescence reflectance index
PSSR	Pigment specific spectral ratio
Q-Q	The quantile–quantile
QTL	Quantitative trait loci
R	Reflectance
RCBD	Randomized complete block design

RECI	Red edge chlorophyll index
REP	Red edge position
RGRI	Red green ratio index
RNSR	Relatively new spectral reflectance
RVSI	Red-edge vegetation stress index
S	Sufficient
SAVI	Soil adjusted vegetation index
SD	Severely deficient
SIPI	Structure intensive pigment index
SNP	Single nucleotide polymorphism
SPAD	Single-photon avalanche diode
SPRI	Simple ratio pigment index
SR	Simple ratio index
SSR	Simple sequence repeats
SWIR	Short wave infrared
TCARI	Transformed chlorophyll absorption ratio index
TNDVI	Transformed normal difference vegetation index
TVI	Triangular vegetation index
UV	Ultraviolet
VARI	Vegetation atmospherically resistant index
VIgreen	Vegetation index green

VIS	Visible
WBI	Water band index
ZMI	Zarco-Tejada & Miller index

CHAPTER I

INTRODUCTION

Increasing the world's population and expanding the food production industry affect the rising demand for agricultural products to supply their consumption. Rice (*Oryza sativa* L.) is an essential food, because half of the world's population consumes rice as their staple food (Maclean *et al.*, 2013). In Thailand, more than seven million tons of rice has been exported as a major agricultural product in 2019. Nevertheless, productivity has been dropped compared with the previous export year (11 million tons in 2018) (ThaiRiceExportersAssociation, 2020). The decrease in rice productivity might be limited by several factors such as drought, salinity stress, and nutrition deficiency (Batlang *et al.*, 2013). In particular, phosphorus deficiency leads to the disruption of plant growth and development and has become one of the major problems in agricultural products' quality and yields (van de Wiel *et al.*, 2016).

Phosphorus (P) is an essential macro-nutrient for plant growth and development. Lack of P element in plants negatively affects several metabolic processes, including photosynthesis, cellular respiration (Terry and Ulrich, 1973), cellular component synthesis (Li *et al.*, 2016), cellular signaling, and disease resistance (Zhao *et al.*, 2013). Plant adaptation is a response to survive under undesirable conditions. Under P deficiency, plants have developed their metabolic processes to maintain metabolism ability and growth performance, such as root architectural adaptation, uptake adjustment, translocation, utilization efficiency, etc. P-deficiency tolerance is complex adaptation that depends on different morphological, physiological, and biochemical responses in P homeostasis. Therefore, the investigation of genes involving P deficiency response or adaptation is the key to develop tolerance rice cultivars, leading to rice enhancement in tolerance capability. Additionally, the sensitive detection in P deficiency is necessary to identify the

deficient status. The responsible parameters can be applied as phenotypic data in the gene prediction process.

Next generation sequencing (NGS) technology provides high speed and precision of a big genomic dataset, which enables in-depth investigation in genomic function and variation. Genome-wide association study (GWAS) has become an effective method used to dissect the genetic basis of the complex traits by establishing statistical links between phenotypes and genotypes. This procedure, based on single nucleotide polymorphism (SNP) markers, has been extensively applied in rice and other plant species, including sorghum (Shehzad *et al.*, 2009), barley (M. Wang *et al.*, 2012), lettuce (Simko *et al.*, 2009), maize (Li *et al.*, 2013), tomato (Ranc *et al.*, 2012), *Arabidopsis* (Atwell *et al.*, 2010), soybean (Contreras-Soto *et al.*, 2017) and bread wheat (Zanke *et al.*, 2014), to identify causative genes involved in agronomic traits and stress responses. GWAS accuracy to predict the high potential causative loci relies on good phenotypic traits (MacRae and Vasan, 2011). Some biochemical parameters are sensitive and direct measurement for plant responses to stress. However, the phenotyping procedures are often time-consuming and labor-intensive, which are not suitable for large scale phenotyping for GWAS (W. Yang *et al.*, 2014).

Inorganic phosphorus (Pi) content is a sensitive parameter for plant P status, which indicates the internal availability of Pi level in the plant. It can determine the ability of plant adaptation under the P-deficient state. However, a conventional protocol of Pi quantification in plant tissue includes numerous and tedious steps, such as grinding, balancing, and centrifuging, which are time-consuming, and labor-intensive that are inappropriate for high throughput measurement, required for GWAS application (Mori and Nakamura, 1959; Turner and Turner, 1961; Kanno *et al.*, 2016). For quantifying Pi content of thousands of samples for the GWAS application, development of the quantifying method is necessary to improve and establish a faster and easier quantification protocol to handle the large-scale quantification.

Hyperspectral detection, which is fast and non-destructive, has been developed and applied to detect plant response in various stresses. A high-performance sensor has been created to observe photo-reflectance from the plants based on light's physical property. Phenotypes can be indirectly observed from spectral reflectance, which is intensity of each wavelength spectrum reflected by plant tissues. Differences in spectral reflectance can indicate plant status and used as an alternative parameter in several applications (Kokaly *et al.,* 2009). Over the past years, many indices of spectral reflectance are reported to indirectly represent several plant phenotypes, including leaf greenness (Zarco-Tejada *et al.,* 2005), yield quality (Kanning *et al.,* 2018), water stress (Jones *et al.,* 2004), protein (D. Sun *et al.,* 2019), chlorophyll (Yang *et al.,* 2015), carotenoid (Yang *et al.,* 2010), and anthocyanin content (Gu *et al.,* 2018). Thus, hyperspectral indices could be another effective trait that can provide an easy and convenient investigation process for the GWAS application.

Objectives of this study

1. To develop a rapid method for inorganic phosphorus quantification

2. To investigate spectral reflectance indices responsive to phosphorus deficiency in rice

3. To determine SNPs associated with phosphorus deficiency tolerance in Thai rice *via* genome-wide association study (GWAS)

CHAPTER II

LITERATURE REVIEW

1. Rice – the essential agronomical crop

1.1 The global rice productivity

Rice (*Oryza sativa* L.) is one of the world's valuable staple food crops and indispensable for more than half of the globe's population, particularly in Asian countries. Besides, rice is an important food source, which abundantly provides more calories for people's diets than maize, wheat, potato, or cassava (Maclean *et al.*, 2013). In 2019, a total of 495.9 million tons of rice was supplied for world wild consumption. Almost all (90%) rice production is in Asian countries, including China, Vietnam, Philippines, Indonesia, Myanmar, Japan, India, Bangladesh, Cambodia, and Thailand. Thailand was the world's second-biggest exporter after India in the same year (Workman, 2020), which exported 7.58 million tons (130.6 billion baht) (ThaiRiceExportersAssociation, 2020). However, rice productivity has been decreased by several factors when compared with the previous year's export **(Figure 1)**.

RICE EXPORTS BY KEY RICE EXPORTING COUNTRIES

2018	47.64 million tonnes	2019	44.87 million tonnes	2020	45.99 million tonnes

Item	2018	2019*	2020*	% change
India	11.79	10.60	12.00	13.21
Thailand	11.23	7.58	7.50	-1.05
Vietnam	6.59	6.85	7.00	2.19
Pakistan	3.91	4.60	4.40	-4.35
China	2.06	3.00	3.50	16.67
US	2.78	3.05	3.18	4.10
Myanmar	2.75	2.50	2.60	4.00
Cambodia	1.30	1.35	1.40	3.70
Uruguay	0.80	0.80	0.80	0.00

Unit: million tonnes of milled rice   *Forecast

Source: Foreign Trade Department   BKPgraphics

Figure 1 World's top 9 rice exporters (in million tonnes) over three years (2018-2020) and their percentage of relative export changing.

1.2 Genetic variation of rice

A couple of rice species are the most popular and essential cereals for human diets, including *O. sativa* (worldwide grown) and *O. glaberrima* (grown in West Africa). The rice genus (*Oryza*) comprises 27 species, 11 genome classification, and four relation series **(Table 1)**. Each rice species contributes to its specific location around the world. The genome variation of each species was evolved and diversified from the origin since 14 million years ago in Malesia. The labeled AA to LL was applied to classified genome variation among rice species. The number of letters was used to indicate genome copy numbers (diploid or tetraploid) described in **Table 1**. In the ecological diversification of *O. sativa*, the two major variety groups were isolated as indica and japonica. The rices that adapted to grow in the tropical areas, were named indica group, and the others that adapted for the temperate zone, and tropical uplands were named japonica group. Nowadays, an in-depth molecular investigation classified three other divergent groups **(Figure 2)**. The japonica was sub-diversified as temperate and tropical japonica. Besides, aus group was a divergent sub-species from the indica group cultivated in India and Bangladesh (Maclean *et al.*, 2013).

In Thailand, thousands of rice cultivars have been developed by natural selection, human selection, and breeding for over 5000 years (Techarang *et al.*, 2019). From a high variation of Thai rice, the rice population can be sub-classified using ecological growing, light period sensitivity, or amylose content. Moreover, some rice cultivars have a specific character derived from evolution processes, such as purple rice (e.g. Riceberry), fragrant rice 'KDML105', floating rice (Pin Kaew 56), etc. Consequently, Thai rice varieties contain high genetic variation that has provided a treasure of genetic materials for genetic investigation and breeding improvement (Vanavichit *et al.*, 2018). Previous reports showed a potential genetic variation of Thai rice in genetic structure, salt tolerance, and root anatomical structure (Chakhonkaen *et al.*, 2012; Vejchasarn *et al.*, 2016; Chokwiwatkul *et al.*, 2017).
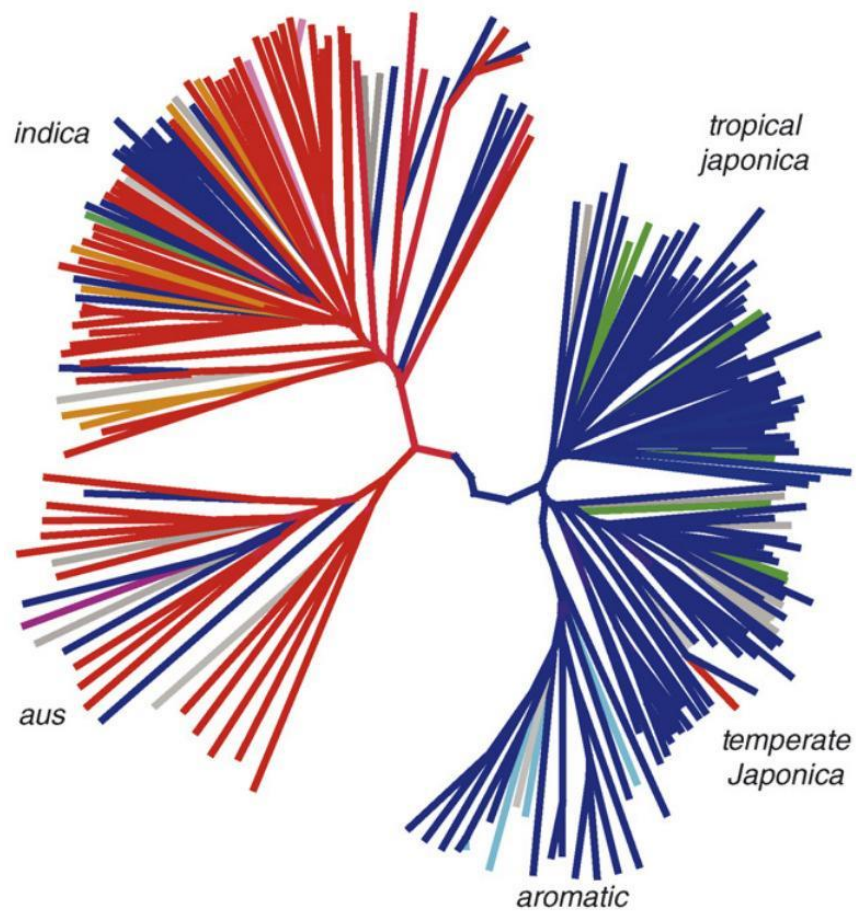
Figure 2 Population structure and relatedness of *O. sativa* over 234 accessions which characterized by the genetic investigation based on nuclear SSR and chloroplast markers (Kovach *et al.*, 2007).

Table 1 Classification and distribution of species in the genus *Oryza* (Maclean et al., 2013).

Taxa	Genome	Distribution	Comments/alternative classification
Section *Oryza*			
Series *Oryza*: *sativa* species complex			
O. sativa	AA	Worldwide	
O. glaberrima	AA	West Africa	
O. nivara	AA	Tropical Asia	Annual ecotype of *O. rufipogon*
O. rufipogon	AA	Tropical Asia to northern Australia	
O. meridionalis	AA	Northern Australia	
O. barthii	AA	Africa	
O. longistaminata	AA	Africa	
O. glumaepatula	AA	South America	South American *O. rufipogon*; *O. glumaepatula*
Series *Latifoliae*: *officinalis* species complex			
O. minuta	BBCC	Philippines, Papua New Guinea	
O. officinalis	CC	Tropical Asia to Papua New Guinea	
O. rhizomatis	CC	Sri Lanka	
O. malampuzhaensis	CCDD	India	Tetraploid race of *O. officinalis*
O. punctata	BB	Africa	
O. schweinfurthiana	BBCC	Africa	Tetraploid race of *O. punctata*
O. eichingeri	CC	West, Central, and East Africa, Sri Lanka	The only species found in both Africa and Asia
O. alta	CCDD	Central and South America	
O. grandiglumis	CCDD	South America	
O. latifolia	CCDD	Central and South America	
Section *Australiensis*			
O. australiensis	EE	Australia	Member of *officinalis* complex
Section *Brachyantha*			
O. brachyantha	FF	Africa	
Section *Padia*			Basal or primitive section of *Oryza*
O. schlechteri	HHKK	Indonesia and Papua New Guinea	
O. coarctata	KKLL	South Asia to Myanmar	
Series *Ridleyanae*: *ridleyi* species complex			
O. longiglumis	HHJJ	Indonesia and Papua New Guinea	
O. ridleyi	HHJJ	Southeast Asia to Papua New Guinea	
Series *Meyerianae*: *meyeriana* species complex			*granulata* species complex
O. granulata	GG	South and Southeast Asia	Variety of *O. meyeriana*
O. meyeriana	GG	South and Southeast Asia	
O. neocaledonica	GG	New Caledonia	

1.3 Stress affects rice productivity

Nowadays, rice production is dramatically reduced by several factors that affect rice growth and development. The high temperature (LÜ *et al.*, 2013), drought (Mukamuhirwa *et al.*, 2019), salinity (Zeng *et al.*, 2003), and nutrient-deficient stress directly caused by poor soil quality (Fageria, 2001) have been reported as factors that affect rice production by inhibition of rice growth. Poor soil quality was found throughout Thailand's area **(Figure 5A)**. Lack of macronutrients (nitrogen, phosphorus, and potassium) in soil negatively results in growth and limits crop productivity (Liu *et al.*, 2011; Sadiq *et al.*, 2017; Lozano Fernández *et al.*, 2018). For improving and raising rice production, the demand for N, P, and K fertilizer is dramatically increased every year (FAO, 2017) **(Table 2)**. Among the macronutrients, potassium is the least of the problems due to its high concentration in soil (up to 20,000 ppm) (Halperin and Kamel, 1998). For N fertilizer, atmospheric nitrogen can be fixed by the Haber-Bosch process or biological nitrogen fixation by microorganisms. Thus, the N fertilizer is unlimited to sustain the world's demand (Basosi *et al.*, 2014). P fertilizer is only derived from non-renewable phosphate rock, which needs at least 300 years in mineral regeneration by the natural process (Samreen and Kausar, 2019). The over-application of P fertilizer in agriculture not only leads to increasing unavailable P forms in the soil, but also dramatically affects the declination of phosphate rock resources in nature.

Table 2 World's trending demand of N, P, and K fertilizers during 2015-2020 (thousand tonnes) (FAO, 2017).

Year	2015	2016	2017	2018	2019	2020
Nitrogen (N)	110,027	111,575	113,607	115,376	117,116	118,763
Phosphate (P_2O_5)	41,151	41,945	43,195	44,120	45,013	45,858
Potash (K_2O)	32,838	33,149	34,048	34,894	35,978	37,042
Total ($N+P_2O_5+K_2O$)	184,017	186,668	190,850	194,390	198,107	201,663

2. Phosphorus deficiency

2.1 Phosphorus - the indispensable plant nutrient

Phosphorus (P) is a necessary and indispensable macronutrient, which is vital for plant metabolism, involving membrane synthesis, energy transfer, enzyme activation, nucleic acid generation, nitrogen fixation, and carbon metabolism (Schachtman *et al.*, 1998). P starvation inhibits plant growth and development (Vance *et al.*, 2003). P deficiency has occurred from two major reasons involving the soil property. Firstly, a shortage of P deficiency happened due to insufficient P addition to the farming system. The deficiency can be easily solved by supplementing P fertilizer input. Secondly, the unavailable form of P causes deficiency by which P is fixed with soil particle or some other elements as a complex. Previous studies reported that high pH could induce P complex with iron (Fe) or aluminum (Al), and low pH could also stimulate precipitation with calcium (Ca). Moreover, overapplication of P fertilizer indirectly leads to a higher rate of unavailable P formation in the soil by increasing soil pH (Haefele *et al.*, 2014).

2.2 Plant response and adaptation to phosphorus deficiency

Rice has developed the complicated mechanism and adaptation to maintain their homeostasis under P deficient condition. The adaptation can be classified into two categories, including P utilization efficiency and P acquisition efficiency (Aziz *et al.*, 2014). The P utilization efficiency is the ability to efficiently use limited P and adjust the internal process to maintain P homeostasis. The internal P remobilization, metabolism modification, membrane reorganization, and growth enhancement with limited P are examples of P use efficiency adaptation. In contrast, P acquisition efficiency adaption mainly focuses on external P foraging *via* root system architecture adaptation, phosphatase exudation releasing, and P uptake enhancement.

In detail, P remobilization tries to translocate stored P from older to younger tissues for maintaining metabolism in young organs (Gill and Ahmad, 2003). Interestingly, the plant can modify an alternative pathway across the P-involving

steps that helps the plant drive the metabolism, such as the alternative pathway of cytosolic glycolysis and electron transport (Plaxton and Carswell, 1999; Gonzàlez-Meler *et al.*, 2001). Sulfo- or galactolipid can be alternatively used instead of phospholipid molecules for membrane components (Pant *et al.*, 2015).   For root system architecture, three major adjustments are modulated under P starvation, including root elongation to forage new resources of available P, lateral root formation to enhance exploration, and root hair development to increase root surface area (López-Bucio *et al.*, 2002) **(Figure 3)**. For transforming unavailable P, root exudates (acid phosphatases or phytases) are excreted from roots to convert P into available P forms (Neumann and Römheld, 1999). Plants had evolved low and high-affinity transporters to increase P acquisition and internal distribution under P starvation (Liu *et al.*, 1998). Moreover, root symbiosis with arbuscular mycorrhiza provides extending surface area and increases uptake ability. Symbiotic interaction is dramatically induced under P starvation by exudating plant-fungi interaction hormone (Bedini *et al.*, 2018). In addition, P deficiency inhibits elongation of the lamina joint by decreasing brassinosteroid biosynthesis that changes leaf angle as an upright leaf phenotype. This phenomenon helps plant to reduce light receiving and photosynthesis under P indigent situation (Ruan *et al.*, 2018).
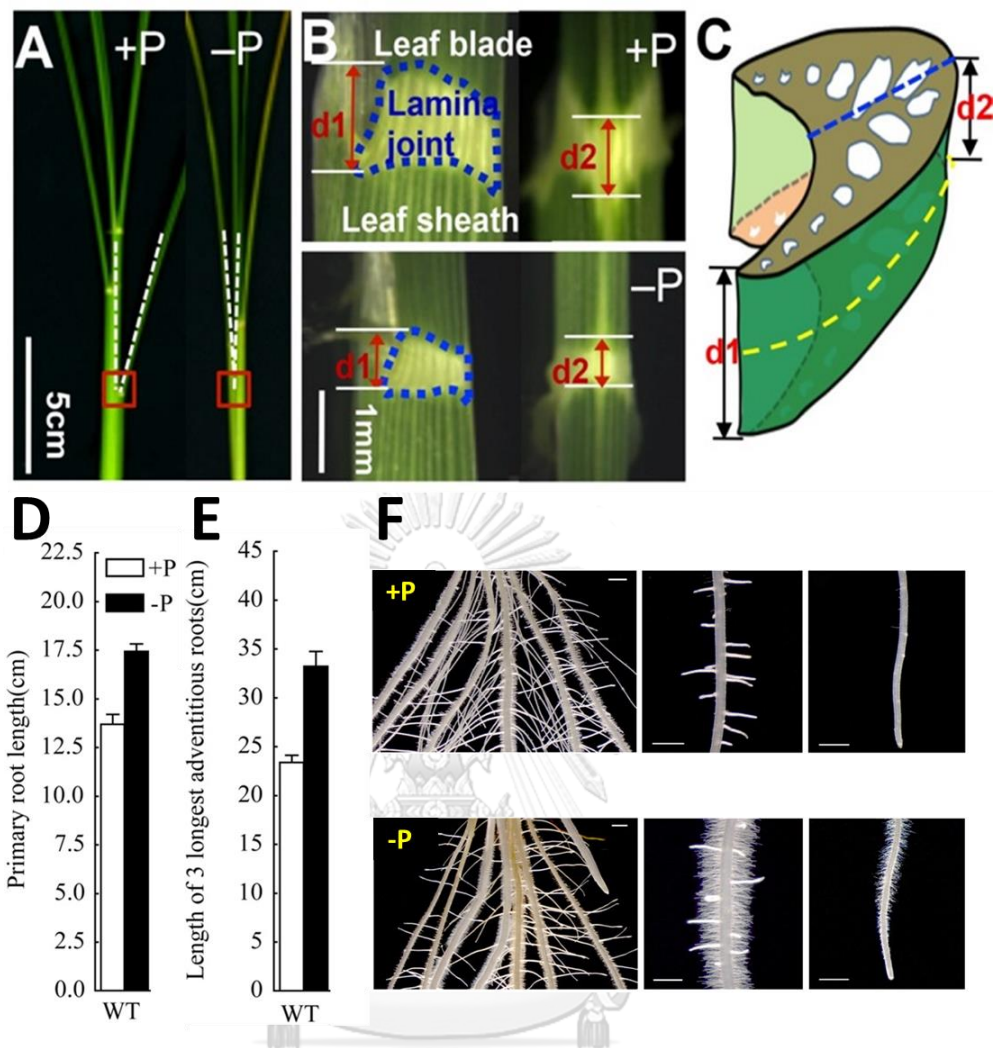
Figure 3 Leaf angle and root system architecture adaptation in rice under phosphorus deficiency (A-F). P deficiency decreased leaf angle (A) by inhibition of lamina joint (B). 3D illustration of different inhibition in both lamina joint sides. P starvation increases root elongation (D-E) and root hair density (F) (Zhou *et al.*, 2008; Ruan *et al.*, 2018).

2.3 Phosphorus responsive and tolerance genes in rice

The adaptation and response to P deprivation are modulated by network regulation of cascade genes. *OsPHR1* and *OsPHR2*, homologous transcription factor genes, are center regulators in P starvation signaling pathway. They directly bind to P1BS cis-element in the promoters of phosphate starvation-induced (PSI) genes to regulate their expression (Zhou *et al.*, 2015). Moreover, *OsPHR2* is negatively controlled by *OsSPX* encoding protein in a Pi-dependent manner, which acts as a Pi detective sensor in plant cells (Wang *et al.*, 2014). Under P deficient condition, expression of PSI genes, including *OsIPS1/2*, *Os-miR399*, *OsPT*s, *OsPAP*s, and *OsSQD2*, are triggered to modulate plant adaptation in both P utilization efficiency and P acquisition efficiency. High expression of *OsPT*s, phosphorus transporter genes, controls higher Pi uptake and remobilization into the essential organs. Similarly, *OsPAP*s and *OsSQD2* promote Pi recycling from membrane phospholipids and releasing of acid phosphatase to breakdown fixed P. *Os-miR399* functions to control the expression level of *OsPHO2,* which negatively regulates other PSI genes. *OsIPS1/2*, which are non-coding genes, act by sequestering miR399 from degrading PHO2 (Franco-Zorrilla *et al.*, 2007).
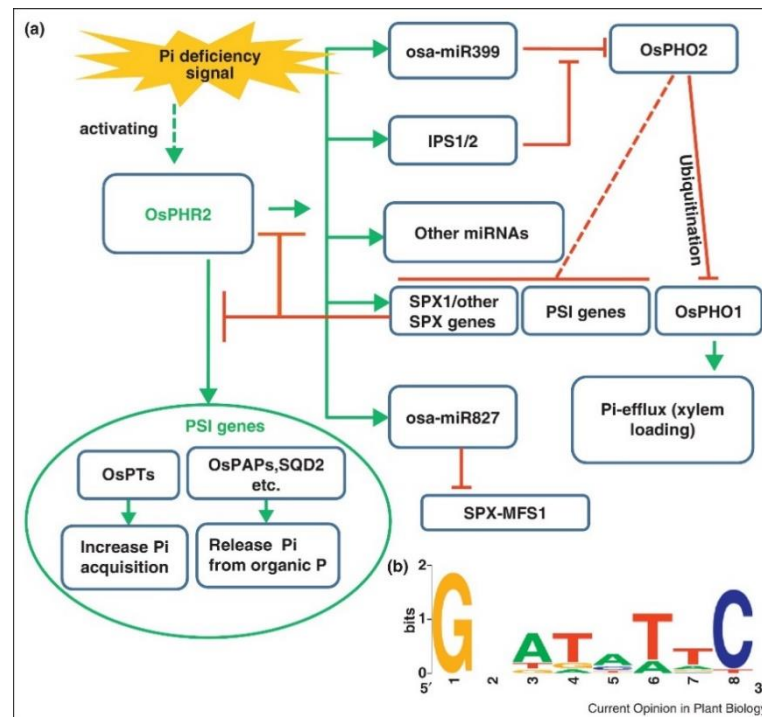
Figure 4 Phosphorus deficiency signaling involved in P deficiency adaptation and response (Wu *et al.,* 2013).

P deficiency signaling pathway is shown in Figure 4. Overexpression of some regulatory genes result in increased adaptation and tolerant efficiency under P starvation, such as *OsPHR2, OsPAP10, OsPT6,* etc. Rice overexpressing *OsPHR2* resulted in the increase of P adaptation by enhanced root elongation, root hair proliferation, Pi transporters, and Pi accumulation (Zhou *et al.,* 2008). In P-fixing soil, *OsPAP10c* overexpressing rice exhibited acid phosphatase activity to breakdown fixed P and then turned it to usable forms. Higher Pi accumulation was found and caused by high root acquisitional performance (Lu *et al.,* 2016). Transgenic rice overexpressing a high-affinity Pi transporter *OsPT6* could store high P content in their leaves and promote greater yield productivity with more numerous tillering under P starvation (Zhang *et al.,* 2014). One well-known P deficiency tolerance gene, *OsPSTOL1*, was identified from tolerance rice cultivars grown under P deficient soil by QTL technique. Pup1 QTL was identified from 30 rice accessions, including aus rice

variety in the population **(Figure 5a)**. In comparison with the Nipponbare genome sequence, 120 kbp of the Pup1 region of Kasalath rice was absent from the Nipponbare genome **(Figure 5b)**. The deletion of *OsPSTOL1* in the Pup1 region causes more susceptibility to P deficiency in Nipponbare (Heuer *et al.*, 2009). Transformation of *OsPSTOL1* into IR64 rice, which is a PSTOL1-absent genotype, could boost tolerance adaptation from P sensitive IR64 rice in both P sufficient and deficient conditions. Improved yield production, P uptake, and root surface area confirmed tolerance enhancing function of the *OsPSTOL1* gene (Gamuyao *et al.*, 2012).
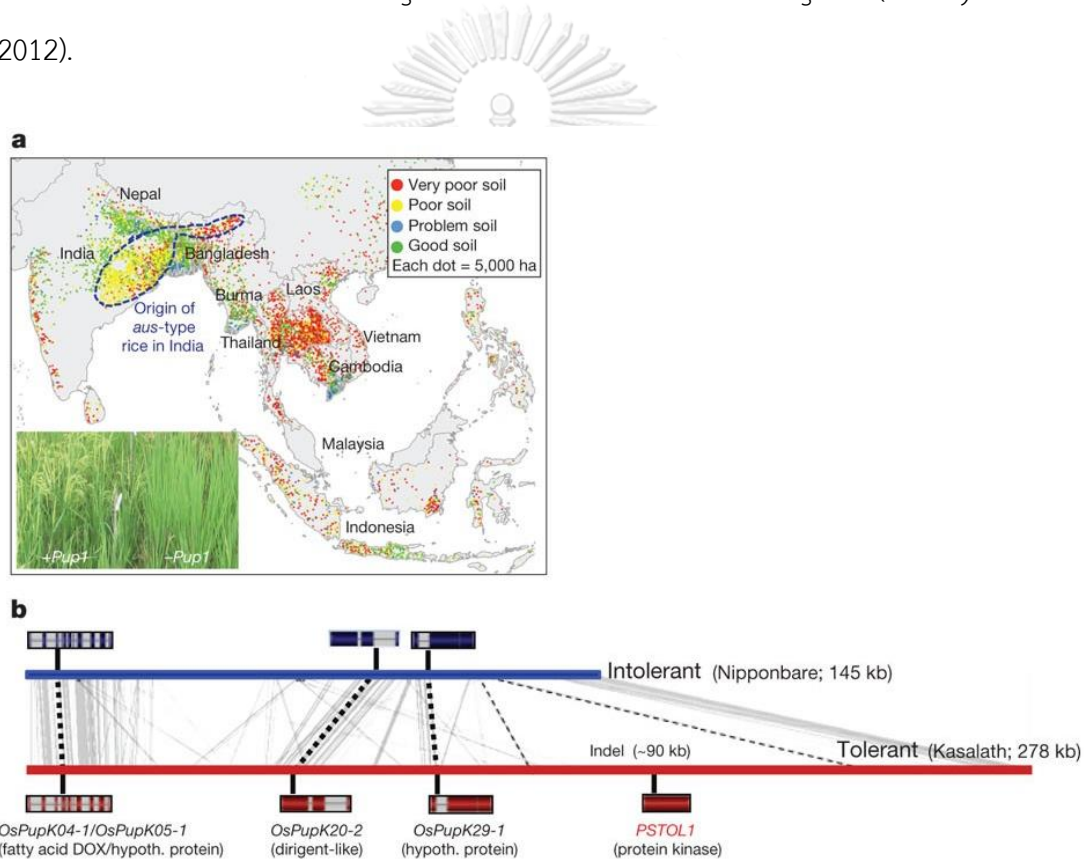
Figure 5 Soil problem in Asia and distribution of aus-type rice (a). The relative position of Pup1 genes between the Kasalath and Nipponbare rice genome (b) (Gamuyao *et al.*, 2012).

3. Phosphorus quantification

3.1 Conventional phosphorus quantification methods

To study phosphorus deficiency and their adaptation in plants, phosphorus determination to understand P concentration changes is essential. Phosphorus quantification techniques are sensitive measurements, particularly in plant tissues. Several quantifying processes have been established for different strengths and weak points, such as colorimetric assay, X-ray spectrometry, inductively coupled plasma (ICP), nuclear magnetic resonance (NMR), etc. But the colorimetric assay is still popular due to its cheap rate and unnecessary complex detecting machine. Recently, molybdenum blue and malachite green are two useful colorimetric assays using for P quantification. The molybdenum blue reaction is more common in the application due to wider range of detection in P concentration than the malachite green approach. Molybdenum blue reaction is used to determine orthophosphate (PO_4^{3-}) molecules, inorganic form of phosphorus in nature, which finally forms blue-colored product. In detail, the reaction includes two major steps that a single orthophosphate (hetero-atom) firstly combines with a dozen molybdate molecule (addenda-atom), and then forms Keggin structure **(Figure 6)**. Secondly, the complex structure is continuously reduced to molybdenum blue species (blue colored molecule) by the reductant, ascorbic acid, as shown in equation (1) and (2) (McKelvie *et al.*, 1995).

$$PO_4^{3-} + 12MoO_4^{2-} + 27H^+ \rightarrow H_3PO_4(MoO_3)_{12} + 12H_2O \qquad \text{------------ (1)}$$

$$H_3PMo(VI)_{12}O_{40} + \text{Reductant} \rightarrow [H_4PMo(VI)_8Mo(V)_4O_{40}]^{3-} \qquad \text{------------ (2)}$$
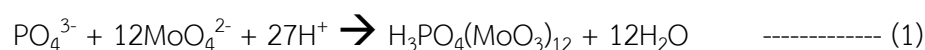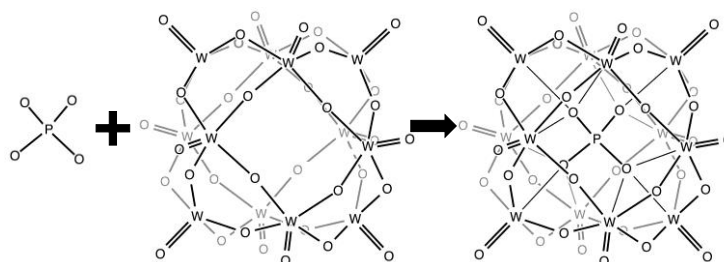
Figure 6 The Keggin structure of phosphomolybdate generating from the combinational reaction of P-hetero atom and molybdenum-addenda atom (Klemperer, 2007).

3.2 Limitations of the conventional quantification methods

By the molybdate blue reaction, the measurement step is not the time-limiting factor of Pi quantification in plants. However, the extraction step, which releases Pi molecule from plant tissues, is precisely the problem from the tedious steps, time consumption, and low throughput. From method consideration, three main issues in the extraction involve sample balancing, numerous times-pipetting, and grinding.

The initial sample's weight is essential and generally used for several quantifications to estimate accurate concentration and interpretation by normalizing the initial sample unit. However, balancing small fresh tissue is inconvenient and error-prone, which needs very sensitive and expensive balance. Besides, working with uncontrollable time and environment affects weight loss from water evaporation in the tissue that influences accurate weight. Alternatively, area normalization had been used to quantification of chlorophyll content (Hamblin *et al.,* 2014; Liang *et al.,* 2017) and root Pi content (Ayadi *et al.,* 2015).

Several times of pipetting, including chemical addition and supernatant transferring, in several repeated step are tedious work and time consuming. The modified method using a microplate reader and multichannel pipette is an alternative way to standardize and encourage high-throughput measurement (Auld *et*

al., 2020). Nowadays, many improved high-throughput methods have developed by performing with microplate and multichannel pipette to enhance the platform speed and easy to perform (Salvo-Chirnside *et al.*, 2011; Hawkins and Storey, 2017; Gilbert-Girard *et al.*, 2020; Koepke *et al.*, 2020). Besides, the fixed location of the microplate provides less labeling in each sample, that I can map the sample description with location of wells in the plate *via* computational mapping (Auld *et al.*, 2020).

Hard-working and loss of uncountable equipment are sacrificed for tissue grounding to release intracellular Pi content. Freeze shattering process provides a single step to permeabilize plant cell walls, containing the excess intracellular substance to the extraction solution by freezing tissue at deep frozen condition (Wasteneys *et al.*, 1997). This technique has previously been demonstrated in plant protoplasts (Tiwari and Polito, 1990), algae cells (Braun, 1996), and various plant materials (Wasteneys *et al.*, 1997).

4. Hyperspectral sensing - a non-destructive detection approach
4.1 Principle and development

Hyperspectral detection is a new and accessible technique to identify plant response against stresses and diseases, subtle symptoms, with non-destructive property (Kokaly *et al.*, 2009). The hyperspectral detection device provides high-fidelity reflectance information over the light spectrum, including visible (VIS) and invisible wavelengths **(Figure 7)**. In the analysis, the large and complicated spectral information can distinguish various responses in plants. The spectrum can be considered from about 250 nm (ultraviolet; UV) to 2,500 nm (short wave infrared; SWIR), which includes a subset of different spectrum type, including UV (250-400 nm), VIS (400-700 nm), NIR (700-1,300 nm), and SWIR (1,300-2,500 nm) (Pandey *et al.*, 2017). Thus, performance of a spectroreflectometer depends on the range coverage and frequency of detective sensor. For plants, the highly potential information is in

the VIS and NIR wavelength regions **(Figure 8)**. VIS is mainly affected by absorbance of pigments, such as chlorophyll, carotenoid, xanthophyll, anthocyanin. In contrast, NIR informs in turgid of plant cell structure, which usually has high reflectance in a healthy plant. Additionally, SWIR indicates leaf water content and lignocellulose (Peñuelas and Filella, 1998). One interesting part is at the red edge position (690-740), in which the reflectance suddenly increases. This change is a specific response to photosynthetic pigments. The reflectance at wavelength up to ~700 nm is low due to dramatical absorption of photosynthetic pigments. After ~720 nm, the reflectance suddenly rises over the red edge region and is then quite steady with high reflectance at the NIR zone (Cho and Skidmore, 2006). Several indices were developed from these interesting spectra, such as NDVI, RECI, TNDVI, MCARI, IRECI, and PSSR. (Psomiadis *et al.*, 2017).
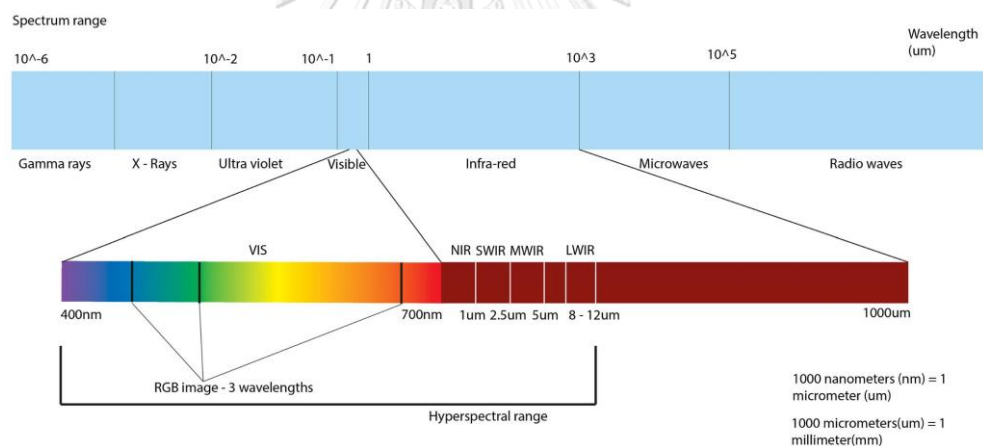
Figure 7 Different types of the electromagnetic spectrum along with wavelength range. The diagram displays visible and infra-red regions (Lowe *et al.*, 2017).

To address plant responses to different conditions, representative wavelengths, which are highly altered under the different conditions, is considered important in the spectrum. The combination of two or more representative wavelengths in the spectrum is used to generate specific vegetative indices. Nowadays, many indices have been investigated to represent plant status and

response indirectly. For example, normalized difference vegetation index (NDVI) was established by NASA scientists to analyze Earth's relative greenness using satellite tele-observation (Rouse Jr *et al.*, 1974). The index was calculated by a simple ratio of the NIR and VIS spectrum. NDVI information helps in environment management by tracking plant vegetation structure, such as agricultural interference, droughts or forest declination (Borowik *et al.*, 2013). Plant pigment indices have been developed to estimate the content of chlorophylls, carotenoids, and anthocyanin. Chlorophyll absorption reflectance index (CARI) (Kim, 1994), modified CARI (MCARI) (Daughtry *et al.*, 2000), and chlorophyll red-edge index (CIred edge) (Gitelson *et al.*, 2006) have been created to improve the accuracy and effectiveness. Different forms of carotenoids, such as violaxanthin and zeaxanthin, can be identified by its individual detective index (CRI1 and CRI2, respectively) (Gitelson *et al.*, 2002). Anthocyanin content indices (ACI) were derived from dividing between green and red reflectance, and the ACI was then modified by normalizing with NIR reflectance (Gamon and Surfus, 1999). Moreover, water deprivation can be determined with the NDII index, which contributed to NIR and SWIR reflectance (Hunt Jr and Rock, 1989). Furthermore, some indices provide multiple purposes, such as NDWI, WBI, SIPI, RGRI, and MSI **(Table 3)** (Roberts *et al.*, 2016).
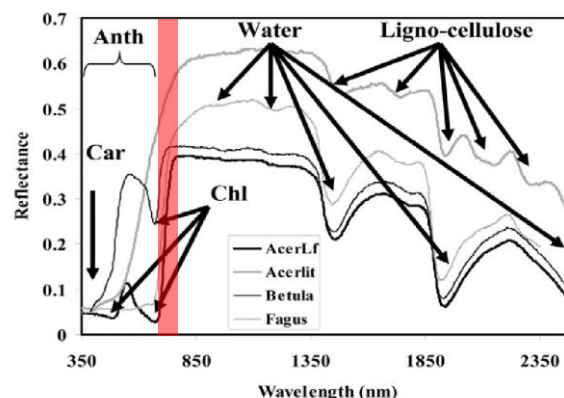
Figure 8 Illustration of reflectance along the spectral wavelength of different samples growing in various locations. The red edge section was highlighted in red (690–740 nm) (Roberts *et al.*, 2016).

Table 3 Summary of some hyperspectral Indices, relevant formulas, and description. Highlight in grey are indices using for multiple purposes (Roberts *et al.*, 2016).

Index	Equation	Reference
Structure (LAI, green biomass, fraction)		
*NDVI	$(R_{NIR}-R_{red})/(R_{NIR}+R_{red})$	Rouse et al.[15]
*SR	R_{NIR}/R_{red}	Jordan [3]
*EVI	$2.5*(R_{NIR}-R_{red})/(R_{NIR}+6*R_{red}-7.5*R_{blue}+1)$	Huete et al.[23]
*NDWI	$(R_{857}-R_{1241})/(R_{857}+R_{1241})$	Gao [29]
**WBI	R_{900}/R_{970}	Peñuelas et al.[28]
*ARVI	$(R_{NIR}-[R_{red}-\gamma*(R_{blue}-R_{red})])/(R_{NIR}+[R_{red}-\gamma*(R_{blue}-R_{red})])$	Kaufman & Tanré [22]
*SAVI	$[(R_{NIR}-R_{red})/(R_{NIR}+R_{red}+L)]*(1+L)$	Huete [21]
**1DL_DGVI	$\sum_{\lambda_{626\,nm}}^{\lambda_{795\,nm}} |R'(\lambda_i) - R'(\lambda_{626\,nm})|\Delta\lambda_i$	Elvidge & Chen [1]
**1DZ_DGVI	$\sum_{\lambda_{626\,nm}}^{\lambda_{795\,nm}} |R'(\lambda_i)|\Delta\lambda_i$	Elvidge & Chen [1]
*VARI	$(R_{green}-R_{red})/(R_{green}+R_{red}-R_{blue})$	Gitelson et al.[13]
*VIgreen	$(R_{green}-R_{red})/(R_{green}+R_{red})$	Gitelson et al.[13]
Biochemical		
Pigments		
**SIPI	$(R_{800}-R_{445})/(R_{800}-R_{680})$	Peñuelas et al. [31]
**PSSR	$(R_{800}/R_{675}); (R_{800}/R_{650})$	Blackburn [30]
**PSND	$[(R_{800}-R_{675})/(R_{800}+R_{675})]; [(R_{800}-R_{650})/(R_{800}+R_{650})]$	Blackburn [32]
**PSRI	$(R_{680}-R_{500})/R_{750}$	Merzlyak et al. [33]
Chlorophyll		
**CARI	$[(R_{700}-R_{670})-0.2*(R_{700}-R_{550})]$	Kim [34]
**MCARI	$[(R_{700}-R_{670})-0.2*(R_{700}-R_{550})]*(R_{700}/R_{670})$	Daughtry et al. [35]
**CI$_{red\,edge}$	$R_{NIR}/R_{red\,edge}-1$	Gitelson et al. [36]
Anthocyanins		
**ARI	$(1/R_{green})-(1/R_{red\,edge})$	Gitelson et al.[40]
**mARI	$[(1/R_{green})-(1/R_{red\,edge})]*R_{NIR}$	Gitelson et al. [36]
**RGRI	R_{red}/R_{green}	Gamon & Surfus [7]
**ACI	R_{green}/R_{NIR}	Van den Berg & Perkins [41]
Carotenoids		
**CRI1	$(1/R_{510})-(1/R_{550})$	Gitelson et al.[42]
**CRI2	$(1/R_{510})-(1/R_{700})$	Gitelson et al. [42]
Water		
*NDII	$(R_{NIR}-R_{SWIR})/(R_{NIR}+R_{SWIR})$	Hunt & Rock [12]
*NDWI, **WBI	See Above	See Above
*MSI	R_{SWIR}/R_{NIR}	Rock et al. [43]
Lignin &Cellulose/Residues		
**CAI	$100*[0.5*(R2031+R2211)-R2101]$	Daughtry [47]
**NDLI	$[\log(1/R_{1754})-\log(1/R_{1680})]/[\log(1/R_{1754})+\log(1/R_{1680})]$	Serrano et al. [48]
Nitrogen		
**NDNI	$[\log(1/R_{1510})-\log(1/R_{1680})]/[\log(1/R_{1510})+\log(1/R_{1680})]$	Serrano et al. [48]
Physiology		
Light Use Efficiency		
RGRI,SIPI	See Above	See Above
**PRI	$(R_{530}-R_{570})/(R_{530}+R_{570})$	Gamon et al. [9]
Stress		
*MSI	See Above	See Above
**REP	I(max first derivitive: 680-750 nm)	Horler et al. [10]
**RVSI	$[(R_{714}+R_{752})/2-R_{733}$	Merton & Huntington [52]

4.2 Hyperspectral application in plant stress response

Hyperspectral observation has been applied for many plant stresses, such as drought, salt stress, plant disease, and nutrient deficiency. Moreover, different plant species also show different response phenotypes, which can be detected by different hyperspectral indices. Jones *et al.* (2004) applied hyperspectral analysis to investigate the effect of water stress in three plant species, including corn, spinach, and snap bean, *via* monitoring of conventional plant water content, spectral bands, and spectral indices. The spectral band at 1,450 nm derived from corn and snap bean resulted in a high correlation with plant water content, while the spinach was the band at 950-970 nm. Reflectance detection at 300-2,550 nm region of corn leaves grown in various irrigation rates showed three representative regions along the spectra (VIS, NIR, and SWIR), which illustrated different responsive spectra between the treatments. Thus, the indices based on ratio across spectral regions could exhibit higher sensitivity in drought stress detection (El-Hendawy *et al.*, 2017). In salinity stress, Moghimi *et al.* (2018) used the hyperspectral imaging pipeline to identify salt stress tolerance in wheat, which offered simple processing and data analysis by associating a machine learning platform. Machine learning helped to investigate complex and high dimensional interaction within hyperspectral information. A similar approach was studied in okra (*Abelmoschus esculentus* L.) under salt stress condition that machine learning-based reflectance analysis provided high-efficiency prediction to calculate the predicted value of SPAD, sodium content, photosynthetic rate, and transpiration rate without traditional phenotyping procedures (Feng *et al.*, 2020). In a complex phenotype as plant disease caused by virulent fungi, charcoal rot disease in soybean could be identified by a novel 3D deep convolutional neural network (3D-DCNN). Based on hyperspectral image acquisition, the 3D-DCNN offered 95.73% accuracy in disease classification by intelligent classification model, which was assessed from the sensitive reflectance information at the NIR region (Nagasubramanian *et al.*, 2019).

Under nutrient deficiency, three major macronutrients (N, P, and K) were mainly focused and attempted to develop the non-destructive measurement processes. Peng *et al.* (2020) applied hyperspectral technology and generated potential indices for degraded vegetation. Three macronutrients in six species were *in situ* performed hyperspectral data collection and nutrient quantification. The exact estimation indices were established from 43 responsive indices, optimized *via* linear regression analysis. These useful indices can be used for airborne and satellite hyperspectral information. For forest observation, hyperspectral tele-capturing or available Google Earth Engine dataset can be analyzed and detected nutrient deficiency area by analyzing a responsive reflectance spectrum (Walshe *et al.*, 2020). For more convenient and accurate use of hyperspectral imaging, in field hyperspectral camera (Hyspex push-broom) was built and automatically used for N content estimation of sugar beet leaves **(Figure 9)**. Predicted N content showed sufficient correlation (r^2=0.86) with actual N content that can be applied to study N content distribution along with leaf samples (Jay *et al.*, 2014). For sensitive detection of P and K in tea leaves, modified NIR based spectral indices were established by pre-processing model improvement to eliminate noise interference of raw spectral data. The developed model could predict high coefficient indices (r^2=0.94 and 0.92) for P and K content in tea leaves, respectively (Wang *et al.*, 2020).

Figure 9 Phenotyping platform with the hyperspectral camera for N content detection (Wang *et al.*, 2020).

5. Genome-wide association study

5.1 Key concept

Since next-generation sequencing technology had been established, the powerful investigating tool called genome-wide association study (GWAS) was also emerged to identify causative genetic positions on the genome in several phenotypes and species of interest. GWAS is the successful method used to dissect the genetic basis of the complex traits by establishing statistical links between phenotypes and genotypes **(Figure 10)**. Based on four different nitrogenous bases (A, C, T, and G) inscribed within billions of DNA molecules of genome sequences, an individual nitrogenous base altering in the same position among the study population is one of potential variations **(Figure 11)**, which called single nucleotide polymorphism (SNP). SNP potentially causes a mutation in an organism that informs the genome history over the past. The non-random interaction of SNPs is the historical evidence representing the mutation or recombination rate of genome passing through the generation, which is called linkage disequilibrium (LD). The different types of variable SNPs can be used to represent the genotype of the population in GWAS analysis. To reduce false positives, the genotypic data are typically pre-processed by performing a quality control process to filter low potential variation before the association step.
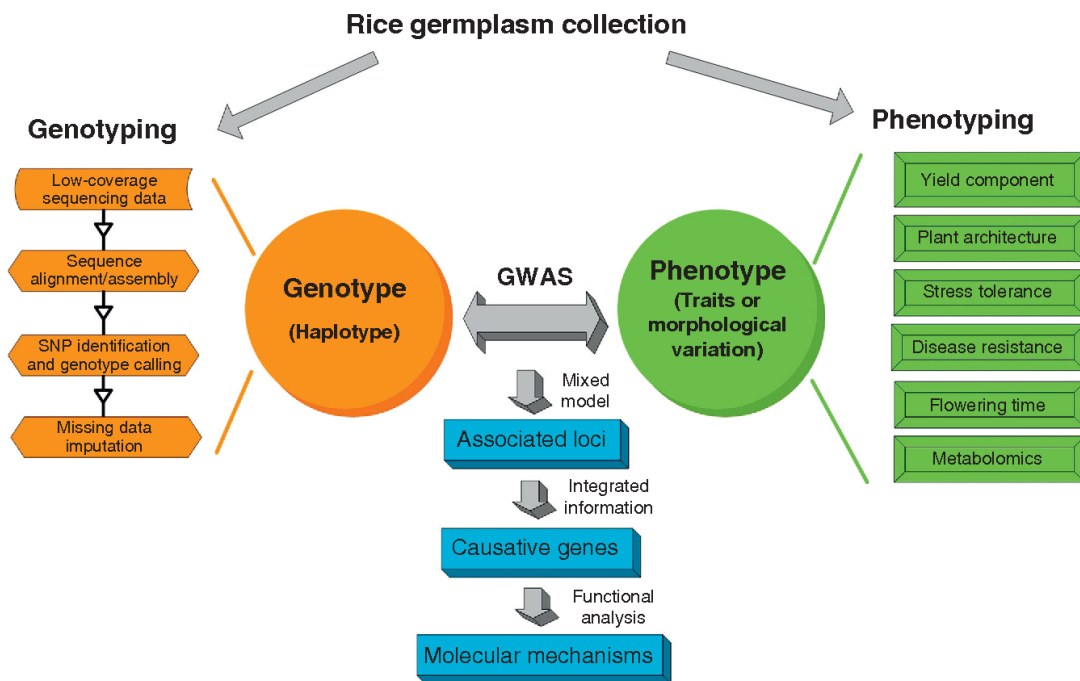
Figure 10 A diagram view of sequencing-based genome-wide association process in rice *(Han and Huang, 2013)*.

Another essential requirement for GWAS is responsive traits of the interesting phenotype, which enables the quantitative or case-control value. Quantitative data are more informative than case-control data in the association by its more dimension of data. For association analysis, each individual SNP is statistically associated and tested the null hypothesis with the phenotypic data. The linear regression model, called the general linear mix model, is typically used for quantitative parameters. Association software, which provides the general linear mix model, includes GEMMA (Zhou and Stephens, 2012) and EMMA (Kang *et al.*, 2008). Moreover, several novel association platforms have been developed to improve the association efficiency, such as the integration of Kruskal–Wallis test with empirical Bayes (pkWemEB) (Ren *et al.*, 2018), easyGWAS (Grimm *et al.*, 2012), GWASpro (Kim *et al.*, 2019), GWAS Atlas (Tian *et al.*, 2020).
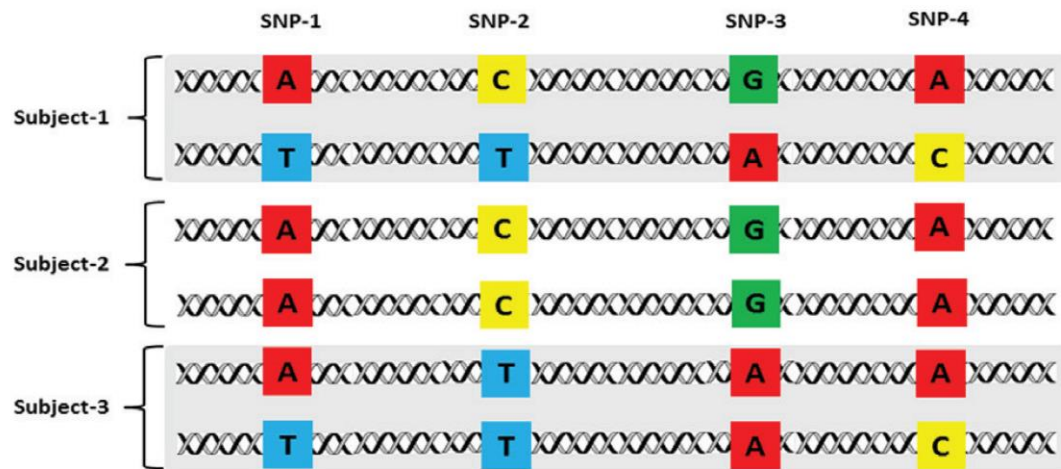
Figure 11 Illustration of four SNPs comparison of three independent genomes.

5.2 Application of genome-wide association study in rice

Since the GWAS launched for research in gene identification, numerous plant species, such as sorghum (Shehzad *et al.*, 2009), barley (M. Wang *et al.*, 2012), lettuce (Simko *et al.,* 2009), maize (Li *et al.,* 2013), tomato (Ranc *et al.,* 2012), *Arabidopsis* (Atwell *et al.,* 2010), soybean (Contreras-Soto *et al.,* 2017), bread wheat (Zanke *et al.,* 2014), pepper (Colonna *et al.,* 2019), and particular rice (Huang *et al.,* 2012; Wu *et al.,* 2015), have been applied with various agronomic parameters under control or stress conditions. Rice is a suitable plant model use for genetic investigation for several reasons. It has a small size of the genome, short-life cycle, diploid alleles, and self-fertilization. Moreover, the complete and informative reference genome databases were already established and available in both indica and japonica varieties (Yu *et al.,* 2002; Kawahara *et al.,* 2013).

For the P deficiency response gene, Wissuwa *et al.* (2015) used the internal P utilization efficiency (PUE) trait derived from 413 rice accessions under comparative P starvation. The significant loci were identified from the association on chromosome 1, 4, 11, and 12, which included 14 candidate genes. Gene expression analysis from rice grown under P starvation showed the high response of the candidate genes.

A responsive gene encodes a nucleic acid-binding protein (LOC_Os01g13090) with an RNA ligase/cyclic nucleotide phosphodiesterase, which was found to be highly expressed in old leaf tissue. Interestingly, GWA of SNPs derived from a comparison between low P tolerant and sensitive rice identified several SNPs located in P responsive and root system architecture genes (Poonam Mehra *et al.*, 2015).

In the case of hyperspectral detection in rice, red edge (680-760 nm) derived indices showed a high correlation with chlorophyll content. GWA association of the indices could identify chlorophyll regulated genes as well as chlorophyll-related traits (Feng *et al.*, 2017). Furthermore, hyperspectral imaging has been used to determine grain quality in rice seeds. The impact ratio spectrum of VIS and NIR regions (702-900 nm) was used as representative indices and associated with the SNP genotypes. The result indicated several grain-quality related genes that could confirm hyperspectral qualification capacity (Barnaby *et al.*, 2020). Similarly, D. Sun *et al.* (2019) could use the hyperspectral NDSI index instead of protein content due to their high correlation efficiency. GWA of both NDSI and protein content identified the same candidate genes. The hyperspectral trait measurement has a potential to apply for GWAS investigation of P deficiency.

CHAPTER III

MATERIALS AND METHODS

1. Materials

1.1 Plant materials

Seeds of 172 Thai rice (*Oryza sativa* L.) accessions, including Thai rice varieties and breeding cultivars used in this study, were obtained from National Rice Seed Storage Laboratory for Genetic Resources, Pathum Thani Rice Research Center, Rice Department, Ministry of Agriculture and Cooperatives **(Table 4)**.

1.2 Equipments

- -20°C deep freezer (Mitsubishi electric, Japan)
- -80°C deep freezer (Thermo-Scientific, USA)
- 3-mm diameter paper puncher
- 4°C refrigerator (Hitachi, Japan)
- 40-liter plastic boxes
- 80-liter foam boxes
- 100-liter plastic tank
- Hot air oven (Binder, USA)
- Ice foam box
- Micropipette (Mettler Toledo Rainin, USA)
- Microplate reader (Molecular Devices, USA)
- Mortar and pistil
- Multichannel micropipette (Mettler Toledo Rainin, USA)
- pH meter (Mettler Toledo, USA)
- Pipetting filler (Mettler Toledo Rainin, USA)
- Plastic net

- PolyPen RP 400 (UV-VIS) (Photon Systems Instruments, Czech Republic)

- Portable pH meter

- PVC pipe

- Refrigerated centrifuge (Hettich Zentrifugen, Germany)

- Reverse osmosis water filter (Colandas, USA)

- Seed Starter Tray

- Vortex shaker (Scientific Industries, Inc., USA)

1.3 Chemical and reagents

All chemical and reagents used in this study were analytical grade and produced by different companies as described below.

- Ammonium molybdate tetrahydrate; $(NH_4)_6.Mo_7O_{24}.4H_2O$ (Alfa Aesar, United Kingdom)

- Ammonium nitrate; NH_4NO_3 (Ajax Finechem, Australia)

- Ascorbic acid; $C_6H_8O_6$ (Acros Organics, Belgium)

- Boric acid; H_3BO_3 (Merck, Germany)

- Calcium chloride hexahydrate; $CaCl_2.6H_2O$ (Ajax Finechem, Australia)

- Commercial bleach (Clorox, USA)

- Copper sulfate pentahydrate; $CuSO_4.5H_2O$ (M&B, England)

- Dipotassium phosphate; K_2HPO_4 (Ajax Finechem, Australia)

- Ferric sodium EDTA; FeNaEDTA (Himedia, India)

- Hydrochloric acid; HCl (Merck, Germany)

- Magnesium sulfate heptahydrate; $MgSO_4.7H_2O$ (Daejung, Korea)

- Manganese chloride tetrahydrate; $MnCl_2.4H_2O$ (M&B, England)

- Molybdate blue reagent (see in Appendix B)

- Perchloric acid; $HClO_4$ (Loba Chemie, India)

- Potassium sulfate; K_2SO_4 (Daejung, Korea)

- Potassium dihydrogen phosphate; KH_2PO_4 (Daejung, Korea)

- Sodium chloride; NaCl (J.T.Baker, Malaysia)

- Sodium hydroxide; NaOH (Daejung, Korea)

- Yoshida solution (see in Appendix A)

- Zinc sulfate heptahydrate; $ZnSO_4.7H_2O$ (Ajax Finechem, Australia)

1.4 Consumables and supplies

- 1.5 ml microtube (Extragene, USA)

- 15 ml plastic tube (Nest Scientific, USA)

- 50 ml plastic tube (Nest Scientific, USA)

- 96-deep well plates (Greiner Bio-One, Austria)

- 96-well plates (Greiner Bio-One, Austria)

- Aluminum foil

- Dry ice

- Glossy paper

- Hydroponic sponge

- Ice

- PP Plastic bag

- Liquid N_2 (TIG, Thailand)

- Multiple channel pipette tips (Mettler Toledo Rainin, USA)

- Pipette tips (Nest Scientific, USA)

- Tissue paper

- Transparent sticker

Table 4 List of rice accessions used in this study.

No.	Name	GS No.	Seq		Location	Parental Lines / parental relations
1	KHIAW HAHNG MAH	2063	Pro	Ex	Thailand	Thai local
2	KHAO SUPAN	2296	Pro	Ex	Thailand	Thai local
3	LUANG PRATAHN	2975	Pro	Ex	Thailand	Thai local
4	HAHNG NAHK	5583	Pro	Ex	Thailand	Thai local
5	KHAO SAMER	7200	-	Ex	Thailand	Thai local
6	LEUANG PUANG TAWNG	7214	Pro	Ex	Thailand	Thai local
7	LEUANG TAH YANG	14685	Pro	Ex	Thailand	Thai local
8	PUANG TAWNG	18442	Pro	Ex	Thailand	Thai local
9	PRATAHN BAN BUNG	20375	Pro	Ex	Thailand	Thai local
10	DAW SAHM DEUAN	21792	Pro	Ex	Thailand	Thai local
11	KHAO GAEW	6152	Pro	Ex	Thailand	Thai local
12	LEUANG NGAHM	12616	Pro	Ex	Thailand	Thai local
13	PUANG TAWNG	574	Pro	Ex	Thailand	Thai local
14	NIAW KHAO	607	Pro	Ex	Thailand	Thai local
15	E-MUM	5639	Pro	Ex	Thailand	Thai local
16	DAWK KHAH	12160	Pro	Ex	Thailand	Thai local
17	RAHK HAENG	12177	Pro	Ex	Thailand	Thai local
18	LEUANG GLAHNG	12498	Pro	Ex	Thailand	Thai local
19	KHAO KOD	12503	Pro	Ex	Thailand	Thai local
20	JAE GAN	12507	Pro	Ex	Thailand	Thai local
21	PRA IN	13967	Pro	Ex	Thailand	Thai local
22	MA GAWK	13972	Pro	Ex	Thailand	Thai local
23	IN PAENG	13981	Pro	Ex	Thailand	Thai local
24	SAM AHANG	13987	Pro	Ex	Thailand	Thai local
25	MA YOM	13988	Pro	Ex	Thailand	Thai local
26	E-LAI	14082	Pro	Ex	Thailand	Thai local
27	GRA DAHD	15905	Pro	Ex	Thailand	Thai local
28	KHAO BAHN POD	19877	-	Ex	Thailand	Thai local
29	TAH BAHN	21695	-	Ex	Thailand	Thai local
30	MAHK YOM	21706	Pro	Ex	Thailand	Thai local

No.	Name	GS No.	Seq		Location	Parental Lines / parental relations
31	HAHNG MAH NAI	21707	Pro	Ex	Thailand	Thai local
32	KHITOM KHAO	21708	Pro	Ex	Thailand	Thai local
33	LEUANG DONG	22046	Pro	Ex	Thailand	Thai local
34	PLAH SEW	22206	-	Ex	Thailand	Thai local
35	RUANG DIAW	22834	Pro	Ex	Thailand	Thai local
36	LAO TAEK	22836	Pro	Ex	Thailand	Thai local
37	DAENG NAH	22850	Pro	Ex	Thailand	Thai local
38	PUANG HAHNG NAHK	23233	Pro	Ex	Thailand	Thai local
39	LEUANG NOI 31-1-39	588	Pro	Ex	Thailand	Thai local
40	JUD MAWN	1693	Pro	Ex	Thailand	Thai local
41	KHAO SA NGUAN	1697	Pro	Ex	Thailand	Thai local
42	CHAW MA GAWK	2042	Pro	Ex	Thailand	Thai local
43	MA FAI	5650	Pro	Ex	Thailand	Thai local
44	JAO RAHK HAENG	12492	Pro	Ex	Thailand	Thai local
45	TA POW GAEW 161	1578	Pro	Ex	Thailand	Thai local
46	KHAO GON JUD	3226	Pro	Ex	Thailand	Thai local
47	PLAH KHAENG	3241	Pro	Ex	Thailand	Thai local
48	JAO KHAO	3330	Pro	Ex	Thailand	Thai local
49	MUAY HIN	5580	Pro	Ex	Thailand	Thai local
50	LEUANG PRATEW	5681	-	Ex	Thailand	Thai local
51	SAO NUENG	5699	-	Ex	Thailand	Thai local
52	GON GAEW	6158	Pro	Ex	Thailand	Thai local
53	KHAO NUAN	6425	-	Ex	Thailand	Thai local
54	TAWNG RAHK SAI	10917	-	Ex	Thailand	Thai local
55	MAHK NAM	14085	-	Ex	Thailand	Thai local
56	DAWK MAI	15127	Pro	Ex	Thailand	Thai local
57	LEUANG PAHK CHONG	21775	-	Ex	Thailand	Thai local
58	LEUANG CHUMPAE	21782	-	Ex	Thailand	Thai local
59	LEUANG KAMIN	21790	-	Ex	Thailand	Thai local
60	KOO MEUANG	21795	-	Ex	Thailand	Thai local

No.	Name	GS No.	Seq		Location	Parental Lines / parental relations
61	TA POW LOM	22357	Pro	Ex	Thailand	Thai local
62	KHAO AH-GAHD	22358	-	Ex	Thailand	Thai local
63	SAI YUD	22366	-	Ex	Thailand	Thai local
64	DI SI	22367	Pro	Ex	Thailand	Thai local
65	NAH KWAN	22379	Pro	Ex	Thailand	Thai local
66	MED MAKHAM	22391	Pro	Ex	Thailand	Thai local
67	HAH RUANG	22395	Pro	Ex	Thailand	Thai local
68	TOM MEUANG LUANG	22784	Pro	Ex	Thailand	Thai local
69	NIAW MALI	22875	Pro	Ex	Thailand	Thai local
70	MA YOM	22802	Pro	Ex	Thailand	Thai local
71	DAW DAWK MAI	22817	Pro	Ex	Thailand	Thai local
72	MAHK NAM	22835	Pro	Ex	Thailand	Thai local
73	KHAO' GAM	23113	Pro	Ex	Thailand	Thai local
74	E-KHAO YAI	23114	-	Ex	Thailand	Thai local
75	KASET DAW	23189	Pro	Ex	Thailand	Thai local
76	GAM PAI	23191	Pro	Ex	Thailand	Thai local
77	KHAO LUANG	7282	Pro	Ex	Thailand	Thai local
78	NAHNG NUAN	3151	Pro	Ex	Thailand	Thai local
79	SEW MAE JAN	3116	Pro	Ex	Thailand	Improved
80	SEW MAE JAN	4001	Pro	Ex	Thailand	Improved
81	PATHUM THANI 1	23898	Pro	Ex	Thailand	BKNA6-18-3-2 / PTT85061-86-3-2-1
82	SANG YOD	15101	Pro	Ex	Thailand	Thai local
83	GWIAN HAK	9064	Pro	Ex	Thailand	Thai local
84	KHAO TAH HAENG 17	828	Pro	Ex	Thailand	Thai local
85	GOW RUANG 88	1193	Pro	Ex	Thailand	Thai local
86	NAHNG MON S-4	1204	Pro	Ex	Thailand	Thai local
87	PIN GAEW 56	1581	-	Ex	Thailand	Thai local
88	HAHNG YI 71	1707	-	Ex	Thailand	Thai local
89	KHAI MOD RIN	1961	-	Ex	Thailand	Thai local
90	BUA NOI	1990	-	Ex	Thailand	Thai local

No.	Name	GS No.	Seq		Location	Parental Lines / parental relations
91	AEW MOD DAENG	10049	-	Ex	Thailand	Thai local
92	NAHNG NGAHM	2066	-	Ex	Thailand	Thai local
93	U-TA POW	2067	-	Ex	Thailand	Thai local
94	PUANG WAHN	2069	-	Ex	Thailand	Thai local
95	PUANG HAHNG MOO	2089	-	Ex	Thailand	Thai local
96	JEK CHUEY	2387	-	Ex	Thailand	Thai local
97	KHAO GAW DIAW	2534	-	Ex	Thailand	Thai local
98	RD9	2601	-	Ex	Thailand	LUANG YAI 34 / TN1 // W1256 /// RD2
99	PUANG NGERN	2963	-	Ex	Thailand	Thai local
100	NAM SAGUI 19	3023	-	Ex	Thailand	Thai local
101	LAM YAI	3028	-	Ex	Thailand	Thai local
102	BUN MAH	3031	-	Ex	Thailand	Thai local
103	RD8	3091	-	Ex	Thailand	IR262/2* NIAW SAN PATONG
104	RD13	3093	-	Ex	Thailand	NAHG PA-YAH 132 / PAK-SIAN(BKN6402-352)
105	JAO DAM	3230	-	Ex	Thailand	Thai local
106	JAO DAENG	3256	-	Ex	Thailand	Thai local
107	DAM DAHNG	3271	Pro	Ex	Thailand	Thai local
108	JAO DAWK KHAO	3285	Pro	Ex	Thailand	Thai local
109	LEUANG TAWNG	3318	Pro	Ex	Thailand	Thai local
110	GAM LIAW	3321	Pro	Ex	Thailand	Thai local
111	TOON CHALAWNG	3637	Pro	Ex	Thailand	Thai local
112	NAHNG MON	3638	Pro	Ex	Thailand	Thai local
113	KHAO PRAGUAD	3677	Pro	Ex	Thailand	Thai local
114	KHAO SAMER	3770	Pro	Ex	Thailand	Thai local
115	KHAO TAH JEUA	3808	Pro	Ex	Thailand	Thai local
116	KHAO TAENG MO	3810	Pro	Ex	Thailand	Thai local
117	LEB NOK	3979	Pro	Ex	Thailand	Thai local
118	RD19	4000	Pro	Ex	Thailand	IR262 / PIN GAEW 56 (BKN6986-147-2)
119	RD17	3999	Pro	Ex	Thailand	IR262 / PIN GAEW 56 (BKN6986-66-2)
120	GAM FEUANG	4490	Pro	Ex	Thailand	Thai local

No.	Name	GS No.	Seq		Location	Parental Lines / parental relations
121	RD10	4790	Pro	Ex	Thailand	Fast neutron mutation (RD1'69-NF1U-G6-6)
122	RD21	4791	Pro	Ex	Thailand	KDML105 / NAHNG MON S4 // IR 26(SPR7419-86-2-5)
123	RD25	4793	Pro	Ex	Thailand	KDML105 / IR2061-213-2-3-3 // KDML105 / IR26 (BKNLR75091-CNT-B- RST-40-2-2)
124	JAMPAH TAWNG	5211	Pro	Ex	Thailand	Thai local
125	KHAO LUANG	5533	Pro	Ex	Thailand	Thai local
126	TAH JEUA	5545	Pro	Ex	Thailand	Thai local
127	LEUANG KWAI LAH	5551	Pro	Ex	Thailand	Thai local
128	SETTI	5678	Pro	Ex	Thailand	Thai local
129	KAN NAH	6442	Pro	Ex	Thailand	Thai local
130	LEUANG TIA	6448	Pro	Ex	Thailand	Thai local
131	LEUANG GAEW	6812	Pro	Ex	Thailand	Thai local
132	LAI MAHK	7025	Pro	Ex	Thailand	Thai local
133	RD27	7125	Pro	Ex	Thailand	KHAO TAH-OO / KHAO TAH HAENG 17
134	LEUANG KWAI LAH	7285	Pro	Ex	Thailand	Thai local
135	SAHM RUANG	7288	Pro	Ex	Thailand	Thai local
136	LEUANG PLAH GIM	7293	Pro	Ex	Thailand	Thai local
137	LEUANG HUAN	7303	Pro	Ex	Thailand	Thai local
138	GWIAN HAK	13201	Pro	Ex	Thailand	Thai local
139	GWIAN HAK	9064	Pro	Ex	Thailand	Thai local
140	KHAO PUANG	9362	Pro	Ex	Thailand	Thai local
141	CHAW PLI KHAO	9742	Pro	Ex	Thailand	Thai local
142	PUANG NAHK	12266	Pro	Ex	Thailand	Thai local
143	KHAO TAH CHEUA	12270	Pro	Ex	Thailand	Thai local
144	LEUANG BAI LOD	14154	Pro	Ex	Thailand	Thai local
145	LEUANG BAI JAEK	14155	Pro	Ex	Thailand	Thai local
146	NAM SAGUI 19	15833	Pro	Ex	Thailand	Thai local
147	HANTRA 60	16232	Pro	Ex	Thailand	Thai local
148	CHUMPAE 60	16235	Pro	Ex	Thailand	Thai local
149	PATHUM THANI 60	17770	Pro	Ex	Thailand	Thai local
150	CHAI NAT 1	20712	Pro	Ex	Thailand	Thai local

No.	Name	GS No.	Seq		Location	Parental Lines / parental relations
151	NIAW DAM LAI	21240	Pro	Ex	Thailand	Thai local
152	PAWNG AEW	21577	Pro	Ex	Thailand	Thai local
153	LAO TAEK	21593	Pro	Ex	Thailand	Thai local
154	LOOK DAENG PATTANI	21963	Pro	Ex	Thailand	Thai local
155	CHIANG PHATTHALUNG	21964	Pro	Ex	Thailand	Thai local
156	SOON	22492	Pro	Ex	Thailand	Thai local
157	GAEN JAN	22653	Pro	Ex	Thailand	Thai local
158	LOOK DAENG PATTANI	23303	Pro	Ex	Thailand	Thai local
159	NIAW PRAE 1	23405	Pro	Ex	Thailand	Thai local
160	PRACHIN BURI 1	23406	Pro	Ex	Thailand	Thai local
161	RD31	24533	Pro	Ex	Thailand	SPR85163-5-1-1-2 / IR54017-131-1-3-2 (SPR93049-PTT-30-4-1-2)
162	KHAO DAWK MALI 105	-	Pro	Ex	Thailand	Improved
163	CSSL11	-	Pro	Ex	Thailand	Derived from KDML105
164	UBN	-	Pro	Ex	Thailand	
165	POKKALI	-	Pro	Ex	India	Indian local
166	DAW KHAO	12155	-	Ex	Thailand	Thai local
167	KHAO READ	21772	-	Ex	Thailand	Thai local
168	PAWNG AEW	21776	-	Ex	Thailand	Thai local
169	LEUANG PRATEW123	869	-	Ex	Thailand	Thai local
170	LEUANG PRATEW 123-TC171	-	Pro	Ex	Thailand	Somaclonal variegation of LEUANGPRATEW123 callus
171	IR29	-	-	Ex	IRRI	R833-6-2-1-1 / IR1561-149-1 // IR24*4 /O.Nivara
172	LUANG PRATAHN	6440	Pro	Ex	Thailand	Thai local

2. Methods

2.1 Development of rapid inorganic phosphorus quantification

2.1.1 Plant cultivation

Thai rice (*Oryza sativa* L.), including LEUANG CHUMPAE (high Pi accumulator) and NAH KWAN (low Pi accumulator) **(Table B2)**, were used to evaluate the method for inorganic phosphorus quantification. Seeds were surface sterilized with 30% commercial bleach (Clorox, containing 6% sodium hypochlorite) for ten minutes and then washed with distilled water three times. Next, the seeds were soaked in distilled water for two days to initiate seed germination. The initiated seeds were continuously floated on a plastic net in half-strength Yoshida solution (Yoshida et al., 1976) for six days. Then, the seed endosperm was cut from the seedlings to remove the phosphorus storage resource, and then the seedlings were transferred to a full-strength Yoshida solution containing different P concentrations, 320, 160, 80, 16, and 0.8 µM NaH_2PO_4, for 16 days. An equal concentration of NaCl was applied to compensate for the decrease of NaH_2PO_4 in the treatments. The nutrient solution was renewed every four days and adjusted pH at 5.8 daily. The experiments were performed in a greenhouse with the natural environment (30-38°C day/26-30°C night temperature; 40-70 % day/70-90% night humidity; 11 h photoperiod of natural light (400-1,900 µmol m^{-2} s^{-1}) using completely randomized design (CRD) with 24 replications.

2.1.2 Conventional extraction method

Leaf tissue was weighed to about 50 mg and grounded using liquid nitrogen. The powder was mixed with 100 µl of 10% (w/v) perchloric acid. Then the homogenate was diluted ten times with 5% (w/v) perchloric acid and incubated on ice for 30 min. The sample was centrifuged at 10,000x g for 10 min at 4 °C (Nanamori *et al.*, 2004). The supernatant was collected and used for the next Pi measurement step.

2.1.3 Pi measurement

The supernatant was added with 160 µl Molybdate Blue reagent, which contained 0.4% (w/v) ammonium molybdate in 0.5 M H_2SO_4 (A solution) with 10% ascorbic acid (B Solution) (A: B = 6:1) and then incubated at 40 °C for 20 min. The absorbance was detected at 820 nm wavelength *via* microplate reader. The Pi content was analyzed by comparing with the standard curve (**Figure D1**) and calculated as nmol per leaf disc area (mm^2) or µmol per gram fresh weight.

2.1.4 Method development

2.1.4.1 Optimization of incubation time

Twenty leaf discs collected from the seedlings grown under 320 or 16 µM NaH_2PO_4 treatment of high and low Pi accumulator, respectively, were separated into five groups (four discs per group) and kept at -80 °C until use. One group was used for the conventional extraction method. The others were used for incubation time optimization. Four discs were put in a 96-well plate, and then, 200 µl of 5.5 % (w/v) perchloric acid was added to each well and incubated on ice for 1, 2, 3, or 4 hours. Then, supernatants were transferred into a new 96-well plate and diluted with 5.5 % (w/v) perchloric acid up to 80 µl of the final volume. The diluted supernatants were used for Pi measurement according to the method in 2.1.3. Suitable incubation time was applied to quantify Pi for the next step. The experiment was performed with ten biological replicates.

2.1.4.2 Validation of the punching quantification method

The validation of the method was performed using the leaf tissues from seedlings of the high (LEUANG CHUMPAE) and low Pi accumulator (NAH KHWAN), grown in the nutrient solution supplemented with different levels of NaH_2PO_4 (320, 160, 80, 16, and 0.8 µM), which resulted in varying levels of Pi contents. For measurement, second fully expanded leaves of 24 day-old seedlings were folded in half twice, put over glossy paper, and punched together to cut the leaves into equal size using paper puncher (3 mm diameter) and put the discs into a 96-well plate.

Four-leaf discs were collected for the newly developed method (punching method), and the residual leaf section was collected for the conventional measurement method, as described in 2.1.2. The tissues were stored at -80 °C. Then, the 96-well plate containing four leaf discs in each well was added with 200 µl of 5.5 % (w/v) perchloric acid and incubated on ice with the appropriate period time as identified in 2.1.4.1. The supernatants were transferred into a new 96-well plate using a multichannel pipette and diluted with 5.5 % (w/v) perchloric acid up to 80 µl of the final volume **(Figure 12)**. The diluted supernatants were used for Pi measurement in 2.1.3. Pi concentration derived from the conventional extraction method and the punching method were calculated. Pearson's correlation was performed to validate Pi content measured by the punching and conventional methods. The experiment was performed with 24 biological replicates.
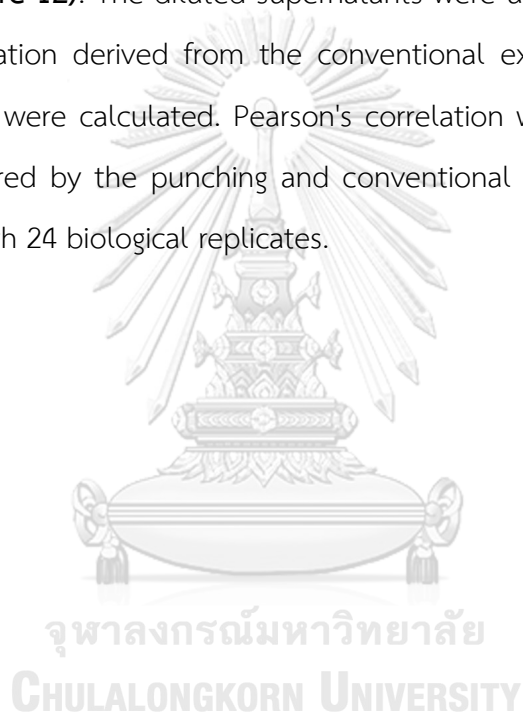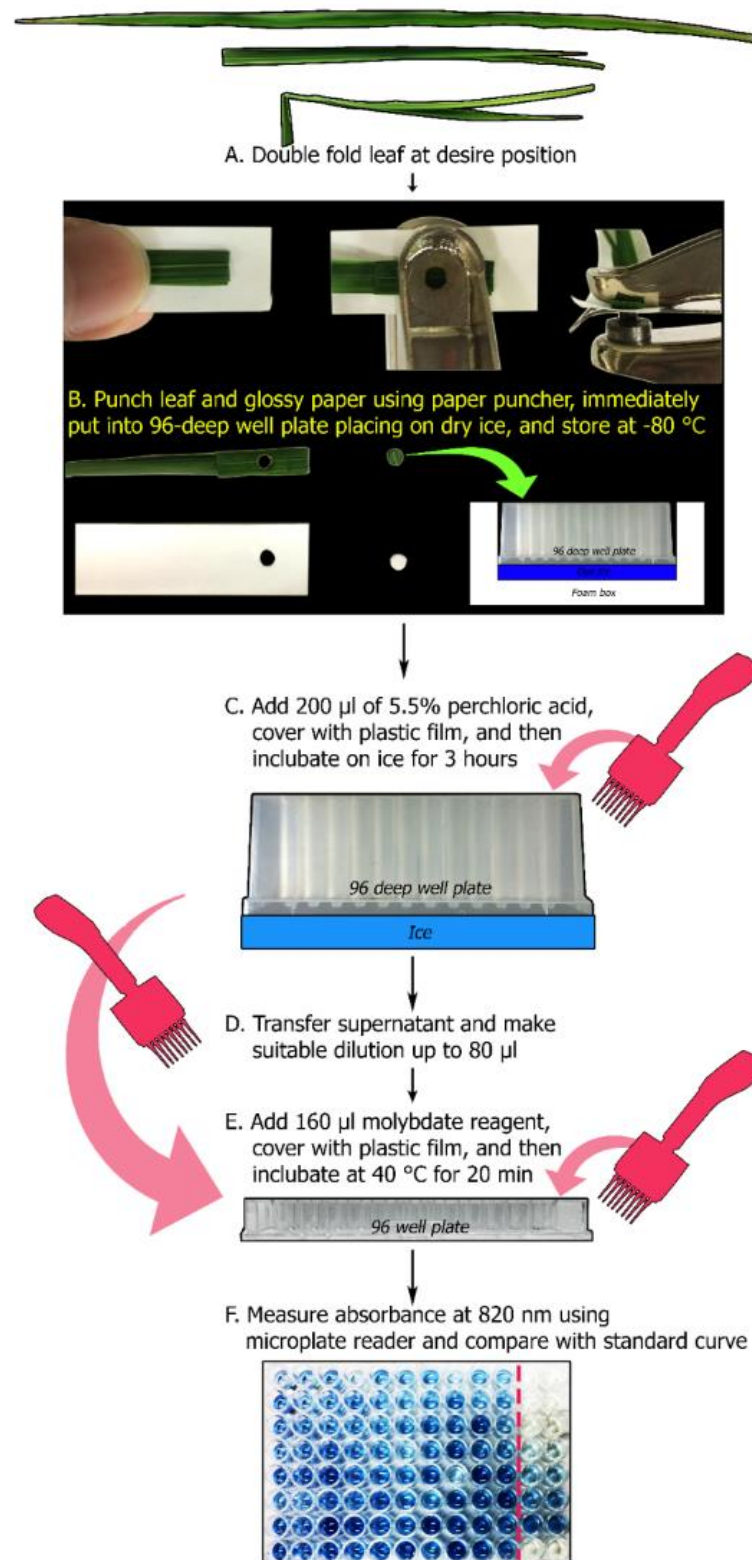
Figure 12 Steps of high-throughput punching method, Pi extraction, and measurement. The leaf was folded in half twice for providing fast tissue harvesting,

then put on glossy paper (A). Both leaf and paper were punched together to produce four-leaf discs at once. The glossy paper functioned as supporting soft leaves and avoiding leaf discs from sticking in the punching hole. Then the leaf discs were suddenly put into a 96-deep well plate, which was placed on dry ice to prevent hydrolysis of organic P. The plates with leaf samples were covered with aluminum foil and then kept at -80 °C until use (B). For extracting Pi content from leaf tissue, 200 µl of 5.5 % (w/v) perchloric acid was added into each well of 96-deep well plate by using a multichannel pipette. The samples were submerged and incubated for 3 hours (C). The supernatant was then transferred to a new 96-well plate and diluted to suitable dilution with 5.5 % (w/v) perchloric acid up to 80 µl of the final volume (D). For quantifying Pi content, 160 µl of Molybdate Blue reagent was added and then incubated at 40 °C for 20 min (E). The absorbance was detected at 820 nm wavelength using a microplate reader. Pi content was compared with the P standard curve and analyzed with a leaf disc area (7.07 mm^2) as $nmol/mm^2$ (F).

2.1.4.3 Pi content detection in different leaf stages and positions

The first, second, third, and fourth fully expanded leaves of 24 day-old plants grown under 320 and 16 µM NaH_2PO_4 treatments of high Pi accumulator were cut into four sections equally. The leaf disc samples from each section were extracted and detected Pi content using the punching method. The experiment was performed with 12 biological replicates.

2.1.4.4 Statistical analysis

Analysis of variance (ANOVA) was performed, and the mean was compared with Duncan's Multiple Range Test (DMRT) by using IBM SPSS Statistics v. 22.

2.2 Phenotyping of local Thai rice cultivars under phosphorus deficiency at seedling stage

2.2.1 Plant culture and treatment

Seeds of 172 Thai rice (*Oryza sativa* L.) accessions, including local Thai rice varieties and breeding cultivars, were provided by the Pathum Thani Rice Research Center **(Table 4)**. The seeds were surface sterilized and pre-cultured, as described in 2.1.1. Then, eight-day old seedlings without endosperm were transferred to 80-litter boxes containing full-strength Yoshida solution with different P supplements, including 320 (sufficient; S), 16 (mildly deficient; MD), and 0.8 µM NaH_2PO_4 (severely deficient; SD) for 16 days. The decrease of NaH_2PO_4 was replaced with an equal concentration of NaCl. The nutrient solution was renewed every four days and adjusted pH at 5.8 every two days **(Appendix E)**. Each growth container contained all rice cultivars for equally nutrient acquired competition. The experiment was performed in a greenhouse with natural light (30-38°C day/26-30°C night temperature; 40-70 % day/70-90% night humidity; 11 h photoperiod of natural light (400-1,700 µmol m^{-2} s^{-1}) using the Randomized Complete Block design (RCBD) with three replicates. Each replicate contains three plants /cultivar.

2.2.2 Reflectance spectra measurement

After 16 days of treatments, the second fully expanded leaves were used for reflectance spectra measurement with non-imaging spectro-reflectometers, PolyPen RP 400 (UV-VIS) **(Table C1)**. The device was calibrated with a white reference standard before use. Leaf adaxial was faced on the PolyPen's detector head to measure the reflectance from two points at the center of each leaf as the technical replicates. The hyperspectral reflectance of 320 – 790 nm wavelength was determined and exported from the device for future analysis as transmittance, computed using the formula below.

$$R_I = Transmittance_I = T_I = I/I_0$$

Where: I_0 is reference light intensity; I is measured light intensity

The same leaf sample was then cut as leaf discs using a paper puncher to be quantified Pi content using the punching method in **2.1.4.2.** Distribution and frequency plot of Pi content in each treatment were illustrated using Seaborn package v. 0.9.0 (Waskom *et al.,* 2014).

2.3 Analysis of spectral reflectance index in Thai rice under phosphorus deficiency and genome-wide association study (GWAS)

2.3.1 Spectral reflectance index analysis

2.3.1.1 Reflectance average and sensitivity

An average of reflectance was calculated and plotted against different spectral wavelength (nm) to distinguish the data characteristics of each treatment. The reflectance sensitivity on phosphorus deficiency was calculated as a percentage ratio between deficiency and sufficiency treatment as below.

$$\text{Reflectance sensitivity} = [(R_l \text{ of P deficient treatment} - R_l \text{ of the control})/ R_l \text{ of the control} \times 100\%]$$

Whereas R_l = received transmittance value at the wavelength of 380, 382, 384,..., 790 nm (Zhao *et al.,* 2005).

The average and sensitivity plots were illustrated by using Seaborn package v. 0.9.0 (Waskom *et al.,* 2014).

2.3.1.2 Test of general spectral indices and the way for improvement

The collected reflectance data were calculated to generate 24 general vegetative indices, as described in **Table C2**. The computed data of the 24 general vegetative indices was tested and observed their property by performing the principal component analysis (PCA), hierarchical clustering analysis, and density plot. The PCA analysis and illustration were performed using Factoextra R package v.1.0.7 (Kassambara and Mundt, 2017). The hierarchical clustering was analyzed and visualized to observe the indices relationship by using Dendextend package v.1.0.1

(Galili, 2015). A density plot was visualized to investigate the deficiency effect in each different treatment by using Caret package v.6.0 (Kuhn, 2012).

I then calculated the mean normalized value of the indices by dividing between SD and S conditions. The mean normalized values of the 24 indices traits were associated with 113,114 SNPs from exome sequences of 172 rice accessions (Lekklar et al., 2019) using GEMMA software as fully described in **2.3.2.** The observation results were used to apply in the next step.

2.3.1.3 Spectral reflectance analysis and new developing indices

Correlation between each wavelength was calculated to observe self-correlation within the reflectance value by using a Spearman correlation model (SciPy package v.1.3.2) on Python (v.3.8.0). The new spectral reflectance indices were then established by the ratio of reflectance at two different wavelengths using NumPy package v. 1.17.4 (Harris *et al.,* 2020).

New spectral reflectance indices (NSR) = $R\lambda_i / R\lambda_i$

Correlation between NSR indices and Pi content was performed using a Spearman correlation model in SciPy package v.1.3.2 (Virtanen *et al.,* 2020). All analyses and illustrations were plotted using Seaborn package v. 0.9.0 (Waskom *et al.,* 2014).

For providing the P deficient phenotype of NSR indices, the ratio between deficiency and sufficiency was calculated as relatively new spectral reflectance indices (RNSR). From the sensitivity result, the RNSR indices of the severely deficient level were selected for GWAS in the next step due to the significant response to P deficiency. In GWAS analysis, the mean data of RNSR indices were used every 10 nm of among reflectance spectrum range to reduce the amount of data in the analysis process.

2.3.2 Association analysis for phosphorus-deficiency responsive traits

The phenotypic data, including Pi content and 217 RNSR traits, were associated using linear mixed model via GEMMA software (Zhou and Stephens, 2012) with 113,114 single nucleotide polymorphisms (SNPs) derived from exome sequences (Lekklar *et al.*, 2019). Manhattan plots and QQ-plots were performed using qqman package v.0.1.4 (Turner, 2014). The visualization of significant SNPs against several spectral indices was illustrated using Seaborn package v. 0.9.0) (Waskom *et al.*, 2014).

2.3.3 Identification of phosphorus-deficiency tolerance genes

Significant SNPs were considered using Bonferroni correction with an experimental type I error rate of a = 0.05, equivalent to a significant threshold -log (p-value) ≥ 6.35. Moreover, the SNP was also identified as significant if its location is within 100kb (upstream and downstream) of a Bonferroni's significant SNP.

CHAPTER IV

RESULTS

1. Development of a rapid inorganic phosphorus quantification

1.1 Optimization of incubation time

For developing a novel Pi quantification protocol, the conventional grinding method was considered three main problems; sample weighing, numerous pipetting, and grinding, which affected fastness and easiness in analysis. Thus, an alternative normalization by using leaf areas instead of leaf weight was proposed in this study. Paper puncher was applied to generate the equal-size leaf discs from each sample, which was used to normalize initial tissue used in the quantification. Moreover, a microplate reader and multi-channel pipettes were used to decrease time and material consumption. The grinding step was removed and replaced with the freeze-shattering technique to permeabilize the plant cell wall and release Pi out of the cell without grinding, and then immerse in extraction buffer.

For finding optimal incubation time for Pi extraction, homogeneously mixed leaf discs from high and low accumulator rice grown under P sufficient (320 μM P) or deficient (16 μM P) condition were kept at - 80 °C and incubated in 5.5% perchloric acid for various period times, 1, 2, 3, and 4 hours. The same mixed leaf discs were also extracted *via* the conventional extraction method. The supernatant was quantified using a molybdate blue reaction. The result showed that 3 hours of incubation indicated the comparable result of Pi extracted content as same as the conventional extraction method in both high and low Pi accumulation rice cultivars, and both P sufficiency and deficiency. Moreover, incubation time less than 3 hours is not enough to release all Pi from leaf tissue. Additionally, prolonged incubation of more than 3 hours led to increased Pi contents likely by hydrolysis of organic P **(Figure 13)**.
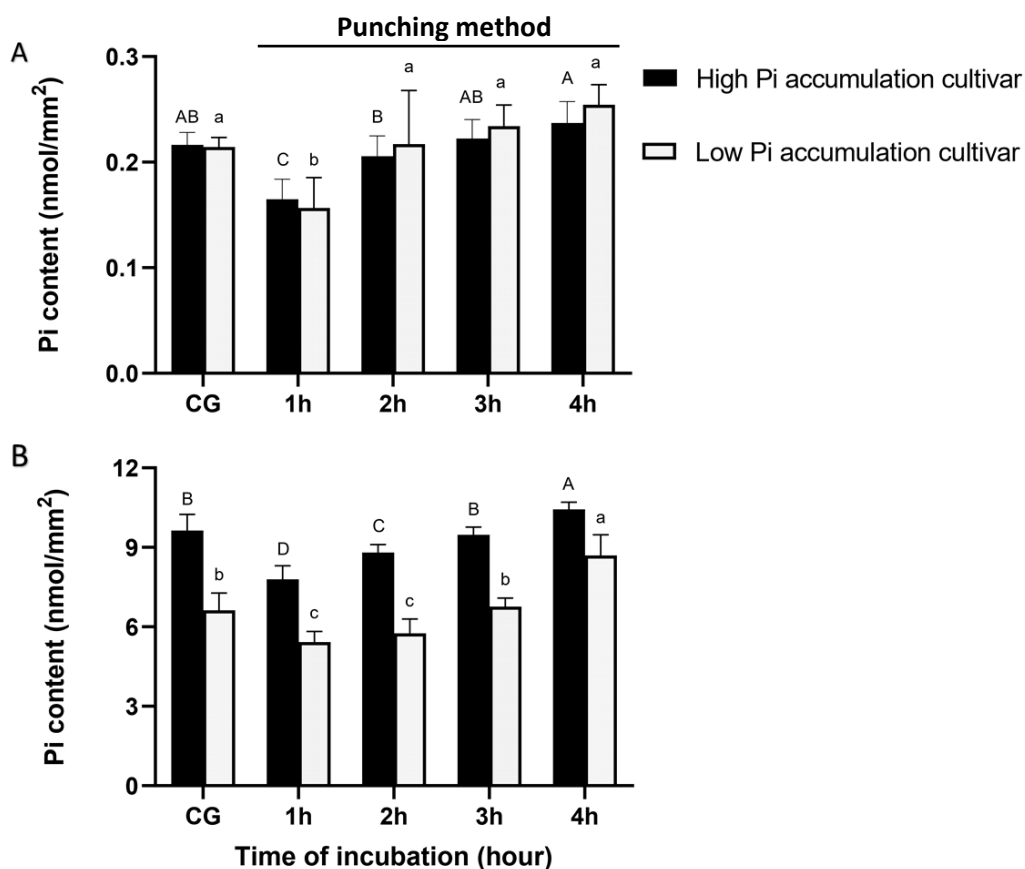
Figure 13 Effect of incubation time on soluble phosphate extraction via punching method comparing with the conventional grinding (CG) method in high and low Pi accumulators under phosphorus-deficient (A) and sufficient (B) conditions. Data are means ± SD (n = 10). Different letters indicate significant differences (P < 0.05), according to Duncan's multiple range test (DMRT).

1.2 Validation of the punching quantification method

To validate the punching method, Pi content quantification via punching method was performed using leaf discs from second fully expanded leaves in low and high Pi accumulator under various five different levels of P supplement, and Pi content via conventional method was quantified by using residue tissues of the same leaves. The Pi content of the punching method and the conventional grinding method were normalized and calculated as $nmol/mm^2$ (leaf disc area) and $\mu mol/g$ FW (leaf fresh weight), respectively. For comparing the result in the comparable unit,

Pi content from the punching method was converted from nmol/mm^2 to μmol/g FW unit by using the average fresh weight of a leaf disc **(Table B1)**.
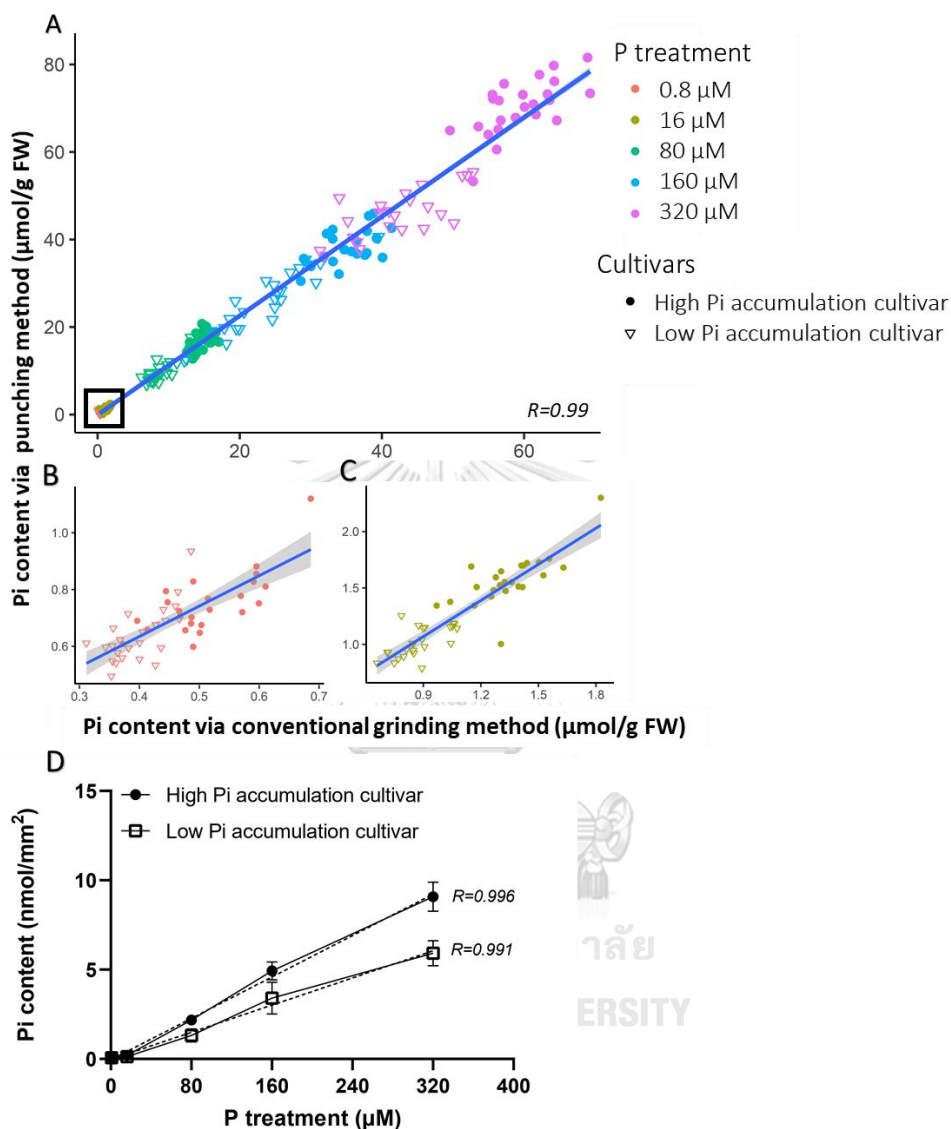
Figure 14 Pi contents of high and low Pi accumulation cultivars grown under different P supply (320, 160, 80, 16, and 0.8 μM P). Linear regression plots of Pi contents determined by punching method (y-axis, μmol/g FW) and conventional grinding method (x-axis, μmol /g FW) (A-C). Data points of plants grown under different levels of P supply (320, 160, 80, 16 and 0.8 μM P) (A), inset shown for 0.8 μM P (B) and 16 μM P (C). Graph showing the average of Pi contents was determined by punching method and fitted by linear regression (D). Data are means ± SD (n =

24). Correlation (r) is determined by Pearson's correlation model. Statistical analyzes were performed with IBM SPSS Statistics ver. 22 and R program.

Comparing the two methods showed comparable Pi content with a high correlation of linear regression ($r=0.99$; when considered with all P supplement level) **(Figure 14A)**. Furthermore, correlations (*r*) of 320, 160, 80, 16 and 0.8 µM P treatment were 0.92, 0.92, 0.92, 0.90 and 0.78, respectively **(Figure 14A-C)**. The result indicated that the punching method yielded similar and reproducible results with the conventional grinding method in various P treatments. However, low level of P supplement of 0.8 µM P showed reduced correlation, which might be an effect from limited Pi in analyzed leaf tissue, as the plants displayed chlorosis symptom and stunted growth. To avoid this limitation, increasing leaf discs could be applied to increase Pi in the analysis, and the number of leaf discs could be used to normalize the Pi content. I also tested the linearity of the extraction by increasing the leaf disc number. High correlation between number of leaf discs and Pi content detected ($r=0.99$) suggested that the multiplication of leaf disc in the extraction did not affect the quantification **(Figure 15)**. In addition, a comparable result ($r=0.97$) of the punching method with the inductively coupled plasma (ICP) quantification was tested to confirm the sensitivity of the novel method **(Figure B1)**.

The accumulated Pi content in plant tissues was directly related to P concentration in the media solution **(Figure 14D)**. By using the punching method, Pi content of the second fully expanded leaves was directed variation with Pi supplement level. Both high and low Pi accumulators showed a high correlation (*r*) with 0.996 and 0.991, respectively. The result presented that when P in the nutrient solution was increased, the plant also raised its accumulation and stored in their leaves. Moreover, high Pi accumulation cultivar showed higher accumulation ability than low Pi accumulation cultivar at all treatments tested.
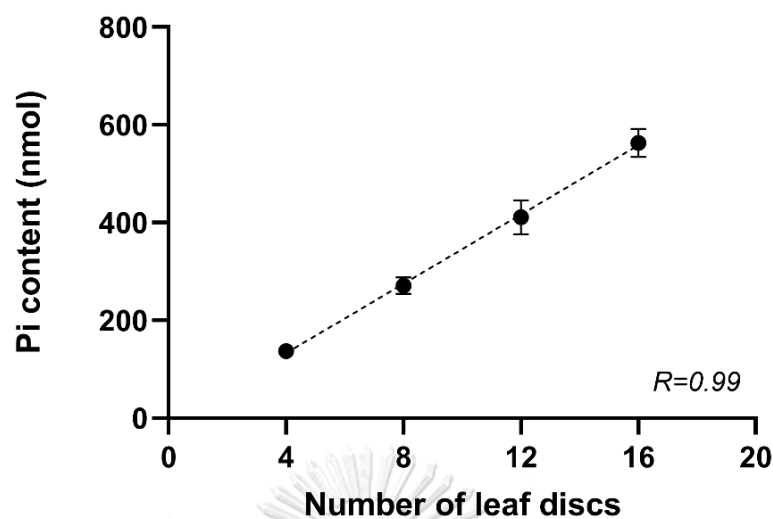
Figure 15 Linearity of the punching method. Graph showing Pi contents (nmol) determined from extracts with varying leaf disc numbers (4, 8, 12, 16 discs) and fitted by linear regression. Correlation (r) is determined by Pearson's correlation model using R software. Each sample was divided from the same pool of leaf discs derived from P-sufficient plants. Data are means ± SD (n = 8).

1.3 Pi content detection in different leaf stages and positions

One of the advantages of the punching method is that the quantification process only needs a small area of leaf tissue that I can apply in any narrow and specific rice leaf position. I tested four different positions, along with leaf length from leaf base to leaf tip, and four different leaf stages applied the punching method to quantify Pi content in different leaf positions and leaf numbers under both P sufficient and deficient conditions **(Figure 16)**. The testing indicated that Pi content was accumulated at the leaf tip lower than the leaf base under P sufficient condition (320 µM). Moreover, the older leaf stage (fourth fully expanded leaf) was found as a higher storage location than the younger leaves. The distribution of Pi content in each leaf position and stage illustrated the gradient concentration of Pi accumulation in the leaf. On the other hand, when P starvation occurred (16 µM), no significant difference in Pi content among leaf positions was found. However, Pi content in

various leaf stages still showed significant variation, but in the different accumulation patterns. Pi content in the youngest leaves (first fully expanded leaf) was more detectable than older leaf stages, caused by a remobilized and re-translocated property that helps the plant transfer limited P content from older leaves to the younger leaves.
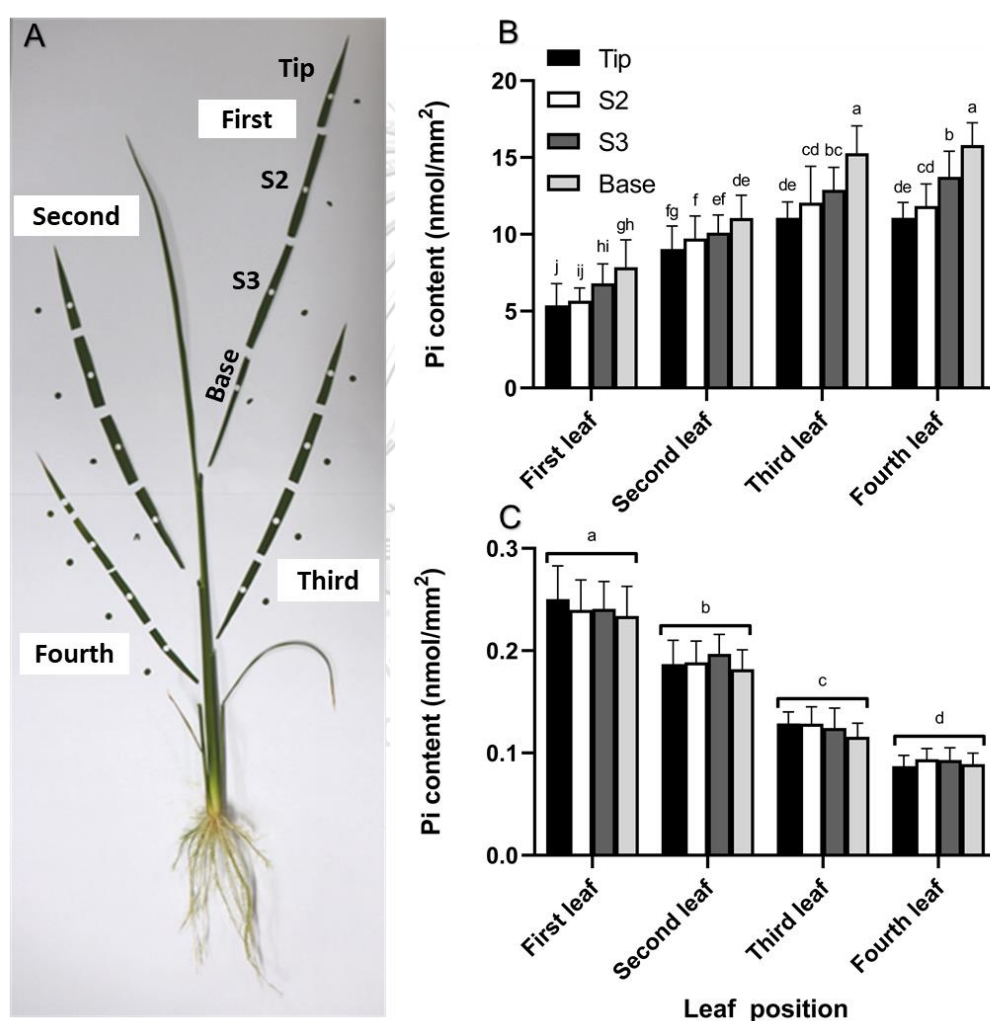
Figure 16 Effect of leaf stages and positions of high Pi accumulation cultivar. (A) Rice leaves were punched at different positions. (B-C) Pi contents of rice grown under phosphorus sufficiency (B) and deficiency (C). Data are means ± SD (n = 12). Different letters indicate significant differences ($P < 0.05$), according to Duncan's multiple range test (DMRT). Statistical analyses were performed with IBM SPSS Statistics ver. 22.

2. Phenotyping of local Thai rice cultivars under phosphorus deficiency at seedling stage

2.1 Phenotyping of rice using Pi quantification and hyperspectral detection

To test for phenotypic variations in the rice population and interaction of destructive and non-destructive measurements of Pi deficiency responses, I determined Pi contents and spectral reflectance in the second fully expanded leaves of 172 rice accessions grown under sufficient (S, 320 µM P), mildly deficient (MD, 16 µM P) and severely deficient (SD, 0.8 µM P) P conditions **(Figure 17)**.
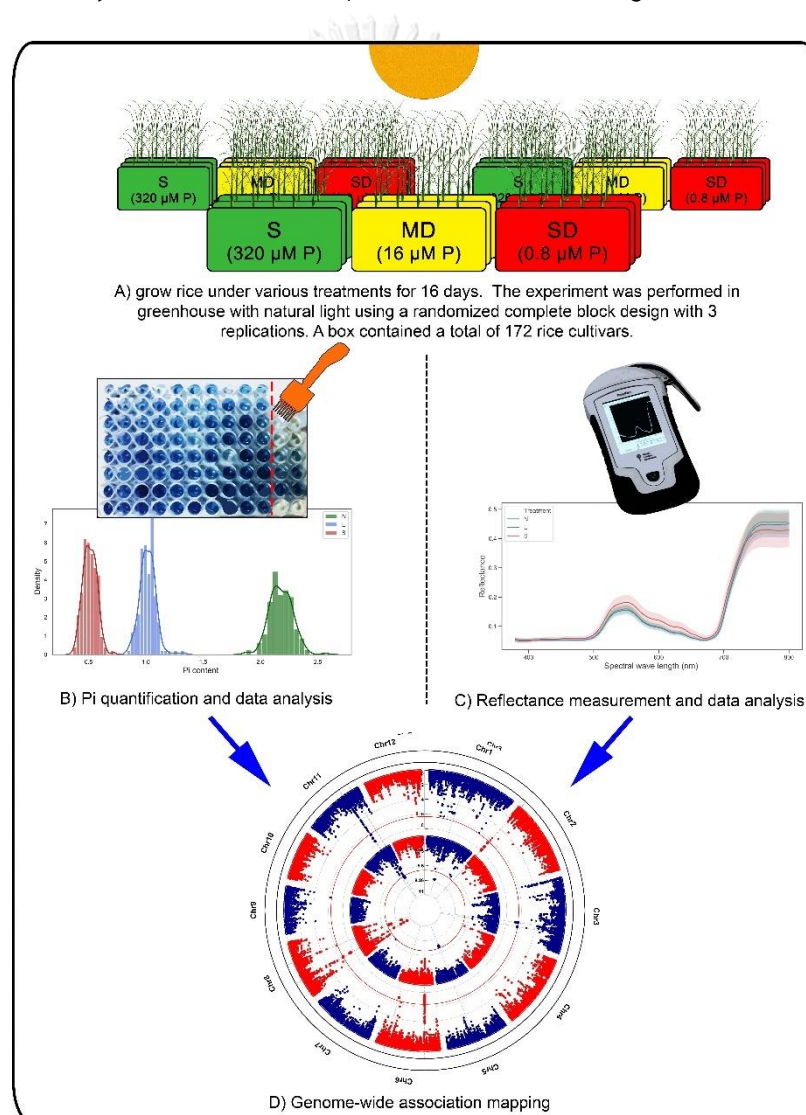
Figure 17 Experimental outline of the GWAS experiment.

In the quantification of Pi content, the leaf tissues were extracted and quantified *via* the punching method to obtain P deficient effect in each different Pi supplement level. The data of Pi contents in various cultivars are shown in **Table B2**. Pi content density and frequency distribution plot against the different concentrations showed a significant decrease of Pi content in various P treatments **(Figure 18A)**. The frequency distribution showed quantitative and continuous information. The general trends of the Pi content parameter indicated the normal distribution that might be affected from polygenes in the plant. Moreover, Pi contents in each P treatment were not overlapped and the Pi levels depended on the P supply. These suggested that Pi content in plant tissue was obviously affected by the deficiency level of culture solution. The result suggested that Pi content should be a useful representative parameter to identify phosphorus-deficiency status, which is confirmed by the previous report that Pi content was a sensitive parameter to determine phosphorus-deficient status and indicated plant tolerant efficiency under phosphorus-deficient stress (Misson *et al.,* 2005).
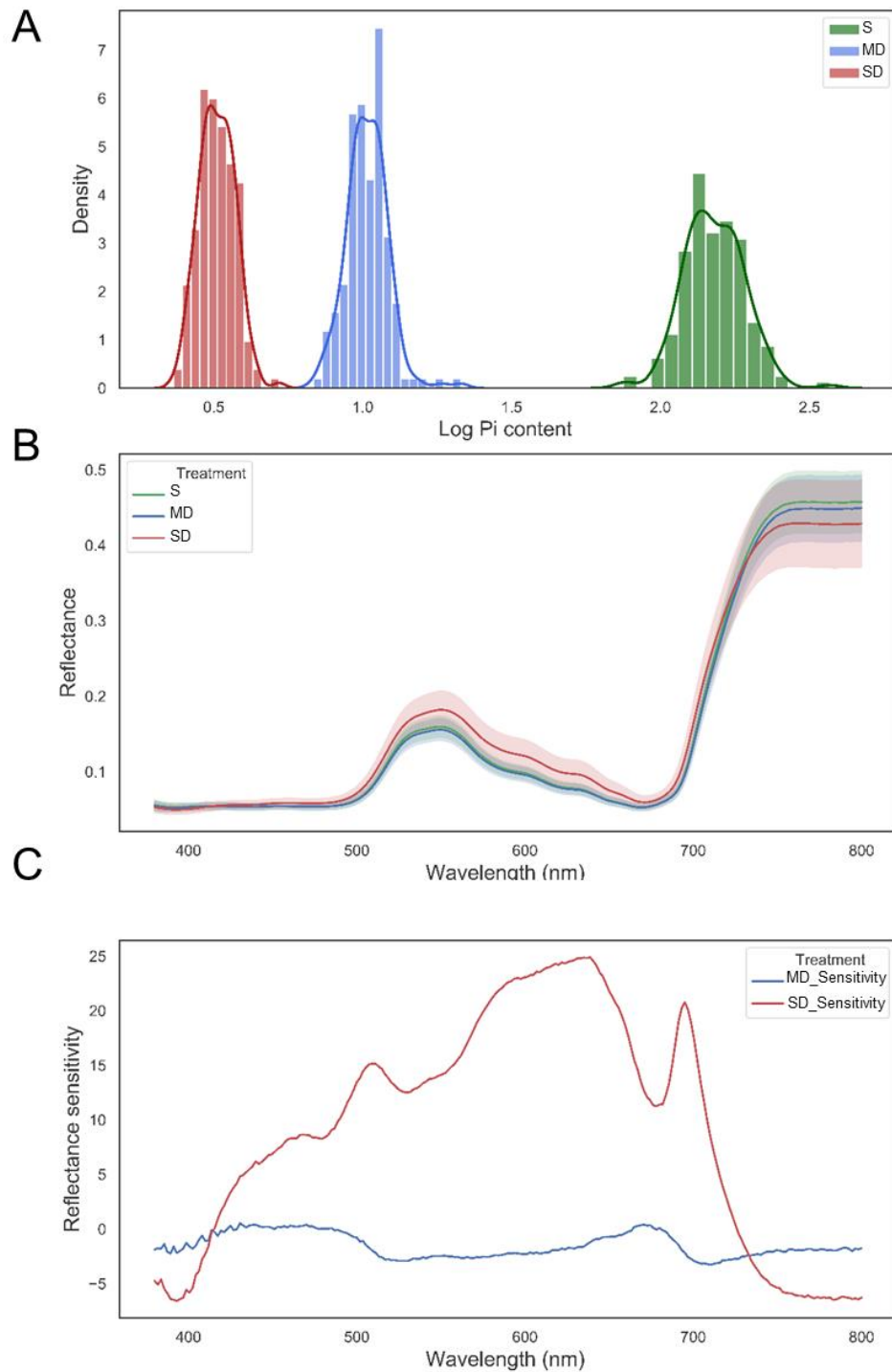
Figure 18 Frequency distribution of Pi content (A), average reflectance spectrum (B) in three different phosphorus treatments (including sufficient (S), mildly deficient (MD), severely deficient (SD)), and sensitivity index (C) of normalized MD and SD treatment with S condition.

For leaf hyperspectral reflectance parameters, the same area used in Pi content quantification was used to measure spectral reflectance along 380-790 nm of the wavelength spectrum. P deficiency affected the increase of visible reflectance spectra and decreased NIR reflectance spectra **(Figure 18B)**. Moreover, different deficiency levels influenced the different responsive effects. The MD treatment showed a less sensitive P deficiency response than SD treatment and looked similar to the S condition.

The P-deficient sensitivity was calculated to represent P response in each reflectance spectrum compared with the control (S) treatment. The result showed that SD treatment showed greater responses to P deficiency than MD treatment **(Figure 18C)**. The sensitivity plot showed three peaks within visible and red edge regions (500-700 nm), in which the most sensitive region was located at 510, 637, and 691 nm. Moreover, two negative sensitivity regions were observed after 730 nm (NIR) wavelength and at around 400 nm or blue reflectance spectrum. The responsive regions of positive and negative sensitivity were focused on their response character to P deficiency in rice.

Though the MD-treated plants had much lower Pi contents than the S-treated plants **(Figure 18B-C)**, they did not show apparent visible symptoms in leaf spectral reflectance. This result suggests that the P-deficient response phenotype in rice can be significantly detected *via* the hyperspectral approach when plants were grown under the SD condition but not the MD condition. However, leaf Pi contents quantification is a more sensitive technique to detect P deficiency response when plants were grown in mildly deficient treatment.

2.2 Analysis of spectral reflectance indices

First, different vegetative indices reported by the PolyPen spectroreflactometer were evaluated. These included 24 vegetative indices, as described in **Table C2**. To observe the performance of each index, distributions of

each of the 24 indices determined from plants grown under different P treatments were visualized by density plots. Most of the indices did not show a differential response result in MD treatment, compared to the S treatment. Some indices, including GM1, GM2, NPQI, PRI, Ctr1, Ctr2, NDVI, SR, and ZMI, showed differential responses, **(Figure 19)**. To observe similarities among the indices, a hierarchical clustering was performed. I found that most of the responsive indices were grouped due to a similar spectral data pattern **(Figure 20)**.
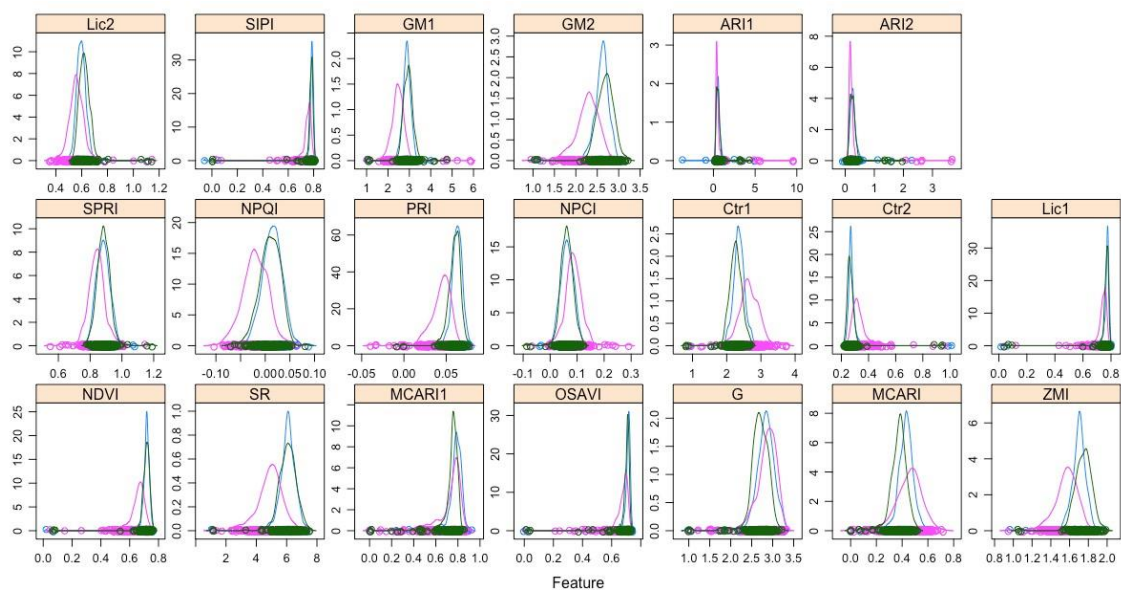
Figure 19 Density plots of 24 general vegetative indices. The color lines determine reflectance data from S (green line), MD (blue line), and SD (pink line) treatment.

Next, traits from the vegetative indices were used to perform genome-wide association studies. The mean normalized values of the 24 indices were calculated by dividing the index value of the SD treatment by that of the S treatment and used for association mapping with 113,114 SNPs from exome sequences of 172 rice accessions (Lekklar *et al.*, 2019) using GEMMA software (Zoubarev *et al.*, 2012). The association result showed that only five indices, including GM1, GM2, NDVI, SR, and ZMI, resulted in identification of significant SNPs **(Figure 20)**. Interestingly, these indices were also shown to be responsive to P deficiency, which could estimate P

response among treatments and had a close relationship of data in the hierarchical clustering **(Figure 21)**. Furthermore, these indices were calculated from ratios between NIR wavelength and VIS wavelength, suggesting that the NIR and VIS spectral ratios are relevant to plant responses to P deficiency. Thus, the NIR and VIS spectrum ratio was used to generate new spectral reflectance indices (NSR) in the next step.
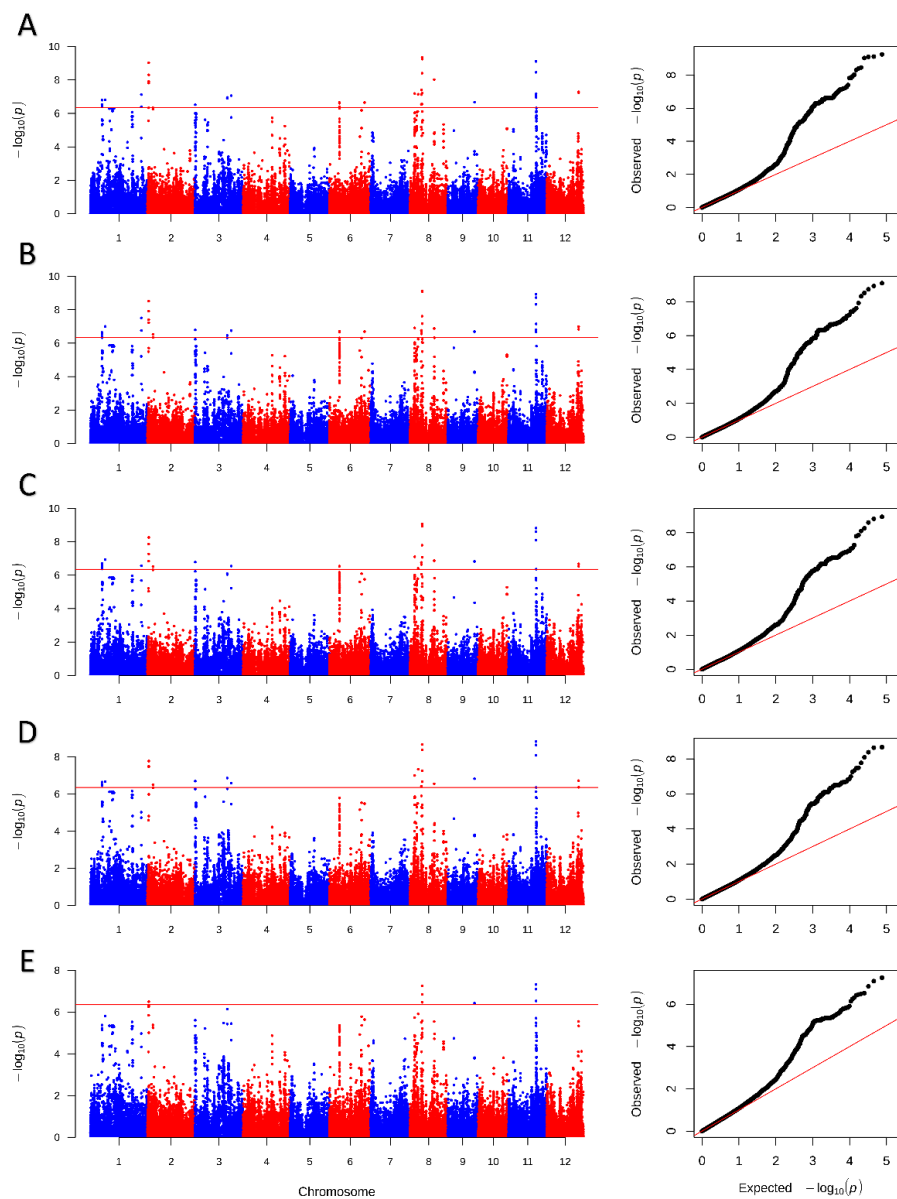
Figure 20 Comparative Manhattan and Q-Q plots on GWAS of normalized GM1 (A), normalized ZMI (B), normalized GM2 (C), normalized SR (D), and normalized NDVI (E)

with P deficient treatment. For Manhattan plots, the x-axis represents SNP positions across the entire rice genome by chromosome, and the y-axis is the -log10 p-value of each SNP. Red lines indicated the threshold line at -log(P-value) ≥ 6.35.

2.3 Hyperspectral analysis and index development

For considering relationship between spectral reflectance and Pi content, the Spearman's correlation between reflectance data at two wavelengths of each spectrum (self-correlation within spectrum) was calculated using SR data from the rice accessions grown under three different P supplements. The correlation matrix heat map displayed that the high self-correlations were found in two regions within visible and NIR zones, respectively. The high self-correlation within the big visible zone was located between spectral reflectance at wavelengths of ~420-720 nm and spectral reflectance of the other wavelengths (r^2 = 0.53-0.99), particularly between 500-650 nm (r^2 = 0.61-0.99) (**Figure 22A**, only data points at every 10 nm were shown). Another small NIR zone with high self-correlation was illustrated between spectral reflectance at wavelengths within ~730-780 nm and spectral reflectance at the other wavelengths (r^2 = 0.91-0.99). But interestingly, spectral reflectance at wavelengths in the NIR range (~730-780 nm) showed a low correlation (r^2 = 0.05-0.54) with spectral reflectance of the other wavelengths in the visible spectrum.

Although spectral reflectance at the range of 380-410 nm also showed low correlation with any wavelength measured (380-790 nm), they still had those of the adjacent wavelengths (e.g., within 10 nm). This implies that the reflectances at the 380-410 nm wavelength is noisy and might not suit for application in this investigation. Thus, they were not considered in this analysis.
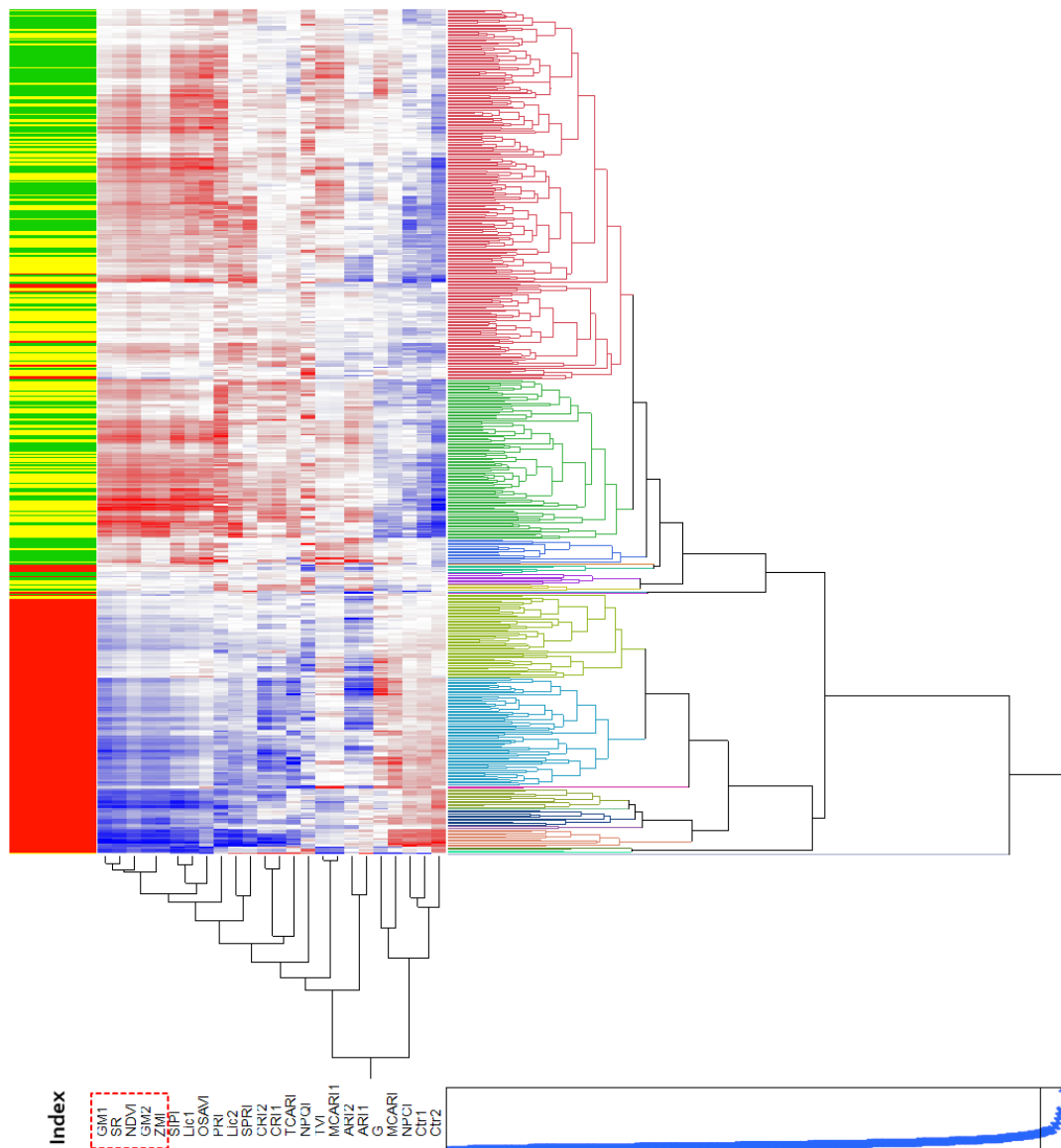
Figure 21 Cluster heat map of 24 different vegetative indices. The hierarchical clustering was performed using values of all 24 vegetative indices. The left-colored y-axis represents S (green), MD (yellow), and SD (red) treatment. The X-axis represents 24 vegetative indices (red box indicates the potential and closed correlation indices). Red and blue colors in the heat map represents a negative and positive value, respectively.
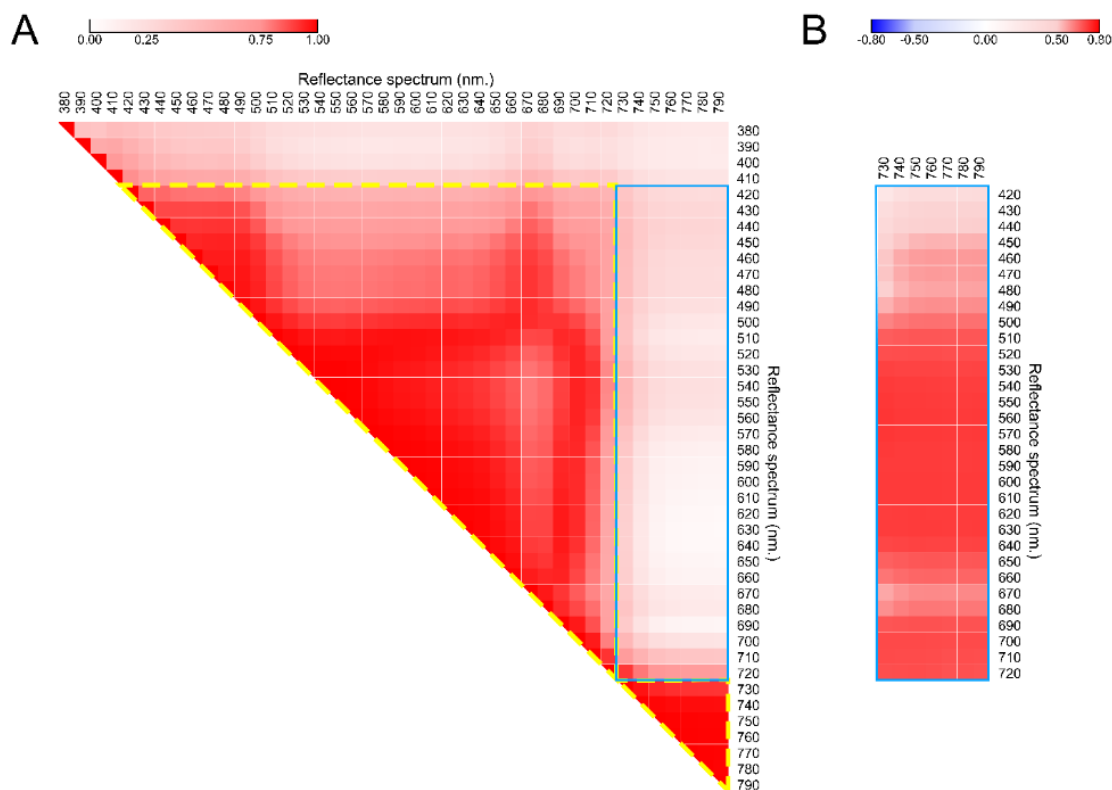
Figure 22 Matrix correlation between its reflectance wavelength (self-correlation) (A) and matrix correlation between each reflectance index with Pi content (B). Blueline indicates the selected area.

Thus, the two ranges of potential spectra, including the visible range (R_{VIS}) and the NIR range (R_{NIR}), were considered from the spectral reflectance information of the full spectrum (420-790 nm). Ratios between two different spectral types of reflectances (R_{NIR} /R_{VIS}) were calculated for further analysis by using only SR values at every 10 nm (e.g., R_{420}, R_{430}, ..., R_{790}) to decrease the amount of data in the analysis. A total of 217 indices were generated and called New spectral reflectance indices (NSR) by pairwise analysis of the dividing ratio between 7 R_{NIR} (R_{730}, R_{740}, ..., R_{790}) and 31 R_{VIS} (R_{420}, R_{430}, ..., R_{720}) values.

Spearman correlation analysis between each of the 217 NSR indices and leaf Pi content measured from the same leaves was performed to estimate the

interaction between NSR (R_{NIR}/R_{VIS}) indices and leaf Pi content. The data were derived from a total of 172 rice accessions grown under MD and SD conditions. A correlation matrix heat map showed that the significant correlation ($r^2 > 0.69$) with leaf Pi content appears in the indices with the range of 730-790 nm (λ_{NIR}) and indices with the range of 530-630 nm or 700-720 nm (λ_{VIS}) **(Figure 22B)**. The whole correlation matrix heat map was provided in **Figure B2**. The results indicate that the NSR ratio indices between 730-780 nm (NIR spectra) and of 530-630 nm (green to red spectra) or 700-720 nm (red edge spectra) could potentially be used to predict Pi contents in rice leaves. In P-sufficient leaves (S treatment), the ratio NSRs did not indicate a meaningful association with the leaf Pi content and were thus omitted from the evaluation.

Additionally, to check for false positives, I reordered the dataset to destroy data structure. The randomized dataset was used to calculate self-correlation and correlation with Pi content. The result showed that the self-correlation matrix and the correlation matrix with Pi content showed low correlation **(Figure B3)**. The randomized dataset showed the significance of the data structure compared with the original dataset. The result and interpretation of data are not likely due to false positives.

2.4 Genome-wide association mapping of Pi content and hyperspectral indices

For the Pi content association, the mean Pi content measured from leaves grown under different P supplement (Pi_S, Pi_MD, and Pi_SD) were associated with 113,114 SNPs derived from exome sequences of 172 rice accessions using GEMMA software. The significant SNPs were considered using the threshold cutoff at -log10(p) >6.35. The significant SNPs were classified as one association signal (locus) by grouping SNPs located approximately within 300 kb. The lowest P-value SNPs were considered as lead SNPs. The results showed that six loci were associated the

Pi_MD trait. The details of these loci are listed in **Table 5** . In contrast, the associations of Pi_S and Pi_SD traits did not show any significant SNPs **(Figure B4)**.

Table 5 Detail of loci associated with Pi content and Spectral reflectance indices

Trait	Loci name	Chr	Number of significant SNPs	Lead SNP position (bp)	(-logP)	Minor allele frequency
Pi_MD	qPi1	1	1	18,062,446	7.81	0.101
	qPi5	5	2	16,423,976	6.83	0.057
	qPi8-1	8	1	8,596,112	10.11	0.052
	qPi8-2	8	3	9,225,490	9.37	0.085
	qPi8-3	8	6	18,346,725	9.19	0.054
	qPi11	11	2	25,844,888	6.68	0.054
SR (740/560, 750/700)	qSR1-1	1	0, 2	11,321,950	6.71	0.06
	qSR1-2	1	0, 1	38,610,955	6.40	0.114
	qSR2	2	5, 4	1,002,248	7.94, 7.92	0.075
	qSR3-1	3	3, 1	24,458,607	6.69, 6.40	0.106
	qSR3-2	3	1, 0	27,448,860	6.39	0.062
	qSR6-1	6	29, 30	7,583,291	7.60, 7.41	0.194
	qSR6-2	6	0, 2	24,291,698	6.54	0.135
	qSR6-3	6	1, 1	26,513,707	6.77, 6.72	0.054
	qSR8-1	8	0, 1	8,596,112	6.47	0.052
	qSR8-2	8	4, 3	9,225,490	7.39, 7.41	0.085
	qSR11	11	5, 3	20,701,489	7.56, 7.47	0.062

จุฬาลงกรณ์มหาวิทยาลัย

CHULALONGKORN UNIVERSITY
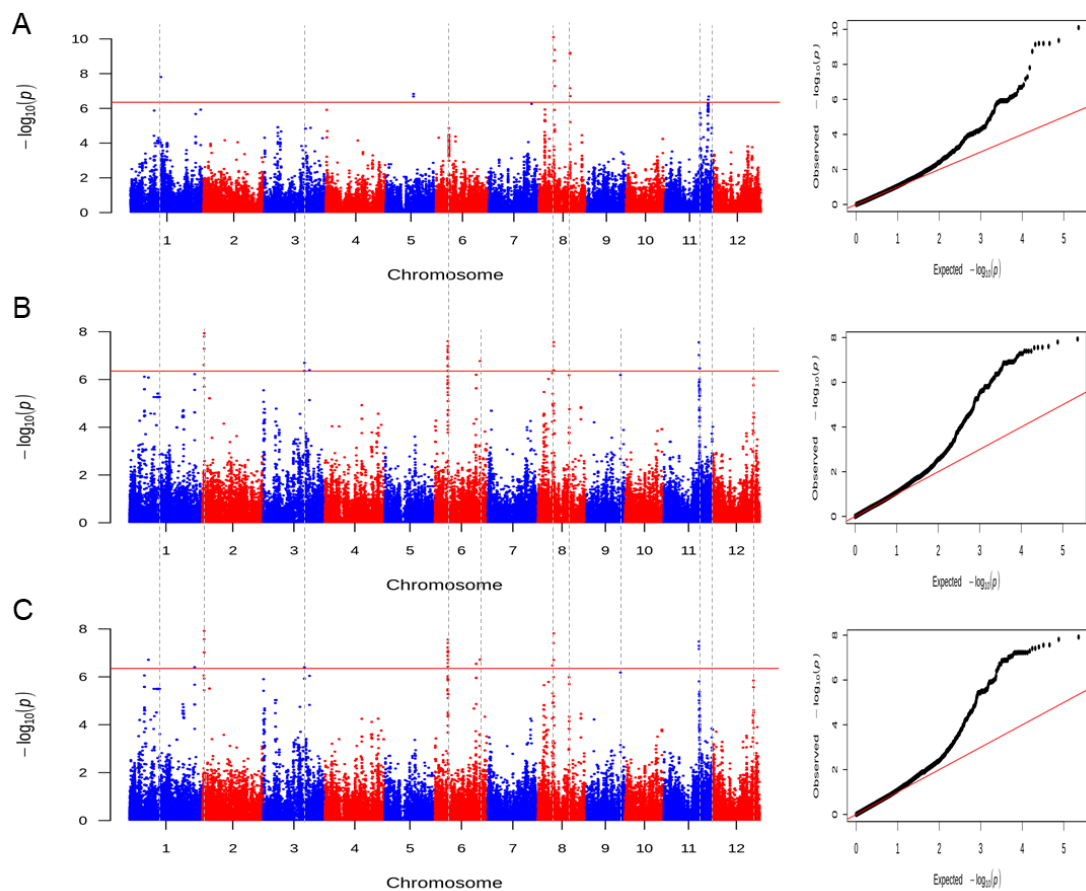
Figure 23 Manhattan and Q-Q plots based on GWAS of Pi content (A), normalized 740/560 index (B), and normalized 750/700 index (C) under SD treatment. For Manhattan plots, the x-axis represents SNP positions across the entire rice genome by chromosome, and the y-axis is the -log10 p-value of each SNP. Red lines indicated the threshold line at -log(P-value) = 6.35.

For NSR traits, the 217 ratio indices (R_{NIR}/R_{VIS}) from 7 R_{NIR} and 31 R_{VIS} were used as the phenotypic data. For representing the P deficiency response effect without the background variation, relative NSR (RNSR) indices were calculated by dividing the means of the NSR indices from SD treatment and S treatment. The MD treatment was not used in the association analysis because its reflectance spectrum did not demonstrate an apparent response to P deficiency **(Figure 18)**. The associations were

performed using the same procedure for Pi content association. From 217 RNSR traits, 104 traits identified upto 48 significant SNPs **(Table 6)**, while the other 113 traits did not show any significant SNP. The significant SNPs from each association were highly overlapped, which might be due to high correlations of the NSR indices **(Figure 23)**. In detail, two groups of ratio spectral indices, including NIR/green to red spectra (530-630 nm) and NIR/red edge spectrum, with R_{740}/R_{560} and R_{750}/R_{700} index, yielded significant SNPs with the lowest p-value from each group, respectively. Hierarchical clustering of -log P-value of candidate genes derived from all indices association grouped the 77 significance of NIR/530-630 reflectance indices and the 27 significance of NIR/700-720 reflectance indices **(Figure 24)**.
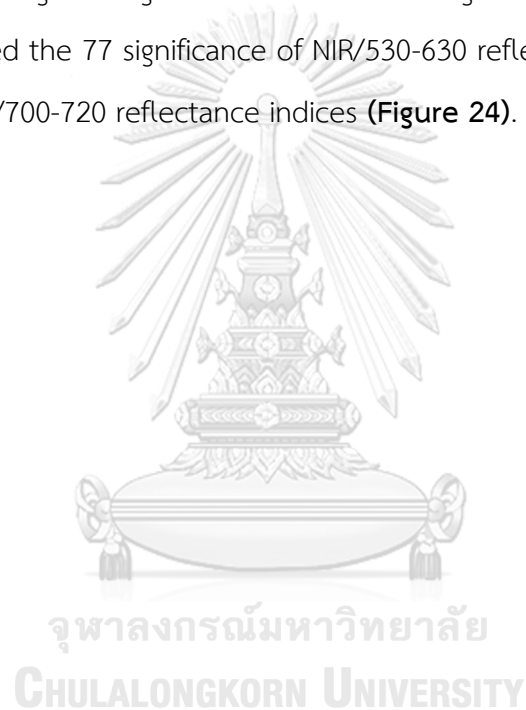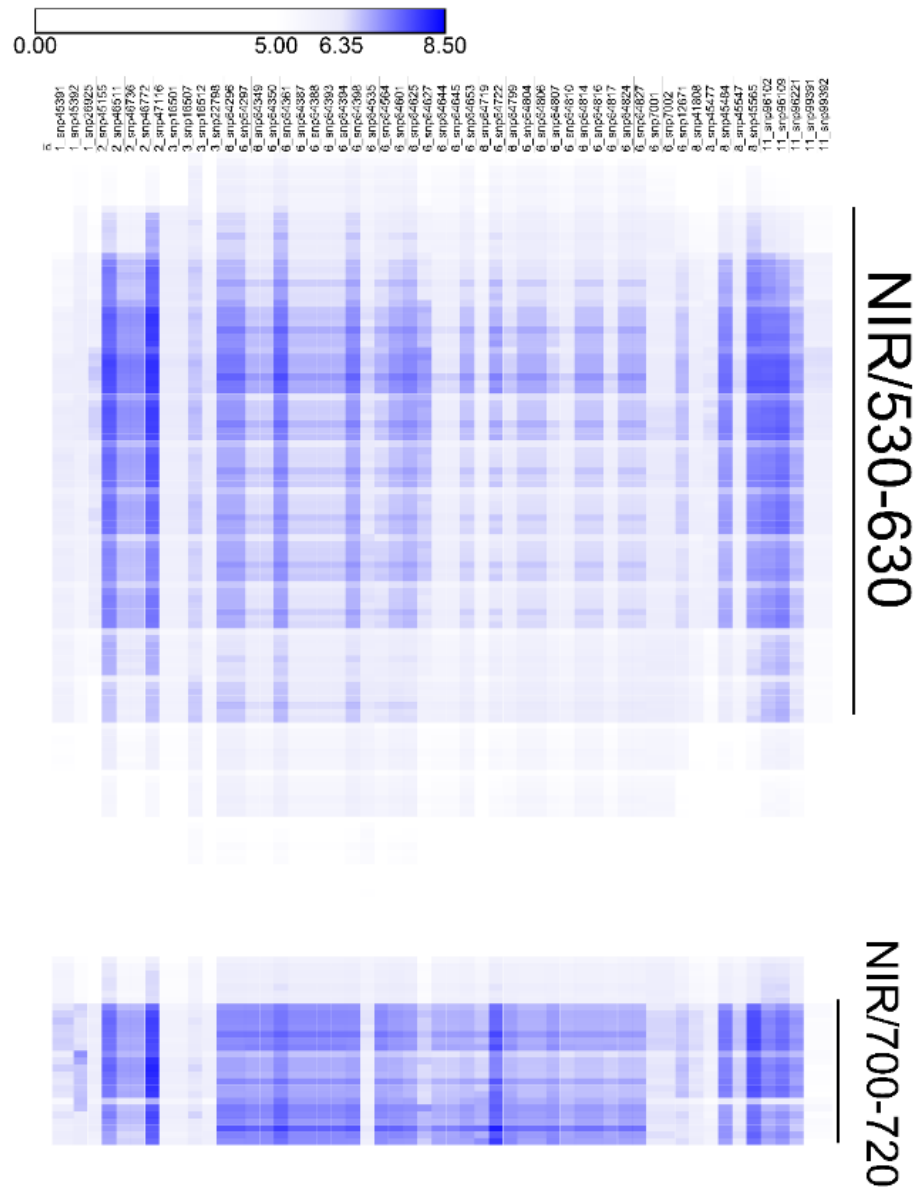
Figure 24 Heatmap of significant SNPs derived from spectral reflectance indices. Blue color represented a significant threshold at -log(P-value) ≥ 6.35.

Overall, 11 loci were summarized from all significant association SNPs of RNSR indices, which included ten loci of 48 significant SNPs derived from the trait R_{740}/R_{560} and seven loci of 48 significant SNPs derived from the trait R_{750}/R_{700} **(Figure 25)**. Almost all of the significant SNPs (41 SNPs or 20 candidate genes) were the same between these spectral index groups. Only seven significant SNPs or four candidate genes of each were found to be specific in NIR/VIS group. Interestingly, three significant SNPs located in two candidate genes were found as SNPs identified in common from hyperspectral indices and Pi content traits.
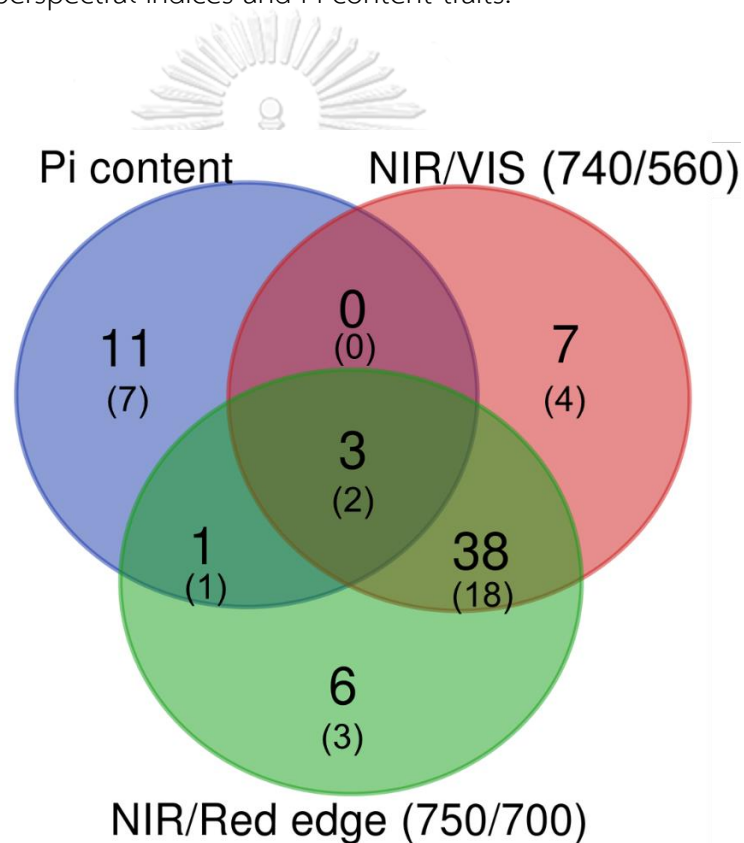
Figure 25 Venn diagram representing the number of significant SNPs (or significant candidate genes in parentheses) from the association of Pi content, NIR/VIS (R_{740}/R_{560} index), and NIR/Red edge (R_{750}/R_{700} index) traits.

Heat maps showing -log p-value of two significant SNPs of *LOC_Os08g15330* and *LOC_Os08g15230* from all of the 217 RNSR traits indicated that the wide range of RNSR indices were also associated with the significant SNPs with p-values passed the threshold cutoff **(Figure 26)**. Not only SNPs located in these two genes but the potential SNPs in the other ten genes were also associated with a similar trend **(Figure B5)**. In addition, the significantly associated region of these two SNP heat maps overlapped with the high correlation zone of the spectral reflectance and Pi content. Such patterns suggest that the identified SNPs are likely not a false positive from noisy data.
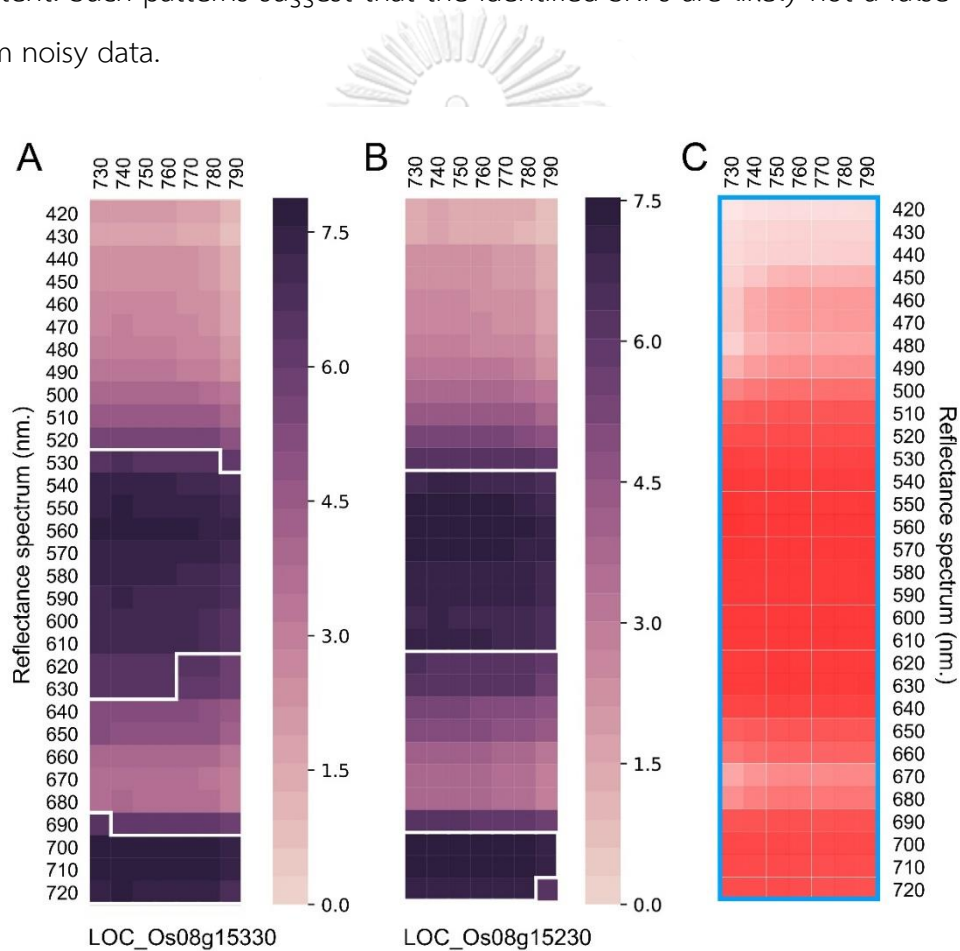
Figure 26 Heat map representing -log P-value of LOC_Os08g15330 (A) and LOC_Os08g15230 (B) significant candidate genes comparing with heat map showing correlation between the indices and Pi content (C). The surrounding white line indicated passed significant threshold line at -log(P-value) ≥ 6.35.

Table 6 List of significant candidate genes associated with Pi content and spectral reflectance indices

Loci name	MSU_id	RAP_id	Annotation	Ref.
qSR1-1	LOC_Os01g19950	-	expressed protein	-
qPi1	LOC_Os01g32890	Os01g0512400	expressed protein	-
qSR1-2	LOC_Os01g66490	Os01g0888300	no apical meristem protein, putative, expressed	-
qSR2	LOC_Os02g02370	Os02g0114800	myb-like DNA-binding domain containing protein, putative, expressed	-
	LOC_Os02g02670	Os02g0118875	NBS-LRR disease resistance protein, putative, expressed	-
	LOC_Os02g02690	Os02g0119100	expressed protein	-
qSR3-1	LOC_Os03g43720	Os03g0638200	transporter family protein, putative, expressed	-
qSR3-1	LOC_Os03g43730	Os03g0638300	tesmin/TSO1-like CXC domain containing protein, expressed	-
qSR3-2	LOC_Os03g48230	Os03g0687900	expressed protein	-
qPi5	LOC_Os05g28090	Os05g0348100	expressed protein	-
qSR6-1	LOC_Os06g13650	Os06g0245700	alpha-mannosidase 2, putative, expressed	-
	LOC_Os06g13660	Os06g0245800	alanyl-tRNA synthetase, putative, expressed	-
	LOC_Os06g13670	Os06g0245900	E2F family transcription factor protein, putative, expressed	-
	LOC_Os06g13680	Os06g0246000	B12D protein, putative, expressed	-
	LOC_Os06g13710	Os06g0246400	glycosyltransferase, putative, expressed	Lin et al., 2011
	LOC_Os06g13730	Os06g0246600	glutamate receptor precursor, putative, expressed	-
	LOC_Os06g13750	-	expressed protein	-
	LOC_Os06g13760	Os06g0247000	glycosyl transferase 8 domain containing protein, putative, expressed	-
	LOC_Os06g13780	Os06g0247200	expressed protein	-
	LOC_Os06g13810	Os06g0247500	PFP1, pyrophosphate--fructose 6-phosphate 1-phosphotransferase subunit beta	Lim et al., 2014
	LOC_Os06g13820	Os06g0247800	dynamin, putative, expressed	-
qSR6-2	LOC_Os06g40740	Os06g0609800	expressed protein	-
qSR6-3	LOC_Os06g44020	Os06g0649100	expressed protein	-
qPi8-2, qSR8-2	LOC_Os08g15230	Os08g0250900	SMAX1-like protein	Choi et al., 2020
	LOC_Os08g15330	Os08g0253100	anthocyanidin 3-O-glucosyltransferase, putative, expressed	-
qPi8-3	LOC_Os08g29854	Os08g0388300	RGH1A, putative, expressed	-
	LOC_Os08g29870	Os08g0388400	expressed protein	-
	LOC_Os08g30070	Os08g0390100	expressed protein	-
qSR11	LOC_Os11g35300	-	expressed protein	-
	LOC_Os11g35320	Os11g0557300	BSD domain-containing protein, putative, expressed	-
	LOC_Os11g35860	Os11g0565300	OsWAK120 - OsWAK receptor-like protein kinase, expressed	-
qPi11	LOC_Os11g42300	Os11g0642500	OsFBX434 - F-box domain containing protein, expressed	-
	LOC_Os11g42900	Os11g0649000	expressed protein	-

From the overlapped significant loci between Pi content and RNSR association, I found that the loci qSR8-1 and qSR8-2 were co-localized with qPi8-1 and qPi8-2, respectively. The candidate genes in the qPi8-2 and qSR8-2 regions encoded the suppressor of MAX2-like protein (*OsSMAX1*; LOC_Os08g15230) and anthocyanidin 3-O-glucosyltransferase (LOC_Os08g15330). The other 10 qSR loci are specific to the SR traits and the other 3 qPi loci are specific to the Pi traits. The highest candidate gene was found in the qSR6-1 locus that consisted of 30 significant SNPs located in 11 genes **(Table 6)**.

From linkage disequilibrium (LD) analysis, several genes locating in the LD of significant candidate SNPs with $r^2 > 0.25$ was found **(Table 7)**. Interestingly, a known gene related to P-deficient tolerance, *OsMYB4P* (LOC_Os11g35390) was found in LD block of qSR11 lead SNP ($r^2 = 0.84$). Moreover, two known genes involved to P response in Arabidopsis orthologues (*BiP2*; LOC_Os02g02410 and *AIR3*; LOC_Os06g40700), were identified in LD block of qSR2 and qSR6-2 ($r^2 = 0.64, 0.30$).

Table 7 List of LD linked candidate genes associated with Pi content and spectral reflectance indices.

Loci name	MSU_id	RAP_id	R2	Annotation	Ref.
qPi1	LOC_Os01g33040	Os01g0513900	0.65	kinesin motor domain containing protein, expressed	-
	LOC_Os01g33050	Os01g0514000	0.65	ribosomal protein L24, putative, expressed	-
qSR1-2	LOC_Os01g66440	Os01g0888000	0.27	expressed protein	-
	LOC_Os01g66500	Os01g0888500	0.85	phosphoribosylformylglycinamidine synthase, putative, expressed	-
qSR2	LOC_Os02g02410	Os02g0115900	0.30	DnaK family protein, putative, expressed	Naumann et al., 2019
	LOC_Os02g02520	Os02g0117100	0.32	expressed protein	-
	LOC_Os02g02720	Os02g0119400	0.30	SNARE domain containing protein, putative, expressed	-
	LOC_Os02g02730	Os02g0119600	0.32	expressed protein	-
	LOC_Os02g02740	Os02g0119700	0.32	PPR repeat containing protein, expressed	-
	LOC_Os02g02750	Os02g0119800	0.31	CDP-alcohol phosphatidyltransferase, putative, expressed	-
	LOC_Os02g02800	Os02g0120300	0.31	AGAP001222-PA, putative, expressed	-
	LOC_Os02g02850	Os02g0120900	0.33	bifunctional protein folD, putative, expressed	-
	LOC_Os02g02860	Os02g0121000	0.33	glutamyl-tRNA synthetase, putative, expressed	-
qSR3-1	LOC_Os03g43760	Os03g0638800	0.28	protein kinase domain containing protein, expressed	-
qSR3-2	LOC_Os03g48190	Os03g0687200	0.92	expressed protein	-
	LOC_Os03g48260	Os03g0688200	0.49	expressed protein	-
qSR6-1	LOC_Os06g13590	None	0.33	PE-PGRS family protein, putative, expressed	-
	LOC_Os06g13600	Os06g0244700	0.33	HEAT repeat family protein, putative, expressed	-
	LOC_Os06g13620	None	0.33	expressed protein	-
	LOC_Os06g13640	Os06g0245600	0.26	expressed protein	-
	LOC_Os06g13690	None	0.61	expressed protein	-
	LOC_Os06g13860	Os06g0248400	0.55	RCD1, putative, expressed	-
	LOC_Os06g13890	Os06g0248900	0.33	expressed protein	-
qSR6-2	LOC_Os06g40590	Os06g0608100	0.28	expressed protein	-
	LOC_Os06g40630	Os06g0608600	0.55	SFT2, putative, expressed	-
	LOC_Os06g40680	None	0.58	expressed protein	-
	LOC_Os06g40700	Os06g0609301	0.64	OsSub50 - Putative Subtilisin homologue, expressed	Al-Ghazi et al., 2003
	LOC_Os06g40704	Os06g0609450	0.64	stromal membrane-associated protein, putative, expressed	-
	LOC_Os06g40710	Os06g0609500	0.62	Myb-like DNA-binding domain containing protein, putative, expressed	-
	LOC_Os06g40720	Os06g0609600	0.61	EF hand family protein, putative, expressed	-
	LOC_Os06g40730	Os06g0609700	0.62	protein with a conserved N-terminal region, putative, expressed	-
	LOC_Os06g40750	Os06g0609900	0.98	expressed protein	-
	LOC_Os06g40770	Os06g0610100	0.98	expressed protein	-
	LOC_Os06g40780	Os06g0610300	0.45	MONOCULM 1, putative, expressed	-
	LOC_Os06g40818	Os06g0610800	0.30	aspartic proteinase, putative, expressed	-
qSR6-3	LOC_Os06g43880	Os06g0646900	0.41	prenyltransferase, putative, expressed	-
	LOC_Os06g43910	Os06g0647200	0.29	two-component response regulator, putative, expressed	-
	LOC_Os06g43920		0.27	hypothetical protein	-
qPi8-1, qSR8-1	LOC_Os08g14440	Os08g0242700	0.50	uridylyltransferase-related, putative, expressed	-
	LOC_Os08g14450	Os08g0242800	0.66	RNA polymerase sigma factor, putative, expressed	-
	LOC_Os08g14460	Os08g0242900	0.26	expressed protein	-
qPi8-2, qSR8-2	LOC_Os08g15204	Os08g0250700	0.83	thioredoxin domain-containing protein 9, putative, expressed	-
	LOC_Os08g15410	None	0.86	expressed protein	-
qPi8-3	LOC_Os08g29809	Os08g0387700	0.62	resistance protein LR10, putative, expressed	-
	LOC_Os08g30014	Os08g0389601	0.31	expressed protein	-
	LOC_Os08g30060	Os08g0390000	0.56	proton pump interactor, putative, expressed	-
qSR11	LOC_Os11g35450	Os11g0558900	0.27	leucine-rich repeat receptor protein kinase EXS precursor	-
	LOC_Os11g35210	Os11g0555300	0.36	NB-ARC domain containing protein, expressed	-
	LOC_Os11g35370	Os11g0558000	0.79	expressed protein	-
	LOC_Os11g35390	Os11g0558200	0.84	MYB family transcription factor, putative, expressed	Yang et al., 2014
	LOC_Os11g35410	Os11g0558400	0.27	expressed protein	-
	LOC_Os11g35425		0.76	expressed protein	-
	LOC_Os11g35440	None	0.31	hypothetical protein	-
	LOC_Os11g35490	Os11g0559100	0.38	leucine rich repeat protein, putative, expressed	-
	LOC_Os11g35500	Os11g0559200	0.57	receptor-like protein kinase 5 precursor, putative, expressed	-
	LOC_Os11g35710	Os11g0562100	0.28	cycloartenol synthase, putative, expressed	-
	LOC_Os11g35850	Os11g0565000	0.84	expressed protein	-
	LOC_Os11g35870	Os11g0565400	0.42	RWD domain containing protein, expressed	-
qPi11	LOC_Os11g42150	None	0.79	hypothetical protein	-
	LOC_Os11g42160	Os11g0641200	0.76	F-box/LRR-repeat protein 3, putative, expressed	-
	LOC_Os11g42170	Os11g0641300	0.79	expressed protein	-
	LOC_Os11g42200	Os11g0641500	0.98	laccase precursor protein, putative, expressed	-
	LOC_Os11g42350	Os11g0642800	0.98	glutathione synthetase, chloroplast precursor, putative, expressed	-
	LOC_Os11g42390	Os11g0643400	0.97	OsSCP64 - Putative Serine Carboxypeptidase homologue, expressed	-
	LOC_Os11g42420	Os11g0643700	0.91	nuclear pore protein 84/107 containing protein, expressed	-
	LOC_Os11g42430	Os11g0643800	0.63	transporter family protein, putative, expressed	Deng et al., 2018
	LOC_Os11g42440	Os11g0644000	0.76	expressed protein	-
	LOC_Os11g42810	Os11g0648200	0.27	expressed protein	-

CHAPTER V

DISCUSSION

1. Development of a rapid inorganic phosphorus quantification

The punching method has been tried to improve the conventional method to supply high throughput performance in Pi quantification. The process in punching method can be done without grinding, balancing, and several transferring steps with validation comparing to the conventional method. The Pi extraction could be finished within 3 hour-incubation time for both high and low accumulation rice cultivar grown under P deficient and sufficient condition **(Figure 12)**. A total available Pi was extracted from the leaf tissue by using a freeze shattering technique without grinding step. Freezing plant organs or tissues affect orientation and distribution of microtubules along with plant cells, which release intracellular substance *via* permeabilization of the cell wall (Wasteneys *et al.*, 1997). This useful technique was applied to various types of materials and organisms (Tiwari and Polito, 1990; Braun, 1996; Wasteneys *et al.*, 1997). Another critical factor in Pi extraction is the incubation time of leaf tissues in the extraction solution. The 4 hours of incubation showed higher Pi content than the conventional process **(Figure 12)**. The increased Pi content can be affected by intracellular enzymes, especially acid phosphatase, which converts organic P and structure binding P to detectable Pi content (Duff *et al.*, 1994; Tazisong *et al.*, 2015). Thus, time control and performing the process under low temperature help to avoid hydrolysis of organic P from the action of the phosphatase enzymes (Gundlach and Luttermann-Semmer, 1987).

Our validation showed that the punching method based on leaf area normalization and non-grinding approach has a comparable result to the conventional method using sample grinding and biomass normalizing processes. Normalization of the Pi content in root tissues with root length has been previously studied in *Arabidopsis* seedlings, which were grown on a one-dimensional agar plate (Ayadi *et al.*, 2015; Kanno *et al.*, 2016). The complex organs, which have a largely

various size or biomass of plant tissues (such as large root system or fruit), may not be appropriate for Pi content calculation by using area normalization techniques. Besides, it should be noted that accuracy may decrease when using this method for P-deficient samples. When I consider a leaf disc weight of high and low Pi accumulators grown under severely P supply levels, I found unequal leaf weight in the lowest P treatment **(Table B1)**. Several studies reported P starvation affects growth and development in the plant, particularly leaf weight and area (HØGH-JENSEN *et al.*, 2002; Chaudhary *et al.*, 2008; Singh *et al.*, 2013). This evidence suggests that level of P deficiency should be considered for the application of this method in your experiment. A comparison between sufficient and severely deficient conditions, which decreases leaf weight or thickness, should be avoided to prevent error interpretation. Optionally, Pi content should be converted by normalizing with average leaf weight per leaf disc before the interpretation to remove the error effect of unequal amount of tissue used. Moreover, the punching method could be limited for small and narrow leaf phenotype in P deficiency condition, which is more difficult to handle with paper punchers. Thus, the level and treatment period of P starvation should be tested before Pi content analysis.

Pi content quantification results from a different position and stage in the same plant showed the various levels of Pi accumulation in the tissue (**Figure 16**). The result suggested that leaf position and stage are essential factors that should be considered to select leaf samples for the analysis. Based on the Pi content in different positions and stages in rice, less than 20 folds difference in Pi content between the plant grown under sufficient (320 µM P) and deficient conditions were detected. Moreover, various fold differences (21-33 and 125-177 folds) were found in the first leaf (youngest) and fourth leaf (older) stage, respectively. Different Pi accumulation in each part and position is controlled by complex regulation in Pi homeostasis to remobilize Pi content to the essential organ during the P starvation period (Irfan *et al.*, 2020). The remobilization of Pi content represents P used

efficiency adaptation in rice under P deficiency (Dissanayaka *et al.,* 2018). Thus, the researchers should carefully decide to choose a suitable leaf position and stage for their experiments. Although this punching method still has some limitation with scarce Pi content and is not optimized for other plant tissues, it can be a quick and easy procedure for initial screening of large number of rice materials and various treatments before validation with the conventional method.

The significant difference in Pi accumulation performance in these two rice cultivars showed the genetic ability to control different accumulation abilities in these rice **(Figure 14D)**. Recently, phenomics studies have become popular and required to unravel the genetic function controlled agronomical traits by integration with the genomic platform. And this developed high-throughput method can be used for application in large-scale detection of Pi content in rice leaf among the big population of the genomic study.

2. Phenotyping of local Thai rice cultivars under phosphorus deficiency at seedling stage

2.1 Phenotyping of rice using Pi quantification and hyperspectral detection

Response phenotype of phosphorus deficiency in rice can be observed from various growth parameters, such as biomass, plant height, root length, etc. (Li *et al.,* 2009; Vejchasarn *et al.,* 2016; Chankaew *et al.,* 2019). However, they may not be obvious to detect P response during the seedling stage. Pi accumulation content in leaves was reported as a sensitive parameter to detect plant deficiency status in plants (Wissuwa and Ae, 2001; Misson *et al.,* 2005; Mehra *et al.,* 2016; Pereira *et al.,* 2020). Currently, hyperspectral measurement has been applied to various plants and purposes due to its sensitive, non-destructive, and rapid property (Bellante *et al.,* 2014; Kim *et al.,* 2015; Kuska *et al.,* 2018; D. Wang *et al.,* 2019). This study is a large-scale detection of rice response under P starvation by using Pi quantification and hyperspectral measurement to evaluate P deficiency effect and P used efficiency in

various rice cultivars. I hydroponically cultured 172 rice accessions in the seedling stage under three different phosphorus levels. The Pi content in the leaves at the same age was estimated *via* the punching method and hyperspectral measurement *via* the Polypen device. The intracellular Pi content in rice leaves grown under different P supplementation showed obviously distinguishing among P deficiency levels **(Figure 18A)**. Pi content is decreased by the use in metabolism processes under P limit, including photosynthesis and cellular respiration (Mikulska *et al.*, 1998; Wang *et al.*, 2015), leading to P starvation in plants.

The Pi quantification refers to the available phosphorus in a plant that directly indicates the residual level of storage Pi content in the plants. In other words, the difference of residual Pi content in the rice population under starvation is controlled by genetic regulatory in the phosphorus homeostasis pathway (Lin *et al.*, 2009; Fabianska *et al.*, 2019) that refers to the variation of Pi used efficiency performance in this rice population. On the other hand, hyperspectral measurement is indirect detection that is not directly used to evaluate P content in the plants. But the hyperspectral approach focuses on the electromagnetic reflection from biochemical molecules such as chlorophyll, anthocyanin, carotenoid, etc. and it is used to distinguish plant response by comparison analysis between treatments. In the hyperspectral analysis, the significant P deficiency response can be observed in only SD treatment, in which the plants were grown in a very low P supplement. In contrast, MD treatment did not show a noticeable difference with sufficient conditions **(Figure 18B-C)**. The appearance of the phenomenon in rice response to P deficiency may be due to the different levels of P starvation that affect occurrent P deficient symptoms (Yaseen *et al.*, 2000; Massawe and Mrema, 2017). The five spectral reflectance indices, GM1, GM2, NDVI, SR, and ZMI, represent the capable detection and predictivity in P deficiency response and gene identification, respectively **(Figures 19 and 20)**. Interestingly, the indices were developed with a high correlation with chlorophyll content to classify green leaves from other objects

and help distinguish stress response in the various plants (Zarco-Tejada *et al.,* 2002; Zagajewski *et al.,* 2018; Caturegli *et al.,* 2020). The result similarly suggested as the previous reports that P starvation reduced biosynthesis of chlorophyll content and photosynthesis activity (Xu *et al.,* 2007; Hernández and Munné-Bosch, 2015). Most of the indices were generated by the dividing ratio between two reflectance spectra in NIR and VIS wavelength, representing the responsible value and used for generating detective indices in several stress-response observations. In this research, the newly generated NIR/VIS ratio indices represented meaningful and correlated results with Pi content **(Figure 21)**. The application of spectral reflectance in P deficiency prediction has been done in some other plants such as grass (Bogrekci and Lee, 2005), rangeland plants (Özyiğit and Bilgen, 2013), soybean (Milton *et al.,* 1991; Guo, 2017), corn (Osborne *et al.,* 2002), and Tomato (G. Sun *et al.,* 2019). Different representative wavelength representing P content was used in different species, which mainly focused at green, red, and NIR spectrum. By their own algorithm and model calculation, different correlation coefficient between generated reflectance index and detected Pi content was found at 0.425, 0.43, 0.6172, 0.68, 0.91, respectively.

2.2 Genome-wide association mapping of Pi content and spectral reflectance indices

Among genome-wide association mapping of 217 spectral reflectance traits, the NIR/green to red (530-630 nm) and NIR/red edge (700-720 nm), which have a high correlation with Pi content, can predict significant SNPs with low P-value **(Figure 23)**. These spectral regions are responsive to P deficiency in the plants with high correlation coefficient to leaf Pi contents. (Peng *et al.,* 2020). Particular the NIR/red edge indices, which were reported and applied to represent several stress responses (Barnes *et al.,* 2000; Furbank and Tester, 2011; Kim *et al.,* 2011), showed significant P-value of the predicted SNPs in the associations. However, the wavelength of the red edge is quite short (about 700-720 nm) that limited the measurement process by the sensitivity of the detective device. NIR/green to red indices similarly identified

significant SNPs. Thus, the NIR/green to red indices may be suitable to be determined with a low cost or DIY hyperspectral tools with high sensitivity (Abd-Elrahman *et al.*, 2011; Huang *et al.*, 2018; Zhao *et al.*, 2018; Ribes *et al.*, 2020).

Comparing significant SNPs between Pi content and spectral reflectance indices associations showed that the same locus and candidate genes were found on chromosome 8 **(Figure 22)**. Two known genes, anthocyanidin 3-O-glucosyltransferase (LOC_Os08g15330) and *OsSMAX1* (LOC_Os08g15230) , has been shown to be related to Pi deficiency responses (Secco et al., 2013; Yin et al., 2012), suggesting the performance of both Pi content and spectral reflectance indices traits in the prediction of genes involved in P deficiency response. The catalytic enzyme in the anthocyanin biosynthesis pathway, anthocyanidin 3-O-glucosyltransferase (EC 2.4.1.115) (Sun *et al.*, 2016), and its expression has been shown to be up-regulated by P deficiency in suspension-cultured grape cells studies (Yin *et al.*, 2012), consistent with P deprivation triggered anthocyanin accumulation (Jiang *et al.*, 2007; Ito *et al.*, 2015; Chen *et al.*, 2018). A recent study showed that *OsSMAX1* plays roles in the karrikin signaling pathway downstream of the Dwarf14-Like (D4L) Karrikin receptor and negatively controls arbuscular mycorrhiza (AM) symbiosis and strigolactone biosynthesis (Choi *et al.*, 2020), which are adaptive strategies to overcome P deficiency (Balzergue *et al.*, 2011; Lanfranco *et al.*, 2018). The symbiosis process was triggered by strigolactone hormone that had been highly accumulated in *smax1* knockout mutant during P deficient condition (Choi et al., 2020).

Another interesting locus, qSR6-1, consisted of 30 significant SNPs located in 12 genes (**Table 6**). *LOC_Os06g13810* encoding the regulatory β-subunit of pyrophosphate-fructose 6-phosphate 1-phosphotransferase (PFP1b) was found in this locus. The PFP enzyme (also called PPi-dependent phosphofructokinase, PPi-PFK; EC 2.7.1.90) catalyzes the reversible phosphorylation of fructose 6-phosphate to fructose 1,6-bisphosphate in the glycolysis pathway and involved in various stress response, including P deficiency and anoxia in which cytoplasmic Pi and ATP are

limited (Mertens *et al.*, 1990; Plaxton and Tran, 2011). Additionally, up-regulation of the *LOC_Os06g13810* gene under P deficiency has also been showed in transgenic rice overexpressing a novel transcription factor (*OsPTF1*) (Yi *et al.,* 2005).

Moreover, three of the LD linked candidate genes were previously reported to be involved in other P-deficient adaptation **(Table 7)**. One of these genes is a known gene related to P-deficient tolerance, *LOC_Os11g35390* encoding R2R3-type MYB transcription factor, OsMYB4P, was identified in the qSR11 locus, whose overexpression in rice promotes Pi uptake by root system architecture adaptation and transporter up-regulation (W. T. Yang *et al.*, 2014). This gene is located in the LD block of qSR11 lead SNP with high correlation (r^2 = 0.84). In the LD block of qSR6-2 (r^2 = 0.64), *LOC_Os06g40700* encoding subtilisin in rice is an ortholog of *Auxin-induced in root cultures 3* (*AIR3*; *AT2G04160*) gene, which was triggered by auxin to promote lateral root formation and thus facilitate lateral root emergence in *Arabidopsis*. This gene showed dramatic and stable up-regulation under P starvation (Al‑Ghazi *et al.,* 2003; Hammond *et al.,* 2003). In the LD block of qSR2 (r^2 = 0.30), I also found an orthologous gene of *LOC_Os02g02410*, DnaK family protein in *Arabidopsis* called BiP2 (AT5G42020), which involved with ER stress response under P starvation. Under P deficiency condition, *AtBiP2* was dramatically increased in root tip to suppress ER stress and autophagy, which was consequently induced by ER stress and P starvation (Naumann *et al.,* 2019).

The candidate genes and their linked genes were checked with the microarray and RNA-seq datasets from several P deficiency experiments (Zheng *et al.,* 2009; X. Dai *et al.,* 2012; Gamuyao *et al.,* 2012; Secco *et al.,* 2013; P. Mehra *et al.,* 2015). Interestingly, I found that most of the candidate genes showed a response to P deficiency condition, suggesting that they might be involved in response to P starvation. There were nine candidate genes that showed up or down-regulation in both microarray and RNA-seq datasets **(Figure 27-30)**; these include *LOC_Os02g02370* (myb-like DNA-binding domain protein), *LOC_Os03g43720*

(transporter family protein), *LOC_Os05g28090* (expressed protein), *LOC_Os06g13660* (alanyl-tRNA synthetase), *LOC_Os06g13680* (B12D protein), *LOC_Os06g13760* (glycosyl transferase8 protein), *LOC_Os08g15230* (SMAX1-like protein), *LOC_Os08g29854* (*RGH1A*), *LOC_Os08g30070* (expressed protein). I found eleven linked candidate genes that showed differential expression in P starvation treatments, including *LOC_Os01g66500* (phosphoribosylformylglycinamidine synthase), *LOC_Os06g13600* (HEAT repeat family protein), *LOC_Os06g40750* (expressed protein), *LOC_Os06g40818* (aspartic proteinase), *LOC_Os08g14450* (RNA polymerase sigma factor), *LOC_Os08g29809* (resistance protein LR10), *LOC_Os11g35210* (NB-ARC domain-containing protein), *LOC_Os11g35710* (cycloartenol synthase), *LOC_Os11g42200* (laccase precursor protein), *LOC_Os11g42390* (Serine Carboxypeptidase), and *LOC_Os11g42430* (transporter family protein). A gene on chromosome 11 encoding transporter protein (LOC_Os11g42430) had strong up- and down-regulated expression in separated P deficient experiment, and also showed significant expression in root sample under P deficiency experiment of wild rice (*Oryza rufipogon* Griff.) (Deng *et al.*, 2018), which were previously reported as P deficient tolerance (Chen *et al.*, 2011).
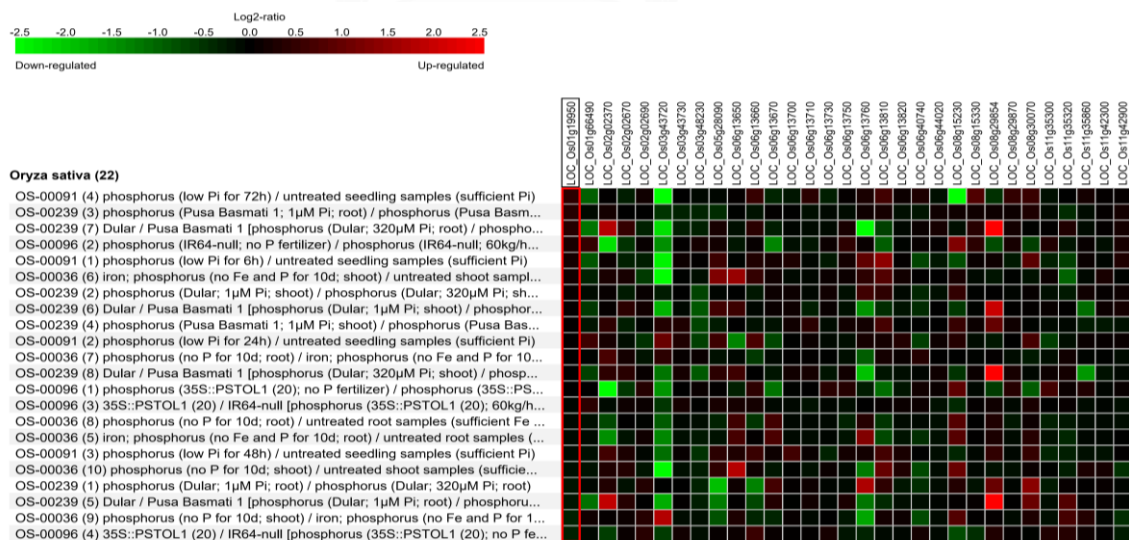
Figure 27 Gene expression heat map of the associated significant genes (rows) from several P deficiency experiments (columns) (Zheng et al., 2009; X. Dai et al., 2012;

Gamuyao et al., 2012; P. Mehra et al., 2015), Affymetrix Rice Genome Array platform from the GENEVESTIGATOR tool was used (Hruz et al., 2008b; 2008a). Down and up-regulation were represented by green and red colors, respectively.
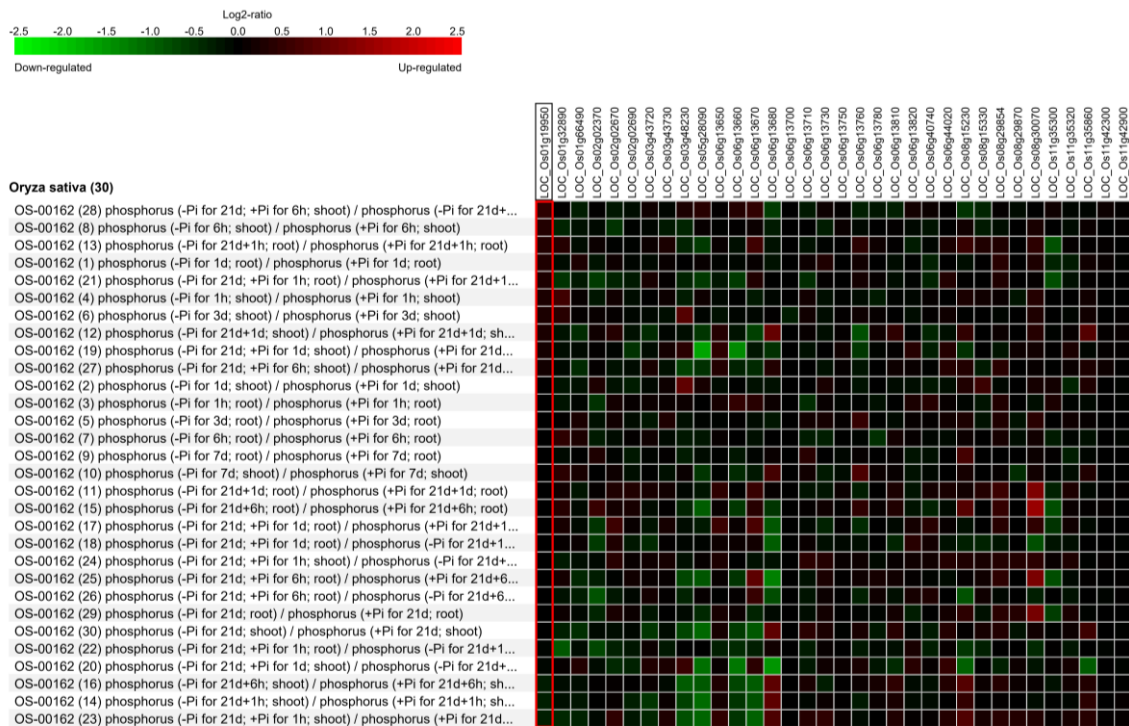
Figure 28 Gene expression heat map of the associated significant genes (rows) from several P deficiency experiments (columns) (Secco et al., 2013), the RNA-Seq platform from the GENEVESTIGATOR tool was used (Hruz et al., 2008b). Down and up-regulation were represented by green and red colors, respectively.
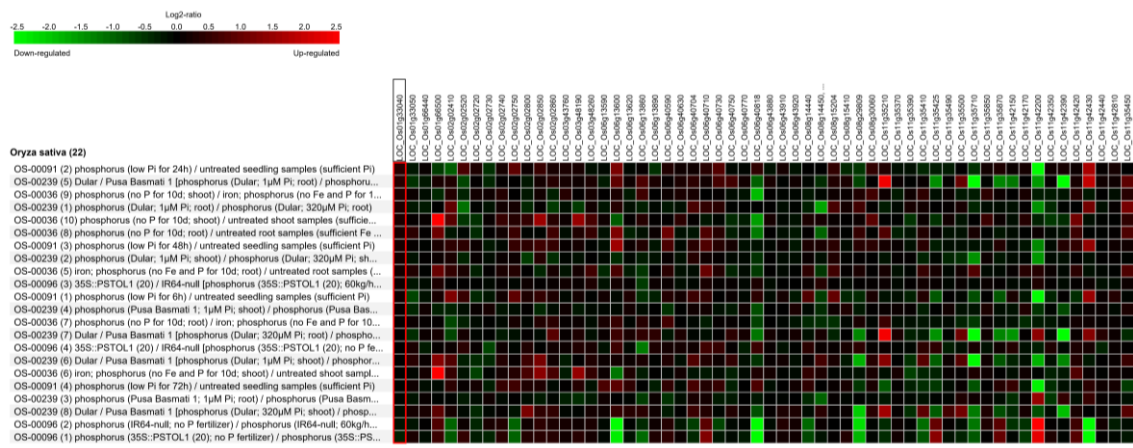
Figure 29 Gene expression heat map of the LD linked candidate genes (rows) from several P deficiency experiments (columns) (Zheng et al., 2009; X. Dai et al., 2012; Gamuyao et al., 2012; P. Mehra et al., 2015), Affymetrix Rice Genome Array platform from the GENEVESTIGATOR tool was used (Hruz et al., 2008b). Down and up-regulation were represented by green and red colors, respectively.
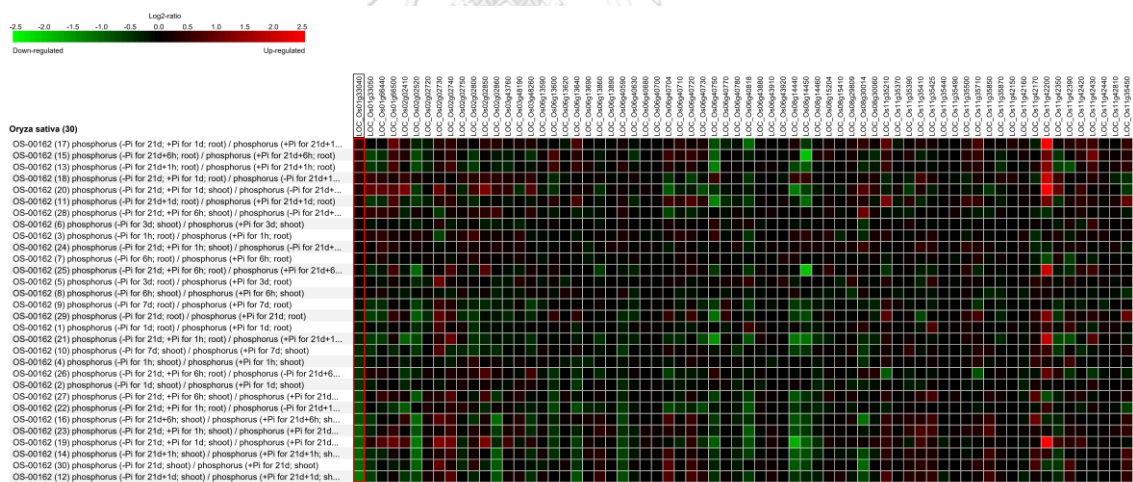
Figure 30 Gene expression heat map of the LD linked candidate genes (rows) from several P deficiency experiments (columns) (Secco et al., 2013), the RNA-Seq platform from the GENEVESTIGATOR tool was used (Hruz et al., 2008b). Down and up-regulation were represented by green and red colors, respectively.

Besides, some candidate genes co-localized with P deficiency-related QTLs, which related to P responsive phenotypes **(Figure 31)**. The candidate genes are located on six chromosomes, including chromosome 1, 2, 3, 6, 8, and 11. Particularly, chromosomes 3 and 6, some of candidate genes were within the reported P deficiency QTL (Ni *et al.*, 1998; Wissuwa *et al.*, 1998; Li *et al.*, 2009; Jewel *et al.*, 2019). Three candidate genes are located within qRN3 and qRFW3a (RM6832-RM3513) on chromosome 3, which are related to root and root fresh weight phenotype. Moreover, another three genes on the same chromosome within qRFW3b and qRRN3 (RM2334-3166) were also detected, which control root-fresh weight and relative total root number under P deficiency condition, respectively. Additionally, 13 candidate genes located within qPH (RM7269-RM5314) on chromosome 6 represent plant height traits grown under P deficiency condition. Moreover, 19 candidate genes are located near qMRL6b (RM402-RM7023) on chromosome 6, which involved with maximum root length phenotype. Twelve candidate gene on chromosome 2 were found near the position of qAE_2.1 marker (SNP_2_542635) that contributed to agronomic efficiency response under P limited condition. , Eight candidate genes on chromosome 8 are located near qPFP_8.2 (SNP_8_8437588) that involves in partial factor productivity in rice. Another group of 7 candidate genes on chromosome 8 located near qRN8a (RM1309- RM1109B), which involved total root number parameter, which is important to forage available phosphorus in soil. Finally, 15 candidate genes are located near qRS11 (RM5349-RM21) involved in the root-shoot ratio under P starvation treatment.
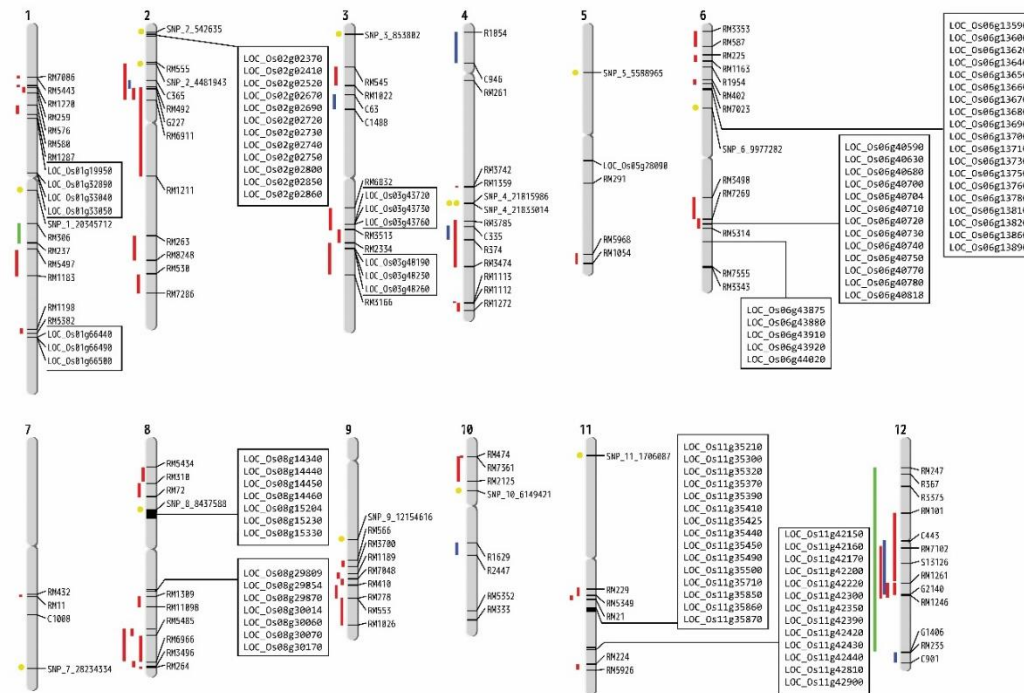
Figure 31 QTL mapping of significant candidate genes and previous P responsive QTL positions. Lines and dots represent P responsive QTL intervals and SNPs from previous reports, respectively. The color symbols include red (Li et al., 2009), green (Ni et al., 1998), blue (Wissuwa et al., 1998), and yellow (Jewel et al., 2019).

Besides, gene expression under P deficiency from several reported experiments of all association candidate genes shows the high response in several predicted genes that also includes known P responsive genes. Moreover, some groups of candidate genes are also in the reported QTL region (Ni *et al.,* 1998; Wissuwa *et al.,* 1998; Li *et al.,* 2009; Jewel *et al.,* 2019) **(Figure 31)**. These indicate potential candidate genes that may involve and regulate P deficient tolerance and regulation in rice. In candidate gene identification process, function-dependent strategy and position-dependent strategy were mainly considered to identify the potential candidate gene (Zhu and Zhao, 2007). Gene expression pattern of some gene can be modulated by some specific environmental factor, such as *PSTOL1* that

is inducted by phosphorus-deficient condition (Gamuyao *et al.*, 2012). Moreover, physical linkage in QTL segment can be provided positive gene (Van Laere *et al.*, 2003), although application of position-dependent strategy could not be guarantee with high accuracy, due to many false-positive, but it can hint to narrow down the potential region (Zhu and Zhao, 2007; Lekklar *et al.*, 2019). From the gene expression and location on reported QTL studies, some genes have high potential on function in P deficiency regulation in rice.

LOC_Os02g02370 (myb-like DNA-binding domain protein; OsMYB61) is one member of the MYB transcription factors, which regulates and involves several plant regulation and abiotic stress response (Katiyar *et al.*, 2012). The orthologue overexpression *Arabidopsis* showed enhancement of root system architecture and resource allocation (Romano *et al.*, 2012). Several R2R3-*MYB* genes are involved in controlling responses to P deficiency in *Arabidopsis* and rice, including *AtMYB62* (Devaiah *et al.*, 2009), *AtMYB103* (Yu *et al.*, 2019), *OsMYB2P-1* (Xiaoyan Dai *et al.*, 2012), *OsMYB5P* (Yang *et al.*, 2018), and particularly *OsMYB4P* (W. T. Yang *et al.*, 2014) which also found in this association.

CAS1 gene (*LOC_Os11g35710*) encoded an important cycloartenol synthase enzyme, which converts isopentenyl pyrophosphate to cycloartenol. The cycloartenol is the key essential compound for multistep brassinosteroid biosynthesis (Bajguz *et al.*, 2020). Brassinosteroid is an essential plant hormone involving in plant development, several stress responses (Planas-Riverola *et al.*, 2019), and particularly the deficiency of nitrogen (Y. Wang *et al.*, 2019), boron (Zhang *et al.*, 2019), iron (B. Wang *et al.*, 2012), and phosphorus (Singh *et al.*, 2014). In rice, brassinosteroid is an important signaling factor regulating P deficiency-induced leaf inclination to decrease excess light reception (Ruan *et al.*, 2018; Zou *et al.*, 2020).

The NiaP transporter encoded gene (*LOC_Os03g43720*) provides nicotinate transporter in plants (Jeanguenin *et al.*, 2012). Nicotinamide is a part of the NADH

and NADPH that important in energy metabolism. P deficiency affects reduced photosynthesis and photorespiration rate (Terry and Ulrich, 1973). Moreover, NADPH and NADH levels are increased to maintain energy homeostasis (Carstensen *et al.,* 2018).

An EF-hand family member or calmodulin-like gene (*LOC_Os06g40720*) is a regulatory member of second messenger calcium (Ca^{2+}) that involves in plant signal transduction various stresses, including P deficiency (Hernández *et al.,* 2007). The obvious calcium signaling in *Arabidopsis* root is dramatically triggered by P starvation but not by N starvation and correlates with a high level of reactive oxygen species (ROS) (Matthus *et al.,* 2019). *AtPsiCaM* (*Arabidopsis* Pi-starvation-induced CaM) had been proven for the interaction between P deficiency and the calmodulin signaling pathway in *Arabidopsis* (Duan *et al.,* 2005).

Two-component response regulator (LOC_Os06g43910) or *Arabidopsis* response regulator (ARR12) orthologue plays a key role in cytokinin signaling (Argyros *et al.,* 2008). The *AtARR12* is the phosphate starvation response protein target. Its expression is upregulated under P deficiency (Bustos *et al.,* 2010). ARR12 is a member of network regulation in root response to P deficiency by regulation of P signaling, auxin, gibberellin, and cytokinin hormone (Crombez *et al.,* 2019).

Less tillering is one of the response plant phenotypes under P starvation (Li *et al.,* 2003). The associated gene, *MONOCULM 1* (*OsMOC1*; *LOC_Os06g40780*) or *AtLAS* in *Arabidopsis*, plays a role in tillering formation by the initiation of meristematic axillary bud (Zhang *et al.,* 2020). *AtLAS* is controlled by SQUAMOSA-PROMOTER BINDING PROTEIN LIKE 9 (SPL9) and microRNA156. Interestingly, *AtSPL*s and microRNA156 are also regulated by P starvation (Lei *et al.,* 2016). Thus, this functional link between these studies makes high confidence in the candidate gene in P deficiency regulation.

CHAPTER VI

CONCLUSION

1. Novel Pi quantification method has been developed.

This study developed the punching method, which provided high throughput quantification based on the conventional Pi extraction and molybdate blue colorimetric assay. The method assisted in processing thousands of samples within 3 hours performing only one researcher. The punching method can be applied in large scale quantification that answers highly quantificational demand in phenomics and genomic study.

2. Hyperspectral reflectance indices can reflect Pi content under P deficient condition and they can be used for GWAS.

Among the 172 rice accessions and three P concentrations, Pi content is a very sensitive parameter that can detect the internal P deficient status within the plant of all the three different P treatments. On the other hand, hyperspectral measurement is clearly detectable in only the severely deficient treatment. I provided R_{740}/R_{560} and R_{750}/R_{700} indices as informative spectral reflectance indices representing the P deficiency phenotype in rice. Moreover, these indices can be used to apply in the genomic study by strong correlation with Pi content.

3. Based on exome sequences of 172 Thai rice cultivars, GWAS with hyperspectral indices can identify more causative genes for P deficient response than Pi content.

In this study, 30 candidate genes were identified by GWAS of leaf Pi content, while based on GWAS with novel hyperspectral indices revealed 78 candidate genes. Among these genes, six of them are known P responsive genes, two of which were predicted by both phenotypic inputs. Based on gene expression information, QTL mapping, and/or their potential functions from gene annotation, six candidate genes were proposed as novel genes involving in P-deficient response in rice, which can be validated and characterized in future studies.

REFERENCES

Abd-Elrahman, A., Pande-Chhetri, R., and Vallad, G. (2011). Design and development of a multi-purpose low-cost hyperspectral imaging system. *Remote Sensing, 3*(3), 570-586.

Al‑Ghazi, Y., Muller, B., Pinloche, S., Tranbarger, T., Nacry, P., Rossignol, M., Tardieu, F., and Doumas, P. (2003). Temporal responses of *Arabidopsis* root architecture to phosphate starvation: evidence for the involvement of auxin signalling. *Plant, Cell & Environment, 26*(7), 1053-1066.

Argyros, R. D., Mathews, D. E., Chiang, Y.-H., Palmer, C. M., Thibault, D. M., Etheridge, N., Argyros, D. A., Mason, M. G., Kieber, J. J., and Schaller, G. E. (2008). Type B response regulators of *Arabidopsis* play key roles in cytokinin signaling and plant development. *The Plant Cell, 20*(8), 2102-2116.

Atwell, S., Huang, Y. S., Vilhjalmsson, B. J., Willems, G., Horton, M., Li, Y., Meng, D., Platt, A., Tarone, A. M., Hu, T. T., *et al.* (2010). Genome-wide association study of 107 phenotypes in *Arabidopsis thalian*a inbred lines. *Nature, 465*(7298), 627-631. doi:10.1038/nature08800

Auld, D. S., Coassin, P. A., Coussens, N. P., Hensley, P., Klumpp-Thomas, C., Michael, S., Sittampalam, G. S., Trask, O. J., Wagner, B. K., and Weidner, J. R. (2020). Microplate selection and recommended practices in high-throughput screening and quantitative biology. *Assay Guidance Manual*.

Ayadi, A., David, P., Arrighi, J.-F., Chiarenza, S., Thibaud, M.-C., Nussaume, L., and Marin, E. (2015). Reducing the genetic redundancy of *Arabidopsis* PHOSPHATE TRANSPORTER1 transporters to study phosphate uptake and signaling. *Plant Physiology, 167*(4), 1511-1526.

Aziz, T., Sabir, M., Farooq, M., Maqsood, M. A., Ahmad, H. R., and Warraich, E. A. (2014). Phosphorus deficiency in plants: responses, adaptive mechanisms, and signaling. In *Plant Signaling: Understanding the Molecular Crosstalk* (pp. 133-148): Springer.

Bajguz, A., Chmur, M., and Gruszka, D. (2020). Comprehensive overview of the

Brassinosteroid biosynthesis pathways: Substrates, products, inhibitors, and connections. *Frontiers in plant science, 11*, 1034.

Balzergue, C., Puech-Pagès, V., Bécard, G., and Rochange, S. F. (2011). The regulation of arbuscular mycorrhizal symbiosis by phosphate in pea involves early and systemic signalling events. *Journal of experimental botany, 62*(3), 1049-1060.

Barnaby, J. Y., Huggins, T. D., Lee, H., McClung, A. M., Pinson, S. R., Oh, M., Bauchan, G. R., Tarpley, L., Lee, K., and Kim, M. S. (2020). Vis/NIR hyperspectral imaging distinguishes sub-population, production environment, and physicochemical grain properties in rice. *Scientific reports, 10*(1), 1-13.

Barnes, E., Clarke, T., Richards, S., Colaizzi, P., Haberland, J., Kostrzewski, M., Waller, P., Choi, C., Riley, E., and Thompson, T. (2000). *Coincident detection of crop water stress, nitrogen status and canopy density using ground based multispectral data.* Paper presented at the Proceedings of the Fifth International Conference on Precision Agriculture, Bloomington, MN, USA.

Basosi, R., Spinelli, D., Fierro, A., and Jez, S. (2014). Mineral nitrogen fertilizers: environmental impact of production and use. *Fertilizers: Components, Uses in Agriculture and Environmental Impacts*, 3-44.

Batlang, U., Baisakh, N., Ambavaram, M. M., and Pereira, A. (2013). Phenotypic and physiological evaluation for drought and salinity stress responses in rice. *Methods in Molecular Biology 956*, 209-225. doi:10.1007/978-1-62703-194-3_15

Bedini, A., Mercy, L., Schneider, C., Franken, P., and Lucic-Mercy, E. (2018). Unraveling the initial plant hormone signaling, metabolic mechanisms and plant defense triggering the endomycorrhizal symbiosis behavior. *Frontiers in plant science, 9*, 1800.

Bellante, G. J., Powell, S. L., Lawrence, R. L., Repasky, K. S., and Dougher, T. (2014). Hyperspectral detection of a subsurface CO_2 leak in the presence of water stressed vegetation. *PloS one, 9*(10), e108299.

Bogrekci, I., and Lee, W. (2005). Spectral phosphorus mapping using diffuse reflectance of soils and grass. *Biosystems Engineering, 91*(3), 305-312.

Borowik, T., Pettorelli, N., Sönnichsen, L., and Jedrzejewska, B. (2013). Normalized difference vegetation index (NDVI) as a predictor of forage availability for

ungulates in forest and field habitats. *European journal of wildlife research, 59*(5), 675-682.

Braun, M. (1996). Immunolocalization of myosin in rhizoids of *Chara globularis* Thuill. *Protoplasma, 191*(1-2), 1-8.

Bustos, R., Castrillo, G., Linhares, F., Puga, M. I., Rubio, V., Pérez-Pérez, J., Solano, R., Leyva, A., and Paz-Ares, J. (2010). A central regulatory system largely controls transcriptional activation and repression responses to phosphate starvation in *Arabidopsis*. *Plos Genetics, 6*(9), e1001102.

Carstensen, A., Herdean, A., Schmidt, S. B., Sharma, A., Spetea, C., Pribil, M., and Husted, S. (2018). The impacts of phosphorus deficiency on the photosynthetic electron transport chain. *Plant Physiology, 177*(1), 271-284.

Caturegli, L., Matteoli, S., Gaetani, M., Grossi, N., Magni, S., Minelli, A., Corsini, G., Remorini, D., and Volterrani, M. (2020). Effects of water stress on spectral reflectance of bermudagrass. *Scientific reports, 10*(1), 1-12.

Chakhonkaen, S., Pitnjam, K., Saisuk, W., Ukoskit, K., and Muangprom, A. (2012). Genetic structure of Thai rice and rice accessions obtained from the International Rice Research Institute. *Rice, 5*(1), 19.

Chankaew, S., Monkham, T., Pinta, W., Sanitchon, J., Kaewpradit, W., and Srinives, P. (2019). Screening tolerance to phosphorus deficiency and validation of phosphorus uptake 1 (Pup1) gene-linked markers in Thai indigenous upland rice germplasm. *Agronomy, 9*(2), 81.

Chaudhary, M. I., Adu-Gyamfi, J. J., Saneoka, H., Nguyen, N. T., Suwa, R., Kanai, S., El-Shemy, H. A., Lightfoot, D. A., and Fujita, K. (2008). The effect of phosphorus deficiency on nutrient uptake, nitrogen fixation and photosynthetic rate in mashbean, mungbean and soybean. *Acta Physiologiae Plantarum, 30*(4), 537-544.

Chen, X., Chen, M., He, H., Zhu, C., Peng, X., He, X., Fu, J., and Ouyang, L. (2011). Low-phosphorus tolerance and related physiological mechanism of Xieqingzao B//Xieqingzao B/Dongxiang wild rice BC1F9 populations. *Journal of Applied Ecology, 22*(5), 1169-1174.

Chen, Y., Wu, P., Zhao, Q., Tang, Y., Chen, Y., Li, M., Jiang, H., and Wu, G. (2018).

Overexpression of a phosphate starvation response AP2/ERF gene from physic nut in *Arabidopsis* alters root morphological traits and phosphate starvation-induced anthocyanin accumulation. *Frontiers in plant science, 9*, 1186.

Cho, M. A., and Skidmore, A. K. (2006). A new technique for extracting the red edge position from hyperspectral data: The linear extrapolation method. *Remote sensing of Environment, 101*(2), 181-193.

Choi, J., Lee, T., Cho, J., Servante, E. K., Pucker, B., Summers, W., Bowden, S., Rahimi, M., An, K., and An, G. (2020). The negative regulator SMAX1 controls mycorrhizal symbiosis and strigolactone biosynthesis in rice. *Nature communications, 11*(1), 1-13.

Chokwiwatkul, R., Tantipirom, N., Khunpolwatatna, N., Imyim, A., Suriya-aroonroj, D., Buaboocha, T., Pongpanich, M., Comai, L., and Chadchawan, S. (2017). Identification of genes involving in salt tolerance using GWAS data based on Na$^+$ content in local Thai rice leaves. *Genomics and Genetics, 10*(1&2), 27-37.

Colonna, V., D'Agostino, N., Garrison, E., Albrechtsen, A., Meisner, J., Facchiano, A., Cardi, T., and Tripodi, P. (2019). Genomic diversity and novel genome-wide association with fruit morphology in *Capsicum*, from 746k polymorphic sites. *Scientific reports, 9*(1), 1-14.

Contreras-Soto, R. I., Mora, F., de Oliveira, M. A. R., Higashi, W., Scapim, C. A., and Schuster, I. (2017). A genome-wide association study for agronomic traits in soybean using SNP markers and SNP-based haplotype analysis. *PloS one, 12*(2), e0171105.

Crombez, H., Motte, H., and Beeckman, T. (2019). Tackling plant phosphate starvation by the roots. *Developmental Cell, 48*(5), 599-615.

Dai, X., Wang, Y., Yang, A., and Zhang, W.-H. (2012). OsMYB2P-1, an R2R3 MYB transcription factor, is involved in the regulation of phosphate-starvation responses and root architecture in rice. *Plant Physiology, 159*(1), 169-183.

Dai, X., Wang, Y., Yang, A., and Zhang, W. H. (2012). OsMYB2P-1, an R2R3 MYB transcription factor, is involved in the regulation of phosphate-starvation responses and root architecture in rice. *Plant Physiol, 159*(1), 169-183. doi:10.1104/pp.112.194217

Daughtry, C., Walthall, C., Kim, M., De Colstoun, E. B., and McMurtrey Iii, J. (2000). Estimating corn leaf chlorophyll concentration from leaf and canopy reflectance. *Remote sensing of Environment, 74*(2), 229-239.

Deng, Q.-W., Luo, X.-D., Chen, Y.-L., Zhou, Y., Zhang, F.-T., Hu, B.-L., and Xie, J.-K. (2018). Transcriptome analysis of phosphorus stress responsiveness in the seedlings of Dongxiang wild rice (*Oryza rufipogon* Griff.). *Biological research, 51*(1), 1-12.

Devaiah, B. N., Madhuvanthi, R., Karthikeyan, A. S., and Raghothama, K. G. (2009). Phosphate starvation responses and gibberellic acid biosynthesis are regulated by the MYB62 transcription factor in *Arabidopsis*. *Molecular plant, 2*(1), 43-58.

Dissanayaka, D., Plaxton, W. C., Lambers, H., Siebers, M., Marambe, B., and Wasaki, J. (2018). Molecular mechanisms underpinning phosphorus-use efficiency in rice. *Plant, Cell & Environment, 41*(7), 1483-1496.

Duan, R.-J., Yi, K.-K., and Wu, P. (2005). The structure and phosphorus or potassium deficiency induced expression of a calmodulin-like protein gene in *Arabidopsis*. *Journal of Plant Physiology and Molecular Biology, 31*(5), 520-526.

Duff, S. M., Sarath, G., and Plaxton, W. C. (1994). The role of acid phosphatases in plant phosphorus metabolism. *Physiologia plantarum, 90*(4), 791-800.

El-Hendawy, S., Al-Suhaibani, N., Hassan, W., Tahir, M., and Schmidhalter, U. (2017). Hyperspectral reflectance sensing to assess the growth and photosynthetic properties of wheat cultivars exposed to different irrigation rates in an irrigated arid region. *PloS one, 12*(8), e0183262.

Fabianska, I., Bucher, M., and Häusler, R. E. (2019). Intracellular phosphate homeostasis– A short way from metabolism to signaling. *Plant Science, 286*, 57-67.

Fageria, N. (2001). Nutrient management for improving upland rice productivity and sustainability. *Communications in Soil Science and Plant Analysis, 32*(15-16), 2603-2629.

FAO, F. (2017). Agriculture organization of the United Nations. 2012. *FAO statistical yearbook*.

Feng, H., Guo, Z., Yang, W., Huang, C., Chen, G., Fang, W., Xiong, X., Zhang, H., Wang, G., and Xiong, L. (2017). An integrated hyperspectral imaging and genome-wide

association analysis platform provides spectral and genetic insights into the natural variation in rice. *Scientific reports, 7*(1), 1-10.

Feng, X., Zhan, Y., Wang, Q., Yang, X., Yu, C., Wang, H., Tang, Z., Jiang, D., Peng, C., and He, Y. (2020). Hyperspectral imaging combined with machine learning as a tool to obtain high-throughput plant salt-stress phenotyping. *The Plant Journal, 101*(6), 1448-1461.

Franco-Zorrilla, J. M., Valli, A., Todesco, M., Mateos, I., Puga, M. I., Rubio-Somoza, I., Leyva, A., Weigel, D., García, J. A., and Paz-Ares, J. (2007). Target mimicry provides a new mechanism for regulation of microRNA activity. *Nature genetics, 39*(8), 1033-1037.

Furbank, R. T., and Tester, M. (2011). Phenomics–technologies to relieve the phenotyping bottleneck. *Trends in plant science, 16*(12), 635-644.

Galili, T. (2015). Dendextend: an R package for visualizing, adjusting and comparing trees of hierarchical clustering. *Bioinformatics, 31*(22), 3718-3720.

Gamon, J., and Surfus, J. (1999). Assessing leaf pigment content and activity with a reflectometer. *The New Phytologist, 143*(1), 105-117.

Gamuyao, R., Chin, J. H., Pariasca-Tanaka, J., Pesaresi, P., Catausan, S., Dalid, C., Slamet-Loedin, I., Tecson-Mendoza, E. M., Wissuwa, M., and Heuer, S. (2012). The protein kinase Pstol1 from traditional rice confers tolerance of phosphorus deficiency. *Nature, 488*(7412), 535-539.

Gilbert-Girard, S., Savijoki, K., Yli-Kauhaluoma, J., and Fallarero, A. (2020). Optimization of a High-Throughput 384-Well Plate-Based Screening Platform with *Staphylococcus aureus* ATCC 25923 and *Pseudomonas aeruginosa* ATCC 15442 Biofilms. *International journal of molecular sciences, 21*(9), 3034.

Gill, M., and Ahmad, Z. (2003). Inter-varietal differences of absorbed-phosphorus utilization in cotton exposed to P-free nutrition: Part II. P-absorption and remobilization in plant. *Pakistan Journal of Scientific Research*.

Gitelson, A. A., Keydan, G. P., and Merzlyak, M. N. (2006). Three-band model for noninvasive estimation of chlorophyll, carotenoids, and anthocyanin contents in higher plant leaves. *Geophysical research letters, 33*(11).

Gitelson, A. A., Zur, Y., Chivkunova, O. B., and Merzlyak, M. N. (2002). Assessing carotenoid content in plant leaves with reflectance spectroscopy. *Photochemistry and photobiology, 75*(3), 272-281.

Gonzàlez-Meler, M., Giles, L., Thomas, R., and Siedow, J. (2001). Metabolic regulation of leaf respiration and alternative pathway activity in response to phosphate supply. *Plant, Cell & Environment, 24*(2), 205-215.

Grimm, D., Greshake, B., Kleeberger, S., Lippert, C., Stegle, O., Schölkopf, B., Weigel, D., and Borgwardt, K. (2012). easyGWAS: An integrated interspecies platform for performing genome-wide association studies. *arXiv*.

Gu, X., Cai, W., Fan, Y., Ma, Y., Zhao, X., and Zhang, C. (2018). Estimating foliar anthocyanin content of purple corn via hyperspectral model. *Food science & nutrition, 6*(3), 572-578.

Gundlach, G., and Luttermann-Semmer, E. (1987). The effect of pH and temperature on the stability and enzymatic activity of prostatic acid phosphatase. Studies on the optimization of a continuous monitored determination of acid phosphatase, II. *Clinical Chemistry and Laboratory Medicine 25*(7).

Guo, R. (2017). Simulation of Soybean Canopy Nutrient Contents by Hyperspectral Remote Sensing. *Applied Ecology and Environmental Research, 15*(4), 1185-1198. doi:10.15666/aeer/1504_11851198

Haefele, S., Nelson, A., and Hijmans, R. (2014). Soil quality and constraints in global rice production. *Geoderma, 235*, 250-259.

Halperin, M. L., and Kamel, K. S. (1998). Potassium. *The Lancet, 352*(9122), 135-140.

Hamblin, J., Stefanova, K., and Angessa, T. T. (2014). Variation in chlorophyll content per unit leaf area in spring wheat and implications for selection in segregating material. *PloS one, 9*(3), e92529.

Hammond, J. P., Bennett, M. J., Bowen, H. C., Broadley, M. R., Eastwood, D. C., May, S. T., Rahn, C., Swarup, R., Woolaway, K. E., and White, P. J. (2003). Changes in gene expression in *Arabidopsis* shoots during phosphate starvation and the potential for developing smart plants. *Plant Physiology, 132*(2), 578-596.

Han, B., and Huang, X. (2013). Sequencing-based genome-wide association study in rice.

Current opinion in plant biology, 16(2), 133-138.

Harris, C. R., Millman, K. J., van der Walt, S. J., Gommers, R., Virtanen, P., Cournapeau, D., Wieser, E., Taylor, J., Berg, S., Smith, N. J*., et al.* (2020). Array programming with NumPy. *Nature, 585*(7825), 357-362. doi:10.1038/s41586-020-2649-2

Hawkins, L. J., and Storey, K. B. (2017). Improved high-throughput quantification of luminescent microplate assays using a common Western-blot imaging system. *MethodsX, 4,* 413-422.

Hernández, G., Ramírez, M., Valdés-López, O., Tesfaye, M., Graham, M. A., Czechowski, T., Schlereth, A., Wandrey, M., Erban, A., and Cheung, F. (2007). Phosphorus stress in common bean: root transcript and metabolic responses. *Plant Physiology, 144*(2), 752-767.

Hernández, I., and Munné-Bosch, S. (2015). Linking phosphorus availability with photo-oxidative stress in plants. *Journal of experimental botany, 66*(10), 2889-2900.

Heuer, S., Lu, X., Chin, J. H., Tanaka, J. P., Kanamori, H., Matsumoto, T., De Leon, T., Ulat, V. J., Ismail, A. M., and Yano, M. (2009). Comparative sequence analyses of the major quantitative trait locus phosphorus uptake 1 (Pup1) reveal a complex genetic structure. *Plant Biotechnology Journal, 7*(5), 456-471.

HØGH-JENSEN, H., Schjoerring, J. K., and SOUSSANA, J. F. (2002). The influence of phosphorus deficiency on growth and nitrogen fixation of white clover plants. *Annals of Botany, 90*(6), 745-753.

Hruz, T., Laule, O., Szabo, G., Wessendorp, F., Bleuler, S., Oertle, L., Widmayer, P., Gruissem, W., and Zimmermann, P. (2008a). Genevestigator V3: A Reference Expression Database for the Meta-Analysis of Transcriptomes. *Advances in bioinformatics, 2008*, 420747. doi:10.1155/2008/420747

Hruz, T., Laule, O., Szabo, G., Wessendorp, F., Bleuler, S., Oertle, L., Widmayer, P., Gruissem, W., and Zimmermann, P. (2008b). Genevestigator v3: a reference expression database for the meta-analysis of transcriptomes. *Advances in bioinformatics, 2008*.

Huang, P., Luo, X., Jin, J., Wang, L., Zhang, L., Liu, J., and Zhang, Z. (2018). Improving high-throughput phenotyping using fusion of close-range hyperspectral camera

and low-cost depth sensor. *Sensors, 18*(8), 2711.

Huang, X., Zhao, Y., Li, C., Wang, A., Zhao, Q., Li, W., Guo, Y., Deng, L., Zhu, C., and Fan, D. (2012). Genome-wide association study of flowering time and grain yield traits in a worldwide collection of rice germplasm. *Nature genetics, 44*(1), 32-39.

Hunt Jr, E. R., and Rock, B. N. (1989). Detection of changes in leaf water content using near-and middle-infrared reflectances. *Remote sensing of Environment, 30*(1), 43-54.

Irfan, M., Aziz, T., Maqsood, M. A., Bilal, H. M., Siddique, K. H., and Xu, M. (2020). Phosphorus (P) use efficiency in rice is linked to tissue-specific biomass and P allocation patterns. *Scientific reports, 10*(1), 1-14.

Ito, S., Nozoye, T., Sasaki, E., Imai, M., Shiwa, Y., Shibata-Hatta, M., Ishige, T., Fukui, K., Ito, K., and Nakanishi, H. (2015). Strigolactone regulates anthocyanin accumulation, acid phosphatases production and plant growth under low phosphate condition in *Arabidopsis*. *PloS one, 10*(3), e0119724.

Jay, S., Hadoux, X., Gorretta, N., and Rabatel, G. (2014). *Potential of hyperspectral imagery for nitrogen content retrieval in sugar beet leaves.* Paper presented at the International Conference on Agricultural Engineering (AgEng 2014).

Jeanguenin, L., Lara-Núñez, A., Rodionov, D. A., Osterman, A. L., Komarova, N. Y., Rentsch, D., Gregory, J. F., and Hanson, A. D. (2012). Comparative genomics and functional analysis of the NiaP family uncover nicotinate transporters from bacteria, plants, and mammals. *Functional & integrative genomics, 12*(1), 25-34.

Jewel, Z. A., Ali, J., Mahender, A., Hernandez, J., Pang, Y., and Li, Z. (2019). Identification of quantitative trait loci associated with nutrient use efficiency traits, using SNP markers in an early backcross population of rice (*Oryza sativa* L.). *International journal of molecular sciences, 20*(4), 900.

Jiang, C., Gao, X., Liao, L., Harberd, N. P., and Fu, X. (2007). Phosphate starvation root architecture and anthocyanin accumulation responses are modulated by the gibberellin-DELLA signaling pathway in *Arabidopsis*. *Plant Physiology, 145*(4), 1460-1470.

Jones, C. L., Weckler, P. R., Maness, N. O., Stone, M. L., and Jayasekara, R. (2004). *Estimating water stress in plants using hyperspectral sensing.* Paper presented

at the 2004 ASAE Annual Meeting.

Kang, H. M., Zaitlen, N. A., Wade, C. M., Kirby, A., Heckerman, D., Daly, M. J., and Eskin, E. (2008). Efficient Control of Population Structure in Model Organism Association Mapping. *Genetics, 178*(3), 1709. doi:10.1534/genetics.107.080101

Kanning, M., Kühling, I., Trautz, D., and Jarmer, T. (2018). High-resolution UAV-based hyperspectral imagery for LAI and chlorophyll estimations from wheat for yield prediction. *Remote Sensing, 10*(12), 2000.

Kanno, S., Cuyas, L., Javot, H., Bligny, R., Gout, E., Dartevelle, T., Hanchi, M., Nakanishi, T. M., Thibaud, M.-C., and Nussaume, L. (2016). Performance and limitations of phosphate quantification: guidelines for plant biologists. *Plant and Cell Physiology, 57*(4), 690-706.

Kassambara, A., and Mundt, F. (2017). Package 'factoextra'. Retrieved from http://www.sthda.com/english/rpkgs/factoextra

Katiyar, A., Smita, S., Lenka, S. K., Rajwanshi, R., Chinnusamy, V., and Bansal, K. C. (2012). Genome-wide classification and expression analysis of MYB transcription factor families in rice and *Arabidopsis*. *BMC genomics, 13*(1), 544.

Kawahara, Y., de la Bastide, M., Hamilton, J. P., Kanamori, H., McCombie, W. R., Ouyang, S., Schwartz, D. C., Tanaka, T., Wu, J., and Zhou, S. (2013). Improvement of the Oryza sativa Nipponbare reference genome using next generation sequence and optical map data. *Rice, 6*(1), 1-10.

Kim, B., Dai, X., Zhang, W., Zhuang, Z., Sanchez, D. L., Lübberstedt, T., Kang, Y., Udvardi, M. K., Beavis, W. D., and Xu, S. (2019). GWASpro: a high-performance genome-wide association analysis server. *Bioinformatics, 35*(14), 2512-2514.

Kim, D. M., Zhang, H., Zhou, H., Du, T., Wu, Q., Mockler, T. C., and Berezin, M. Y. (2015). Highly sensitive image-derived indices of water-stressed plants using hyperspectral imaging in SWIR and histogram analysis. *Scientific reports, 5*, 15919.

Kim, M. S. (1994). *The Use of Narrow Spectral Bands for Improving Remote Sensing Estimations of Fractionally Absorbed Photosynthetically Active Radiation.*

Kim, Y., Glenn, D. M., Park, J., Ngugi, H. K., and Lehman, B. L. (2011). Hyperspectral image analysis for water stress detection of apple trees. *Computers and Electronics in*

Agriculture, 77(2), 155-160.

Klemperer, D. G. (2007). Keggin structure. Retrieved from https://en.wikipedia.org/wiki/Keggin_structure

Koepke, L., Winter, B., Grenzner, A., Regensburger, K., Engelhart, S., van der Merwe, J. A., Krebs, S., Blum, H., Kirchhoff, F., and Sparrer, K. M. (2020). An improved method for high-throughput quantification of autophagy in mammalian cells. *Scientific reports, 10*(1), 1-20.

Kokaly, R. F., Asner, G. P., Ollinger, S. V., Martin, M. E., and Wessman, C. A. (2009). Characterizing canopy biochemistry from imaging spectroscopy and its application to ecosystem studies. *Remote sensing of Environment, 113*, S78-S91.

Kovach, M. J., Sweeney, M. T., and McCouch, S. R. (2007). New insights into the history of rice domestication. *Trends in Genetics, 23*(11), 578-587.

Kuhn, M. (2012). The caret package. *R Foundation for Statistical Computing*. Retrieved from https://cran.r-project.org/package=caret

Kuska, M. T., Behmann, J., and Mahlein, A.-K. (2018). Potential of hyperspectral imaging to detect and identify the impact of chemical warfare compounds on plant tissue. *Pure and Applied Chemistry, 90*(10), 1615-1624.

Lanfranco, L., Fiorilli, V., Venice, F., and Bonfante, P. (2018). Strigolactones cross the kingdoms: plants, fungi, and bacteria in the arbuscular mycorrhizal symbiosis. *Journal of experimental botany, 69*(9), 2175-2188.

Lei, K.-J., Lin, Y.-M., Ren, J., Bai, L., Miao, Y.-C., An, G.-Y., and Song, C.-P. (2016). Modulation of the phosphate-deficient responses by microRNA156 and its targeted SQUAMOSA PROMOTER BINDING PROTEIN-LIKE 3 in *Arabidopsis*. *Plant and Cell Physiology, 57*(1), 192-203.

Lekklar, C., Pongpanich, M., Suriya-arunroj, D., Chinpongpanich, A., Tsai, H., Comai, L., Chadchawan, S., and Buaboocha, T. (2019). Genome-wide association study for salinity tolerance at the flowering stage in a panel of rice accessions from Thailand. *BMC genomics, 20*(1), 76. doi:10.1186/s12864-018-5317-2

Li, H., Peng, Z., Yang, X., Wang, W., Fu, J., Wang, J., Han, Y., Chai, Y., Guo, T., and Yang, N. (2013). Genome-wide association study dissects the genetic architecture of oil biosynthesis in maize kernels. *Nature genetics, 45*(1), 43-50.

Li, J., Xie, Y., Dai, A., Liu, L., and Li, Z. (2009). Root and shoot traits responses to phosphorus deficiency and QTL analysis at seedling stage using introgression lines of rice. *Journal of Genetics and Genomics, 36*(3), 173-183.

Li, M., Shi, X., Guo, C., and Lin, S. (2016). Phosphorus deficiency inhibits cell division but not growth in the dinoflagellate *Amphidinium carterae*. *Frontiers in microbiology, 7*, 826.

Li, X., Qian, Q., Fu, Z., Wang, Y., Xiong, G., Zeng, D., Wang, X., Liu, X., Teng, S., and Hiroshi, F. (2003). Control of tillering in rice. *Nature, 422*(6932), 618-621.

Liang, Y., Urano, D., Liao, K.-L., Hedrick, T. L., Gao, Y., and Jones, A. M. (2017). A nondestructive method to estimate the chlorophyll content of *Arabidopsis* seedlings. *Plant methods, 13*(1), 1-10.

Lin, W.-Y., Lin, S.-I., and Chiou, T.-J. (2009). Molecular regulators of phosphate homeostasis in plants. *Journal of experimental botany, 60*(5), 1427-1438.

Liu, C., Muchhal, U. S., Uthappa, M., Kononowicz, A. K., and Raghothama, K. G. (1998). Tomato phosphate transporter genes are differentially regulated in plant tissues by phosphorus. *Plant Physiology, 116*(1), 91-99.

Liu, K., Ma, B., Luan, L., and Li, C. (2011). Nitrogen, phosphorus, and potassium nutrient effects on grain filling and yield of high-yielding summer corn. *Journal of plant nutrition, 34*(10), 1516-1531.

López-Bucio, J., Hernández-Abreu, E., Sánchez-Calderón, L., Nieto-Jacobo, M. F., Simpson, J., and Herrera-Estrella, L. (2002). Phosphate availability alters architecture and causes changes in hormone sensitivity in the *Arabidopsis* root system. *Plant Physiology, 129*(1), 244-256.

Lowe, A., Harrison, N., and French, A. P. (2017). Hyperspectral image analysis techniques for the detection and classification of the early onset of plant disease and stress. *Plant methods, 13*(1), 80.

Lozano Fernández, J., Orozco Orozco, L. F., and Montoya Munera, L. F. (2018). Effect of nitrogen, phosphorus and potassium fertilization on the yield of broccoli cultivars. *Revista Facultad Nacional de Agronomía Medellín, 71*(1), 8375-8386.

LÜ, G.-h., WU, Y.-f., BAI, W.-b., Bao, M., WANG, C.-y., and SONG, J.-q. (2013). Influence of high temperature stress on net photosynthesis, dry matter partitioning and rice

grain yield at flowering and grain filling stages. *Journal of Integrative Agriculture, 12*(4), 603-609.

Lu, L., Qiu, W., Gao, W., Tyerman, S. D., Shou, H., and Wang, C. (2016). OsPAP10c, a novel secreted acid phosphatase in rice, plays an important role in the utilization of external organic phosphorus. *Plant, Cell & Environment, 39*(10), 2247-2259.

Maclean, J., Hardy, B., and Hettel, G. (2013). *Rice Almanac: Source book for one of the most important economic activities on earth*: IRRI.

MacRae, C. A., and Vasan, R. S. (2011). Next-generation genome-wide association studies: time to focus on phenotype? *Circulation Cardiovascular Genetics, 4*(4), 334-336. doi:10.1161/CIRCGENETICS.111.960765

Massawe, P. I., and Mrema, J. (2017). Effects of different phosphorus fertilizers on rice (*Oryza sativa* L.) yield components and grain yields. *Asian Journal of Advances in Agricultural Research*, 1-13.

Matthus, E., Wilkins, K. A., Swarbreck, S. M., Doddrell, N. H., Doccula, F. G., Costa, A., and Davies, J. M. (2019). Phosphate starvation alters abiotic-stress-induced cytosolic free calcium increases in roots. *Plant Physiology, 179*(4), 1754-1767.

McKelvie, I. D., Peat, D. M., and Worsfold, P. J. (1995). *Analytical perspective. Techniques for the quantification and speciation of phosphorus in natural waters.* Paper presented at the Analytical Proceedings Including Analytical Communications.

Mehra, P., Pandey, B. K., and Giri, J. (2015). Comparative Morphophysiological Analyses and Molecular Profiling Reveal Pi-Efficient Strategies of a Traditional Rice Genotype. *Front Plant Sci, 6*, 1184. doi:10.3389/fpls.2015.01184

Mehra, P., Pandey, B. K., and Giri, J. (2015). Genome-wide DNA polymorphisms in low phosphate tolerant and sensitive rice genotypes. *Scientific reports, 5*, 13090.

Mehra, P., Pandey, B. K., and Giri, J. (2016). Comparative morphophysiological analyses and molecular profiling reveal Pi-efficient strategies of a traditional rice genotype. *Frontiers in plant science, 6*, 1184.

Mertens, E., Larondelle, Y., and Hers, H.-G. (1990). Induction of Pyrophosphate:Fructose 6-Phosphate 1-Phosphotransferase by Anoxia in Rice Seedlings. *Plant*

Physiology, 93(2), 584. doi:10.1104/pp.93.2.584

Mikulska, M., Bomsel, J.-L., and Rychter, A. (1998). The influence of phosphate deficiency on photosynthesis, respiration and adenine nucleotide pool in bean leaves. *Photosynthetica, 35*(1), 79-88.

Milton, N., Eiswerth, B., and Ager, C. (1991). Effect of phosphorus deficiency on spectral reflectance and morphology of soybean plants. *Remote sensing of Environment, 36*(2), 121-127.

Misson, J., Raghothama, K. G., Jain, A., Jouhet, J., Block, M. A., Bligny, R., Ortet, P., Creff, A., Somerville, S., and Rolland, N. (2005). A genome-wide transcriptional analysis using *Arabidopsis thaliana* Affymetrix gene chips determined plant responses to phosphate deprivation. *Proceedings of the National Academy of Sciences, 102*(33), 11934-11939.

Moghimi, A., Yang, C., Miller, M. E., Kianian, S. F., and Marchetto, P. M. (2018). A novel approach to assess salt stress tolerance in wheat using hyperspectral imaging. *Frontiers in plant science, 9*, 1182.

Mori, K., and Nakamura, M. (1959). Notes on the colorimetric determination of inorganic orthophosphate: part I. determination of inorganic orthophosphate in the presence of some acid-labile phosphate compounds of biochemical significance part II. determination of total phosphorus. *Journal of the Agricultural Chemical Society of Japan, 23*(4), 272-280.

Mukamuhirwa, A., Persson Hovmalm, H., Bolinsson, H., Ortiz, R., Nyamangyoku, O., and Johansson, E. (2019). Concurrent drought and temperature stress in rice—a possible result of the predicted climate change: effects on yield attributes, eating characteristics, and health promoting compounds. *International journal of environmental research and public health, 16*(6), 1043.

Nagasubramanian, K., Jones, S., Singh, A. K., Sarkar, S., Singh, A., and Ganapathysubramanian, B. (2019). Plant disease identification using explainable 3D deep learning on hyperspectral images. *Plant methods, 15*(1), 98.

Nanamori, M., Shinano, T., Wasaki, J., Yamamura, T., Rao, I. M., and Osaki, M. (2004). Low phosphorus tolerance mechanisms: phosphorus recycling and photosynthate partitioning in the tropical forage grass, *Brachiaria* hybrid cultivar Mulato

compared with rice. *Plant and Cell Physiology, 45*(4), 460-469.

Naumann, C., Müller, J., Sakhonwasee, S., Wieghaus, A., Hause, G., Heisters, M., Bürstenbinder, K., and Abel, S. (2019). The Local Phosphate Deficiency Response Activates Endoplasmic Reticulum Stress-Dependent Autophagy. *Plant Physiology, 179*(2), 460. doi:10.1104/pp.18.01379

Neumann, G., and Römheld, V. (1999). Root excretion of carboxylic acids and protons in phosphorus-deficient plants. *Plant and Soil, 211*(1), 121-130.

Ni, J., Wu, P., Senadhira, D., and Huang, N. (1998). Mapping QTLs for phosphorus deficiency tolerance in rice (*Oryza sativa* L.). *Theoretical and Applied Genetics, 97*(8), 1361-1369.

Osborne, S., Schepers, J. S., Francis, D., and Schlemmer, M. R. (2002). Detection of phosphorus and nitrogen deficiencies in corn using spectral radiance measurements. *Agronomy journal, 94*(6), 1215-1221.

Özyiğit, Y., and Bilgen, M. (2013). Use of spectral reflectance values for determining nitrogen, phosphorus, and potassium contents of rangeland plants. *Journal of Agricultural Science and Technology, 15*(7), 1537-1545.

Pandey, P., Ge, Y., Stoerger, V., and Schnable, J. C. (2017). High throughput in vivo analysis of plant leaf chemical properties using hyperspectral imaging. *Frontiers in plant science, 8*, 1348.

Pant, B. D., Burgos, A., Pant, P., Cuadros-Inostroza, A., Willmitzer, L., and Scheible, W.-R. (2015). The transcription factor PHR1 regulates lipid remodeling and triacylglycerol accumulation in *Arabidopsis thaliana* during phosphorus starvation. *Journal of experimental botany, 66*(7), 1907-1918.

Peng, Y., Zhang, M., Xu, Z., Yang, T., Su, Y., Zhou, T., Wang, H., Wang, Y., and Lin, Y. (2020). Estimation of leaf nutrition status in degraded vegetation based on field survey and hyperspectral data. *Scientific reports, 10*(1), 1-12.

Peñuelas, J., and Filella, I. (1998). Visible and near-infrared reflectance techniques for diagnosing plant physiological status. *Trends in plant science, 3*(4), 151-156.

Pereira, J. F., Pimentel, M. F., Amigo, J. M., and Honorato, R. S. (2020). Detection and identification of *Cannabis sativa* L. using near infrared hyperspectral imaging and machine learning methods. A feasibility study. *Spectrochimica Acta Part A:*

Molecular and Biomolecular Spectroscopy, 118385.

Planas-Riverola, A., Gupta, A., Betegón-Putze, I., Bosch, N., Ibañes, M., and Caño-Delgado, A. I. (2019). Brassinosteroid signaling in plant development and adaptation to stress. *Development, 146*(5).

Plaxton, W. C., and Carswell, M. C. (1999). *Metabolic aspects of the phosphate starvation response in plants*. New York: Marcel Dekker.

Plaxton, W. C., and Tran, H. T. (2011). Metabolic adaptations of phosphate-starved plants. *Plant Physiology, 156*(3), 1006-1015.

PSI. (2018). *POLYPEN RP400 & RP410 : Manual and User Guide*. In P. S. Instruments (Ed.). Retrieved from https://handheld.psi.cz/documents/PolyPen%20RP400_RP410_Manual_03_2020.pdf

Psomiadis, E., Dercas, N., Dalezios, N. R., and Spyropoulos, N. V. (2017). *Evaluation and cross-comparison of vegetation indices for crop monitoring from sentinel-2 and worldview-2 images.* Paper presented at the Remote Sensing for Agriculture, Ecosystems, and Hydrology XIX.

Ranc, N., Muños, S., Xu, J., Le Paslier, M.-C., Chauveau, A., Bounon, R., Rolland, S., Bouchet, J.-P., Brunel, D., and Causse, M. (2012). Genome-wide association mapping in tomato (*Solanum lycopersicum*) is possible using genome admixture of *Solanum lycopersicum* var. cerasiforme. *G3: Genes, Genomes, Genetics, 2*(8), 853-864.

Ren, W.-L., Wen, Y.-J., Dunwell, J. M., and Zhang, Y.-M. (2018). pKWmEB: integration of Kruskal–Wallis test with empirical Bayes under polygenic background control for multi-locus genome-wide association study. *Heredity, 120*(3), 208-218.

Ribes, M., Russias, G., Tregoat, D., and Fournier, A. (2020). Towards low-cost hyperspectral single-pixel imaging for plant phenotyping. *Sensors, 20*(4), 1132.

Roberts, D. A., Roth, K. L., and Perroy, R. L. (2016). 14 hyperspectral vegetation indices. *Hyperspectral remote sensing of vegetation.*, 309.

Romano, J. M., Dubos, C., Prouse, M. B., Wilkins, O., Hong, H., Poole, M., Kang, K. Y., Li, E., Douglas, C. J., and Western, T. L. (2012). AtMYB61, an R2R3‑MYB transcription

factor, functions as a pleiotropic regulator via a small gene network. *New Phytologist, 195*(4), 774-786.

Rouse Jr, J., Haas, R., Deering, D., Schell, J., and Harlan, J. (1974). *Monitoring the Vernal Advancement and Retrogradation (Green Wave Effect) of Natural Vegetation.[Great Plains Corridor].* Retrieved from https://ntrs.nasa.gov/api/citations/19730017588/downloads/19730017588.pdf

Ruan, W., Guo, M., Xu, L., Wang, X., Zhao, H., Wang, J., and Yi, K. (2018). An SPX-RLI1 module regulates leaf inclination in response to phosphate availability in rice. *The Plant Cell, 30*(4), 853-870.

Sadiq, G., Khan, A. A., Inamullah, A. R., Fayyaz, H., Naz, G., Nawaz, H., Ali, I., Raza, H., Amin, J., and Ali, S. (2017). Impact of phosphorus and potassium levels on yield and yield components of maize. *Pure and Applied Biology, 6*(3), 1071-1078.

Salvo-Chirnside, E., Kane, S., and Kerr, L. E. (2011). Protocol: high throughput silica-based purification of RNA from *Arabidopsis* seedlings in a 96-well format. *Plant methods, 7*(1), 40.

Samreen, S., and Kausar, S. (2019). Phosphorus fertilizer: the original and commercial sources. In *Phosphorus-Recovery and Recycling*: IntechOpen.

Schachtman, D. P., Reid, R. J., and Ayling, S. M. (1998). Phosphorus uptake by plants: from soil to cell. *Plant Physiology, 116*(2), 447-453.

Secco, D., Jabnoune, M., Walker, H., Shou, H., Wu, P., Poirier, Y., and Whelan, J. (2013). Spatio-temporal transcript profiling of rice roots and shoots in response to phosphate starvation and recovery. *The Plant Cell, 25*(11), 4285-4304.

Shehzad, T., Iwata, H., and Okuno, K. (2009). Genome-wide association mapping of quantitative traits in sorghum (*Sorghum bicolor* (L.) Moench) by using multiple models. *Breeding science, 59*(3), 217-227.

Simko, I., Pechenick, D. A., McHale, L. K., Truco, M. J., Ochoa, O. E., Michelmore, R. W., and Scheffler, B. E. (2009). Association mapping and marker-assisted selection of the lettuce dieback resistance gene Tvr1. *BMC plant biology, 9*(1), 135.

Singh, A. P., Fridman, Y., Friedlander-Shani, L., Tarkowska, D., Strnad, M., and Savaldi-Goldstein, S. (2014). Activity of the brassinosteroid transcription factors BRASSINAZOLE RESISTANT1 and BRASSINOSTEROID INSENSITIVE1-ETHYL

METHANESULFONATE-SUPPRESSOR1/BRASSINAZOLE RESISTANT2 blocks developmental reprogramming in response to low phosphate availability. *Plant Physiology, 166*(2), 678-688.

Singh, S., Badgujar, G., Reddy, V., Fleisher, D., and Timlin, D. (2013). Effect of phosphorus nutrition on growth and physiology of cotton under ambient and elevated carbon dioxide. *Journal of Agronomy and Crop Science, 199*(6), 436-448.

Sun, D., Cen, H., Weng, H., Wan, L., Abdalla, A., El-Manawy, A. I., Zhu, Y., Zhao, N., Fu, H., and Tang, J. (2019). Using hyperspectral analysis as a potential high throughput phenotyping tool in GWAS for protein content of rice quality. *Plant methods, 15*(1), 54.

Sun, G., Ding, Y., Wang, X., Lu, W., Sun, Y., and Yu, H. (2019). Nondestructive determination of nitrogen, phosphorus and potassium contents in greenhouse Tomato plants based on multispectral three-dimensional imaging. *Sensors, 19*(23), 5295.

Sun, W., Liang, L., Meng, X., Li, Y., Gao, F., Liu, X., Wang, S., Gao, X., and Wang, L. (2016). Biochemical and molecular characterization of a flavonoid 3-O-glycosyltransferase responsible for anthocyanins and flavonols biosynthesis in *Freesia hybrida*. *Frontiers in plant science, 7*, 410.

Tazisong, I. A., Senwo, Z. N., and He, Z. (2015). Phosphatase hydrolysis of organic phosphorus compounds. *Advances in Enzyme Research, 3*(02), 39.

Techarang, J., Phanchaisri, B., and Yu, L. D. (2019). Rice Breeding for Rice Farmers of Thailand 4.0 Retrieved from http://thep-center.org/src2/views/network-academic-news_en.php?news_id=226

Terry, N., and Ulrich, A. (1973). Effects of phosphorus deficiency on the photosynthesis and respiration of leaves of sugar beet. *Plant Physiology, 51*(1), 43-47.

ThaiRiceExportersAssociation. (2020). Rice Exports Statistics Retrieved from http://www.thairiceexporters.or.th/List_%20of_statistic.htm

Tian, D., Wang, P., Tang, B., Teng, X., Li, C., Liu, X., Zou, D., Song, S., and Zhang, Z. (2020). GWAS Atlas: a curated resource of genome-wide variant-trait associations in plants and animals. *Nucleic Acids Research, 48*(D1), D927-D932.

Tiwari, S. C., and Polito, V. (1990). The initiation and organization of microtubules in

germinating pear (*Pyrus communis* L.) pollen. *European journal of cell biology, 53*(2), 384-389.

Turner, D. H., and Turner, J. F. (1961). The use of perchloric acid in the extraction of phosphoric compounds from plant tissues. *Biochimica et Biophysica Acta, 51*(3), 591-593.

Turner, S. D. (2014). qqman: an R package for visualizing GWAS results using QQ and manhattan plots. *Biorxiv*, 005165.

van de Wiel, C. C., van der Linden, C. G., and Scholten, O. E. (2016). Improving phosphorus use efficiency in agriculture: opportunities for breeding. *Euphytica, 207*(1), 1-22.

Van Laere, A.-S., Nguyen, M., Braunschweig, M., Nezer, C., Collette, C., Moreau, L., Archibald, A. L., Haley, C. S., Buys, N., Tally, M., *et al.* (2003). A regulatory mutation in IGF2 causes a major QTL effect on muscle growth in the pig. *Nature, 425*(6960), 832-836. doi:10.1038/nature02064

Vanavichit, A., Kamolsukyeunyong, W., Siangliw, M., Siangliw, J. L., Traprab, S., Ruengphayak, S., Chaichoompu, E., Saensuk, C., Phuvanartnarubal, E., and Toojinda, T. (2018). Thai Hom Mali Rice: origin and breeding for subsistence rainfed lowland rice system. *Rice, 11*(1), 20.

Vance, C. P., Uhde-Stone, C., and Allan, D. L. (2003). Phosphorus acquisition and use: critical adaptations by plants for securing a nonrenewable resource. *New Phytologist, 157*(3), 423-447.

Vejchasarn, P., Lynch, J. P., and Brown, K. M. (2016). Genetic variability in phosphorus responses of rice root phenotypes. *Rice, 9*(1), 29.

Virtanen, P., Gommers, R., Oliphant, T. E., Haberland, M., Reddy, T., Cournapeau, D., Burovski, E., Peterson, P., Weckesser, W., and Bright, J. (2020). SciPy 1.0: fundamental algorithms for scientific computing in Python. *Nature methods, 17*(3), 261-272.

Walshe, D., McInerney, D., Van De Kerchove, R., Goyens, C., Balaji, P., and Byrne, K. A. (2020). Detecting nutrient deficiency in spruce forests using multispectral satellite imagery. *International Journal of Applied Earth Observation and*

Geoinformation, 86, 101975.

Wang, B., Li, Y., and Zhang, W.-H. (2012). Brassinosteroids are involved in response of cucumber (*Cucumis sativus*) to iron deficiency. *Annals of Botany, 110*(3), 681-688.

Wang, D., Vinson, R., Holmes, M., Seibel, G., Bechar, A., Nof, S., and Tao, Y. (2019). Early detection of tomato spotted wilt virus by hyperspectral imaging and outlier removal auxiliary classifier generative adversarial nets (OR-AC-GAN). *Scientific reports, 9*(1), 1-14.

Wang, M., Jiang, N., Jia, T., Leach, L., Cockram, J., Waugh, R., Ramsay, L., Thomas, B., and Luo, Z. (2012). Genome-wide association mapping of agronomic and morphologic traits in highly structured populations of barley cultivars. *Theoretical and Applied Genetics, 124*(2), 233-246.

Wang, Y.-J., Jin, G., Li, L.-Q., Liu, Y., Kalkhajeh, Y. K., Ning, J.-M., and Zhang, Z.-Z. (2020). NIR hyperspectral imaging coupled with chemometrics for nondestructive assessment of phosphorus and potassium contents in tea leaves. *Infrared Physics & Technology, 108*, 103365.

Wang, Y., Cao, J.-J., Wang, K.-X., Xia, X.-J., Shi, K., Zhou, Y.-H., Yu, J.-Q., and Zhou, J. (2019). BZR1 mediates brassinosteroid-induced autophagy and nitrogen starvation in tomato. *Plant Physiology, 179*(2), 671-685.

Wang, Z.-Q., Huang, H., Deng, J.-M., and Liu, J.-Q. (2015). Scaling the respiratory metabolism to phosphorus relationship in plant seedlings. *Scientific reports, 5*, 16377.

Wang, Z., Ruan, W., Shi, J., Zhang, L., Xiang, D., Yang, C., Li, C., Wu, Z., Liu, Y., and Yu, Y. (2014). Rice SPX1 and SPX2 inhibit phosphate starvation responses through interacting with PHR2 in a phosphate-dependent manner. *Proceedings of the National Academy of Sciences, 111*(41), 14953-14958.

Waskom, M., Botvinnik, O., Hobson, P., Warmenhoven, J., Cole, J., Halchenko, Y., Vanderplas, J., Hoyer, S., Villalba, S., and Quintero, E. (2014). Seaborn: statistical data visualization. *URL: https://seaborn. pydata. org/(visited on 2017-05-15)*.

Wasteneys, G., Willingale-Theune, J., and Menzel, D. (1997). Freeze shattering: a simple

and effective method for permeabilizing higher plant cell walls. *Journal of Microscopy, 188*(1), 51-61.

Wissuwa, M., and Ae, N. (2001). Genotypic variation for tolerance to phosphorus deficiency in rice and the potential for its exploitation in rice improvement. *Plant Breeding, 120*(1), 43-48.

Wissuwa, M., Kondo, K., Fukuda, T., Mori, A., Rose, M. T., Pariasca-Tanaka, J., Kretzschmar, T., Haefele, S. M., and Rose, T. J. (2015). Unmasking Novel Loci for Internal Phosphorus Utilization Efficiency in Rice Germplasm through Genome-Wide Association Analysis. *PloS one, 10*(4), e0124215. doi:10.1371/journal.pone.0124215

Wissuwa, M., Yano, M., and Ae, N. (1998). Mapping of QTLs for phosphorus-deficiency tolerance in rice (Oryza sativa L.). *Theoretical and Applied Genetics, 97*(5-6), 777-783.

Workman, D. (2020). Rice Exports by Country. Retrieved from http://www.worldstopexports.com/rice-exports-country/

Wu, J., Feng, F., Lian, X., Teng, X., Wei, H., Yu, H., Xie, W., Yan, M., Fan, P., and Li, Y. (2015). Genome-wide Association Study (GWAS) of mesocotyl elongation based on re-sequencing approach in rice. *BMC plant biology, 15*(1), 1-10.

Wu, P., Shou, H., Xu, G., and Lian, X. (2013). Improvement of phosphorus efficiency in rice on the basis of understanding phosphate signaling and homeostasis. *Current opinion in plant biology, 16*(2), 205-212.

Xu, H. X., Weng, X. Y., and Yang, Y. (2007). Effect of phosphorus deficiency on the photosynthetic characteristics of rice plants. *Russian Journal of Plant Physiology, 54*(6), 741-748. doi:10.1134/s1021443707060040

Yang, J., Tian, Y., Yao, X., Cao, W., and Zhu, Y. (2010). Estimating leaf carotenoid content with hyperspectral parameters in rice. *Journal of Plant Ecology, 34*(7), 845-854.

Yang, W., Guo, Z., Huang, C., Duan, L., Chen, G., Jiang, N., Fang, W., Feng, H., Xie, W., and Lian, X. (2014). Combining high-throughput phenotyping and genome-wide association studies to reveal natural genetic variation in rice. *Nature communications, 5*, 5087.

Yang, W. T., Baek, D., Yun, D.-J., Hwang, W. H., Park, D. S., Nam, M. H., Chung, E. S.,

Chung, Y. S., Yi, Y. B., and Kim, D. H. (2014). Overexpression of OsMYB4P, an R2R3-type MYB transcriptional activator, increases phosphate acquisition in rice. *Plant Physiology and Biochemistry, 80*, 259-267.

Yang, W. T., Baek, D., Yun, D.-J., Lee, K. S., Hong, S. Y., Bae, K. D., Chung, Y. S., Kwon, Y. S., Kim, D. H., and Jung, K. H. (2018). Rice OsMYB5P improves plant phosphate acquisition by regulation of phosphate transporter. *PloS one, 13*(3), e0194628.

Yang, X., Yu, Y., and Fan, W. (2015). Chlorophyll content retrieval from hyperspectral remote sensing imagery. *Environmental monitoring and assessment, 187*(7), 456.

Yaseen, M., Khan, R., Gill, M., Aziz, A., Aslam, M., and Khan, A. (2000). Genetic variability among different rice cultivars for Zn uptake and utilization. *Pakistan Journal of Biological Sciences, 3*(7), 1174-1176.

Yi, K., Wu, Z., Zhou, J., Du, L., Guo, L., Wu, Y., and Wu, P. (2005). OsPTF1, a novel transcription factor involved in tolerance to phosphate starvation in rice. *Plant Physiology, 138*(4), 2087-2096.

Yin, Y., Borges, G., Sakuta, M., Crozier, A., and Ashihara, H. (2012). Effect of phosphate deficiency on the content and biosynthesis of anthocyanins and the expression of related genes in suspension-cultured grape (*Vitis* sp.) cells. *Plant Physiology and Biochemistry, 55*, 77-84.

Yu, F., Wang, S., Zhang, W., Wang, H., Yu, L., Fei, Z., and Li, J. (2019). An R2R3-type MYB transcription factor MYB103 is involved in phosphate remobilization in *Arabidopsis thaliana*. *Research Square*. doi:10.21203/rs.2.16579/v1

Yu, J., Hu, S., Wang, J., Wong, G. K.-S., Li, S., Liu, B., Deng, Y., Dai, L., Zhou, Y., Zhang, X., *et al.* (2002). A Draft Sequence of the Rice Genome (*Oryza sativa* L. ssp. *indica*). *Science, 296*(5565), 79. doi:10.1126/science.1068037

Zagajewski, B., Kycko, M., Tømmervik, H., Bochenek, Z., Wojtun, B., Bjerke, J. W., and Kłos, A. (2018). Feasibility of hyperspectral vegetation indices for the detection of chlorophyll concentration in three high Arctic plants: *Salix polaris, Bistorta vivipara*, and *Dryas octopetala*. *Acta Societatis Botanicorum Poloniae, 87*(4). doi:10.5586/asbp.3604

Zanke, C., Ling, J., Plieske, J., Kollers, S., Ebmeyer, E., Korzun, V., Argillier, O., Stiewe, G., Hinze, M., and Beier, S. (2014). Genetic architecture of main effect QTL for

heading date in European winter wheat. *Frontiers in plant science, 5*, 217.

Zarco-Tejada, P. J., Berjón, A., López-Lozano, R., Miller, J. R., Martín, P., Cachorro, V., González, M., and De Frutos, A. (2005). Assessing vineyard condition with hyperspectral indices: Leaf and canopy reflectance simulation in a row-structured discontinuous canopy. *Remote sensing of Environment, 99*(3), 271-287.

Zarco-Tejada, P. J., Miller, J. R., Mohammed, G., Noland, T. L., and Sampson, P. (2002). Vegetation stress detection through chlorophyll a+ b estimation and fluorescence effects on hyperspectral imagery. *Journal of environmental quality, 31*(5), 1433-1441.

Zeng, L., Lesch, S. M., and Grieve, C. M. (2003). Rice growth and yield respond to changes in water depth and salinity stress. *Agricultural Water Management, 59*(1), 67-75.

Zhang, C., He, M., Wang, S., Chu, L., Wang, C., Yang, N., Ding, G., Cai, H., Shi, L., and Xu, F. (2019). Boron deficiency-induced root growth inhibition is mediated by brassinosteroid signalling regulation in *Arabidopsis*. *Biorxiv*.

Zhang, F., Wu, X.-N., Zhou, H.-M., Wang, D.-F., Jiang, T.-T., Sun, Y.-F., Cao, Y., Pei, W.-X., Sun, S.-B., and Xu, G.-H. (2014). Overexpression of rice phosphate transporter gene OsPT6 enhances phosphate uptake and accumulation in transgenic rice plants. *Plant and Soil, 384*(1-2), 259-270.

Zhang, Q. Q., Wang, J. G., Wang, L. Y., Wang, J. F., Wang, Q., Yu, P., Bai, M. Y., and Fan, M. (2020). Gibberellin repression of axillary bud formation in *Arabidopsis* by modulation of DELLA-SPL9 complex activity. *Journal of Integrative Plant Biology, 62*(4), 421-432.

Zhao, D., Reddy, K. R., Kakani, V. G., and Reddy, V. R. (2005). Nitrogen deficiency effects on plant growth, leaf photosynthesis, and hyperspectral reflectance properties of sorghum. *European Journal of Agronomy, 22*(4), 391-403.

Zhao, H., Sun, R., Albrecht, U., Padmanabhan, C., Wang, A., Coffey, M. D., Girke, T., Wang, Z., Close, T. J., and Roose, M. (2013). Small RNA profiling reveals phosphorus deficiency as a contributing factor in symptom expression for citrus

huanglongbing disease. *Molecular plant, 6*(2), 301-310.

Zhao, T., Koumis, A., Niu, H., Wang, D., and Chen, Y. (2018). *Onion irrigation treatment inference using a low-cost hyperspectral scanner.* Paper presented at the Multispectral, Hyperspectral, and Ultraspectral Remote Sensing Technology, Techniques and Applications VII.

Zheng, L., Huang, F., Narsai, R., Wu, J., Giraud, E., He, F., Cheng, L., Wang, F., Wu, P., Whelan, J*., et al.* (2009). Physiological and transcriptome analysis of iron and phosphorus interaction in rice seedlings. *Plant Physiol, 151*(1), 262-274.

Zhou, J., Jiao, F., Wu, Z., Li, Y., Wang, X., He, X., Zhong, W., and Wu, P. (2008). OsPHR2 is involved in phosphate-starvation signaling and excessive phosphate accumulation in shoots of plants. *Plant Physiology, 146*(4), 1673-1686.

Zhou, X., and Stephens, M. (2012). Genome-wide efficient mixed-model analysis for association studies. *Nature genetics, 44*(7), 821-824.

Zhou, Z., Wang, Z., Lv, Q., Shi, J., Zhong, Y., Wu, P., and Mao, C. (2015). SPX proteins regulate Pi homeostasis and signaling in different subcellular level. *Plant Signaling & Behavior, 10*(9), e1061163.

Zhu, M., and Zhao, S. (2007). Candidate gene identification approach: progress and challenges. *International journal of biological sciences, 3*(7), 420-427. doi:10.7150/ijbs.3.420

Zou, L., Qu, M., Zeng, L., and Xiong, G. (2020). The molecular basis of the interaction between Brassinosteroid induced and phosphorous deficiency induced leaf inclination in rice. *Plant Growth Regulation*, 1-14.

Zoubarev, A., Hamer, K. M., Keshav, K. D., McCarthy, E. L., Santos, J. R. C., Van Rossum, T., McDonald, C., Hall, A., Wan, X., and Lim, R. (2012). Gemma: a resource for the reuse, sharing and meta-analysis of expression profiling data. *Bioinformatics, 28*(17), 2272-2273.

APPENDICES

Appendix A
Solution Formulas

A1. Yoshida's Solution (Stock Solution)

Stock code	Nutrient element	Chemical (AR grade)	g/liter
A	N	NH_4NO_3	91.400
B	P	$NaH_2PO_4.2H_2O$	40.300
C	K	K_2SO_4	71.400
D	Ca	$CaCl_2.2H_2O$	117.372
E	Mg	$MgSO_4.7H_2O$	324.000
	Mn	$MnCl_2.4H_2O$	1.500
	Mo	$(NH_4)_6.Mo_7O_{24}.4H_2O$	0.074
F	B	H_3BO_3	0.934
	Zn	$ZnSO_4.7H_2O$	0.035
	Cu	$CuSO_4.5H_2O$	0.031
G	Fe	Fe-EDTA	10.712
H	Na (instead of P deficient treatment)	NaCl	15.096

**A liter of working Yoshida's solution is prepared by using 1.25 ml of stock A-G.

For P deficient treatment, stock H is used instead of decreasing stock B in equal concentration to maintain comparable Na concentration.

A2. Molybdate Blue reagent

A solution

ammonium molybdate	4 g
0.5 M H_2SO_4	1000 ml

B solution

ascorbic acid	10 g
distil water	100 ml

A and B solution are mixed together in 6:1 ratio, respectively, before use.

Appendix B

Supplementary results

Table B1 Leaf disc weight (mg/disc) of high and low Pi accumulators grown under different levels of P supply (320, 160, 80, 16, and 0.8 µM P). Data are means ± SD (n = 3 samples; each sample was derived from an averaged pool of 80 leaf discs). Different letters indicate significant differences ($P < 0.05$), according to Duncan's multiple range test (DMRT).

Cultivar	P supply (µM)	Fresh weight of leaf disc (mg/disc)			
High Pi accumulator	0.8	0.887	±	0.013	b
	16	1.025	±	0.003	a
	80	1.037	±	0.024	a
	160	1.036	±	0.028	a
	320	1.039	±	0.060	a
Low Pi accumulator	0.8	0.886	±	0.009	b
	16	1.022	±	0.022	a
	80	1.035	±	0.051	a
	160	1.035	±	0.025	a
	320	1.038	±	0.045	a

Table B2 Pi content (μmol/mm^2) from rice leaf grown under 320 (sufficient; S), 16 (mildly deficient; MD), and 0.8 μM NaH$_2$PO$_4$ (severely deficient; SD). Data are means ± SD (n = 9 samples).

No.	Name	S	MD	SD
1	KHIAW HAHNG MAH	4.005 ± 2.045	0.149 ± 0.048	0.060 ± 0.022
2	KHAO SUPAN	5.060 ± 0.733	0.188 ± 0.016	0.061 ± 0.035
3	LUANG PRATAHN	4.075 ± 1.951	0.232 ± 0.059	0.069 ± 0.024
4	HAHNG NAHK	4.222 ± 1.930	0.168 ± 0.049	0.079 ± 0.034
5	KHAO SAMER	2.534 ± 1.024	0.210 ± 0.059	0.079 ± 0.023
6	LEUANG PUANG TAWNG	3.600 ± 1.173	0.195 ± 0.094	0.076 ± 0.029
7	LEUANG TAH YANG	3.881 ± 2.523	0.248 ± 0.053	0.064 ± 0.029
8	PUANG TAWNG	5.148 ± 2.224	0.193 ± 0.030	0.075 ± 0.021
9	PRATAHN BAN BUNG	3.682 ± 1.279	0.170 ± 0.043	0.065 ± 0.030
10	DAW SAHM DEUAN	3.033 ± 1.054	0.210 ± 0.055	0.075 ± 0.026
11	KHAO GAEW	4.583 ± 0.821	0.196 ± 0.076	0.064 ± 0.019
12	LEUANG NGAHM	3.621 ± 1.479	0.183 ± 0.048	0.077 ± 0.026
13	PUANG TAWNG	3.899 ± 1.155	0.198 ± 0.090	0.074 ± 0.030
14	NIAW KHAO	4.606 ± 1.595	0.214 ± 0.034	0.085 ± 0.021
15	E-MUM	4.948 ± 2.141	0.232 ± 0.055	0.113 ± 0.045
16	DAWK KHAH	4.138 ± 2.683	0.205 ± 0.041	0.083 ± 0.031
17	RAHK HAENG	4.110 ± 0.705	0.217 ± 0.056	0.083 ± 0.030
18	LEUANG GLAHNG	5.059 ± 0.978	0.229 ± 0.040	0.090 ± 0.030
19	KHAO KOD	3.487 ± 2.805	0.181 ± 0.047	0.074 ± 0.023
20	JAE GAN	3.702 ± 1.087	0.238 ± 0.052	0.081 ± 0.017
21	PRA IN	3.738 ± 0.374	0.244 ± 0.092	0.087 ± 0.028
22	MA GAWK	5.163 ± 1.895	0.254 ± 0.042	0.076 ± 0.020
23	IN PAENG	4.180 ± 1.307	0.263 ± 0.085	0.083 ± 0.036
24	SAM AHANG	3.803 ± 1.854	0.193 ± 0.052	0.082 ± 0.022
25	MA YOM	4.875 ± 3.566	0.239 ± 0.071	0.066 ± 0.038
26	E-LAI	5.480 ± 2.347	0.249 ± 0.062	0.092 ± 0.031
27	GRA DAHD	4.371 ± 2.244	0.222 ± 0.068	0.083 ± 0.048
28	KHAO BAHN POD	3.567 ± 1.830	0.290 ± 0.097	0.069 ± 0.015
29	TAH BAHN	4.923 ± 1.657	0.231 ± 0.056	0.056 ± 0.023
30	MAHK YOM	2.240 ± 1.594	0.228 ± 0.101	0.070 ± 0.057

No.	Name	S	MD	SD
31	HAHNG MAH NAI	3.301 ± 0.974	0.226 ± 0.034	0.102 ± 0.018
32	KHITOM KHAO	2.804 ± 0.916	0.271 ± 0.102	0.089 ± 0.041
33	LEUANG DONG	6.457 ± 3.105	0.219 ± 0.051	0.114 ± 0.074
34	PLAH SEW	3.138 ± 0.998	0.165 ± 0.046	0.090 ± 0.045
35	RUANG DIAW	4.737 ± 1.299	0.204 ± 0.032	0.090 ± 0.027
36	LAO TAEK	3.820 ± 2.250	0.205 ± 0.030	0.069 ± 0.046
37	DAENG NAH	4.410 ± 1.714	0.221 ± 0.039	0.079 ± 0.030
38	PUANG HAHNG NAHK	4.801 ± 2.501	0.239 ± 0.043	0.069 ± 0.024
39	LEUANG NOI 31-1-39	3.198 ± 1.319	0.227 ± 0.057	0.090 ± 0.032
40	JUD MAWN	4.328 ± 1.468	0.178 ± 0.041	0.121 ± 0.068
41	KHAO SA NGUAN	3.150 ± 1.300	0.170 ± 0.015	0.069 ± 0.026
42	CHAW MA GAWK	2.732 ± 1.127	0.193 ± 0.075	0.061 ± 0.012
43	MA FAI	3.119 ± 1.294	0.251 ± 0.063	0.084 ± 0.042
44	JAO RAHK HAENG	3.428 ± 1.791	0.167 ± 0.032	0.061 ± 0.008
45	TA POW GAEW 161	3.269 ± 0.365	0.183 ± 0.051	0.067 ± 0.015
46	KHAO GON JUD	5.310 ± 1.998	0.216 ± 0.070	0.065 ± 0.019
47	PLAH KHAENG	4.391 ± 1.655	0.214 ± 0.102	0.095 ± 0.030
48	JAO KHAO	2.987 ± 2.279	0.181 ± 0.051	0.057 ± 0.029
49	MUAY HIN	3.884 ± 2.091	0.228 ± 0.041	0.067 ± 0.010
50	LEUANG PRATEW	3.770 ± 1.727	0.166 ± 0.048	0.065 ± 0.015
51	SAO NUENG	3.852 ± 1.299	0.220 ± 0.067	0.097 ± 0.034
52	GON GAEW	2.476 ± 1.394	0.238 ± 0.044	0.077 ± 0.028
53	KHAO NUAN	4.762 ± 3.519	0.284 ± 0.049	0.085 ± 0.023
54	TAWNG RAHK SAI	4.918 ± 1.239	0.172 ± 0.021	0.074 ± 0.015
55	MAHK NAM	3.540 ± 2.654	0.206 ± 0.041	0.090 ± 0.030
56	DAWK MAI	4.070 ± 1.802	0.316 ± 0.088	0.074 ± 0.019
57	LEUANG PAHK CHONG	4.127 ± 0.856	0.235 ± 0.075	0.090 ± 0.018
58	LEUANG CHUMPAE	8.651 ± 1.830	0.281 ± 0.037	0.096 ± 0.029
59	LEUANG KAMIN	5.132 ± 2.244	0.247 ± 0.038	0.084 ± 0.028
60	KOO MEUANG	4.288 ± 1.151	0.224 ± 0.077	0.066 ± 0.014

No.	Name	S	MD	SD
61	TA POW LOM	3.205 ± 2.429	0.182 ± 0.085	0.080 ± 0.036
62	KHAO AH-GAHD	3.128 ± 0.455	0.240 ± 0.048	0.091 ± 0.032
63	SAI YUD	3.867 ± 0.985	0.206 ± 0.020	0.091 ± 0.022
64	DI SI	4.991 ± 2.494	0.271 ± 0.140	0.074 ± 0.028
65	NAH KWAN	1.992 ± 0.455	0.234 ± 0.046	0.078 ± 0.045
66	MED MAKHAM	5.032 ± 1.826	0.187 ± 0.032	0.069 ± 0.013
67	HAH RUANG	2.941 ± 0.565	0.178 ± 0.042	0.053 ± 0.028
68	TOM MEUANG LUANG	3.464 ± 0.836	0.281 ± 0.125	0.068 ± 0.019
69	NIAW MALI	4.484 ± 1.584	0.170 ± 0.067	0.078 ± 0.031
70	MA YOM	4.875 ± 3.566	0.239 ± 0.071	0.066 ± 0.038
71	DAW DAWK MAI	5.120 ± 2.575	0.202 ± 0.010	0.058 ± 0.030
72	MAHK NAM	3.540 ± 2.654	0.206 ± 0.041	0.090 ± 0.030
73	KHAO' GAM	2.843 ± 1.038	0.236 ± 0.052	0.083 ± 0.016
74	E-KHAO YAI	3.821 ± 0.902	0.272 ± 0.040	0.077 ± 0.036
75	KASET DAW	3.557 ± 0.885	0.215 ± 0.085	0.107 ± 0.037
76	GAM PAI	6.064 ± 2.514	0.303 ± 0.121	0.087 ± 0.042
77	KHAO LUANG	3.355 ± 2.558	0.197 ± 0.041	0.049 ± 0.013
78	NAHNG NUAN	3.803 ± 1.036	0.168 ± 0.033	0.059 ± 0.030
79	SEW MAE JAN	3.864 ± 3.020	0.235 ± 0.102	0.084 ± 0.035
80	SEW MAE JAN	6.480 ± 1.932	0.153 ± 0.043	0.061 ± 0.005
81	PATHUM THANI 1	3.331 ± 1.568	0.249 ± 0.078	0.080 ± 0.033
82	SANG YOD	3.655 ± 2.070	0.230 ± 0.067	0.075 ± 0.022
83	GWIAN HAK	3.084 ± 0.696	0.236 ± 0.067	0.082 ± 0.028
84	KHAO TAH HAENG 17	2.628 ± 1.645	0.212 ± 0.033	0.066 ± 0.026
85	GOW RUANG 88	3.031 ± 1.439	0.174 ± 0.043	0.090 ± 0.039
86	NAHNG MON S-4	4.311 ± 1.712	0.218 ± 0.042	0.082 ± 0.036
87	PIN GAEW 56	3.693 ± 0.432	0.195 ± 0.103	0.085 ± 0.022
88	HAHNG YI 71	4.650 ± 1.388	0.173 ± 0.036	0.098 ± 0.036
89	KHAI MOD RIN	3.784 ± 1.405	0.193 ± 0.051	0.089 ± 0.033
90	BUA NOI	3.542 ± 1.246	0.220 ± 0.038	0.076 ± 0.019

No.	Name	S	MD	SD
91	AEW MOD DAENG	3.160 ± 1.074	0.179 ± 0.072	0.066 ± 0.020
92	NAHNG NGAHM	3.358 ± 0.424	0.171 ± 0.038	0.069 ± 0.022
93	U-TA POW	3.676 ± 1.866	0.208 ± 0.034	0.078 ± 0.020
94	PUANG WAHN	2.777 ± 0.609	0.173 ± 0.042	0.079 ± 0.029
95	PUANG HAHNG MOO	5.376 ± 3.192	0.201 ± 0.064	0.066 ± 0.037
96	JEK CHUEY	3.134 ± 1.412	0.156 ± 0.052	0.055 ± 0.030
97	KHAO GAW DIAW	3.024 ± 0.583	0.181 ± 0.028	0.100 ± 0.025
98	RD9	4.726 ± 1.484	0.245 ± 0.028	0.081 ± 0.027
99	PUANG NGERN	3.684 ± 1.991	0.192 ± 0.040	0.047 ± 0.023
100	NAM SAGUI 19	2.860 ± 0.948	0.192 ± 0.041	0.066 ± 0.045
101	LAM YAI	3.517 ± 1.843	0.147 ± 0.049	0.069 ± 0.018
102	BUN MAH	3.586 ± 0.836	0.223 ± 0.023	0.073 ± 0.024
103	RD8	4.466 ± 0.523	0.226 ± 0.073	0.089 ± 0.018
104	RD13	3.051 ± 2.019	0.169 ± 0.053	0.052 ± 0.020
105	JAO DAM	3.323 ± 1.743	0.210 ± 0.039	0.073 ± 0.016
106	JAO DAENG	3.601 ± 1.805	0.193 ± 0.055	0.080 ± 0.021
107	DAM DAHNG	2.453 ± 1.125	0.204 ± 0.056	0.057 ± 0.035
108	JAO DAWK KHAO	3.786 ± 1.389	0.187 ± 0.053	0.053 ± 0.030
109	LEUANG TAWNG	4.119 ± 1.882	0.198 ± 0.094	0.083 ± 0.026
110	GAM LIAW	3.666 ± 1.536	0.226 ± 0.104	0.063 ± 0.040
111	TOON CHALAWNG	3.862 ± 1.438	0.209 ± 0.015	0.078 ± 0.013
112	NAHNG MON	4.238 ± 1.234	0.209 ± 0.056	0.060 ± 0.035
113	KHAO PRAGUAD	2.901 ± 0.883	0.222 ± 0.066	0.078 ± 0.034
114	KHAO SAMER	2.534 ± 1.024	0.210 ± 0.059	0.079 ± 0.023
115	KHAO TAH JEUA	3.636 ± 1.235	0.201 ± 0.039	0.087 ± 0.032
116	KHAO TAENG MO	4.349 ± 1.892	0.218 ± 0.051	0.088 ± 0.039
117	LEB NOK	3.514 ± 1.858	0.229 ± 0.083	0.080 ± 0.019
118	RD19	3.545 ± 1.033	0.287 ± 0.195	0.091 ± 0.031
119	RD17	3.995 ± 0.944	0.217 ± 0.059	0.074 ± 0.044
120	GAM FEUANG	3.153 ± 0.974	0.186 ± 0.046	0.084 ± 0.034

No.	Name	S	MD	SD
121	RD10	5.391 ± 3.485	0.392 ± 0.140	0.077 ± 0.027
122	RD21	5.555 ± 2.049	0.262 ± 0.067	0.075 ± 0.044
123	RD25	2.811 ± 1.222	0.271 ± 0.054	0.085 ± 0.032
124	JAMPAH TAWNG	3.462 ± 0.723	0.174 ± 0.027	0.061 ± 0.030
125	KHAO LUANG	3.355 ± 2.558	0.197 ± 0.041	0.049 ± 0.013
126	TAH JEUA	4.082 ± 2.380	0.198 ± 0.030	0.082 ± 0.015
127	LEUANG KWAI LAH	4.333 ± 1.467	0.251 ± 0.055	0.064 ± 0.020
128	SETTI	4.335 ± 1.481	0.218 ± 0.030	0.068 ± 0.048
129	KAN NAH	3.821 ± 1.829	0.205 ± 0.044	0.080 ± 0.005
130	LEUANG TIA	5.377 ± 1.950	0.261 ± 0.047	0.078 ± 0.014
131	LEUANG GAEW	3.894 ± 1.274	0.186 ± 0.046	0.074 ± 0.039
132	LAI MAHK	4.502 ± 1.608	0.160 ± 0.038	0.067 ± 0.022
133	RD27	3.135 ± 0.876	0.202 ± 0.041	0.067 ± 0.029
134	LEUANG KWAI LAH	4.333 ± 1.467	0.251 ± 0.055	0.064 ± 0.020
135	SAHM RUANG	3.970 ± 1.801	0.215 ± 0.046	0.088 ± 0.013
136	LEUANG PLAH GIM	3.163 ± 0.877	0.246 ± 0.054	0.069 ± 0.030
137	LEUANG HUAN	3.117 ± 0.778	0.221 ± 0.042	0.066 ± 0.003
138	GWIAN HAK	3.704 ± 2.140	0.208 ± 0.068	0.074 ± 0.021
139	GWIAN HAK	3.084 ± 0.696	0.236 ± 0.067	0.082 ± 0.028
140	KHAO PUANG	3.287 ± 1.368	0.194 ± 0.030	0.060 ± 0.016
141	CHAW PLI KHAO	3.898 ± 0.973	0.232 ± 0.079	0.077 ± 0.025
142	PUANG NAHK	3.882 ± 2.497	0.237 ± 0.056	0.084 ± 0.039
143	KHAO TAH CHEUA	3.147 ± 1.025	0.166 ± 0.039	0.066 ± 0.020
144	LEUANG BAI LOD	4.361 ± 1.469	0.148 ± 0.073	0.071 ± 0.041
145	LEUANG BAI JAEK	5.495 ± 1.317	0.236 ± 0.011	0.086 ± 0.037
146	NAM SAGUI 19	2.860 ± 0.948	0.192 ± 0.041	0.066 ± 0.045
147	HANTRA 60	3.182 ± 1.478	0.195 ± 0.128	0.070 ± 0.013
148	CHUMPAE 60	4.745 ± 2.265	0.203 ± 0.049	0.084 ± 0.019
149	PATHUM THANI 60	5.014 ± 2.366	0.166 ± 0.035	0.077 ± 0.044
150	CHAI NAT 1	2.804 ± 1.004	0.270 ± 0.047	0.073 ± 0.032

| No.	Name	S	MD	SD
151	NIAW DAM LAI	4.571 ± 1.515	0.202 ± 0.020	0.071 ± 0.027
152	PAWNG AEW	2.514 ± 1.369	0.158 ± 0.038	0.068 ± 0.039
153	LAO TAEK	3.820 ± 2.250	0.205 ± 0.030	0.069 ± 0.046
154	LOOK DAENG PATTANI	2.275 ± 1.341	0.148 ± 0.012	0.077 ± 0.032
155	CHIANG PHATTHALUNG	5.166 ± 2.534	0.269 ± 0.046	0.071 ± 0.046
156	SOON	5.377 ± 2.141	0.219 ± 0.044	0.098 ± 0.028
157	GAEN JAN	3.303 ± 1.422	0.220 ± 0.048	0.087 ± 0.043
158	LOOK DAENG PATTANI	2.275 ± 1.341	0.148 ± 0.012	0.077 ± 0.032
159	NIAW PRAE 1	4.166 ± 0.492	0.290 ± 0.079	0.070 ± 0.040
160	PRACHIN BURI 1	4.724 ± 3.175	0.287 ± 0.081	0.084 ± 0.021
161	RD31	3.943 ± 0.768	0.274 ± 0.070	0.080 ± 0.032
162	KHAO DAWK MALI 105	3.948 ± 1.697	0.179 ± 0.039	0.066 ± 0.018
163	CSSL11	4.308 ± 0.209	0.245 ± 0.048	0.079 ± 0.021
164	UBN	3.971 ± 1.592	0.226 ± 0.087	0.073 ± 0.023
165	POKKALI	4.819 ± 2.161	0.181 ± 0.043	0.073 ± 0.022
166	DAW KHAO	3.050 ± 0.822	0.133 ± 0.016	0.079 ± 0.027
167	KHAO READ	4.393 ± 1.641	0.197 ± 0.036	0.089 ± 0.045
168	PAWNG AEW	2.514 ± 1.369	0.158 ± 0.038	0.068 ± 0.039
169	LEUANG PRATEW123	4.418 ± 2.102	0.235 ± 0.073	0.081 ± 0.036
170	LEUANG PRATEW 123-TC1	4.767 ± 2.233	0.199 ± 0.032	0.082 ± 0.018
171	IR29	2.407 ± 1.465	0.343 ± 0.073	0.082 ± 0.025
172	LUANG PRATAHN	4.075 ± 1.951	0.232 ± 0.059	0.069 ± 0.024
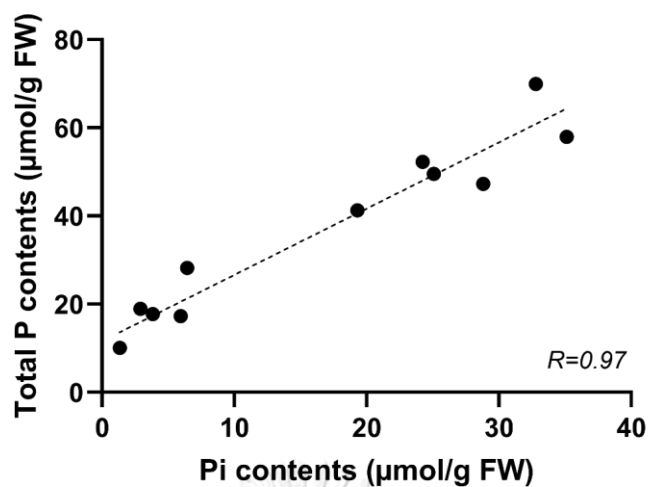
Figure B1 Comparison of Pi contents determined by the punching method and total P contents determined by the ICP method. Data points are fitted by linear regression, and correlation (*r*) is determined by Pearson's correlation model using R software.
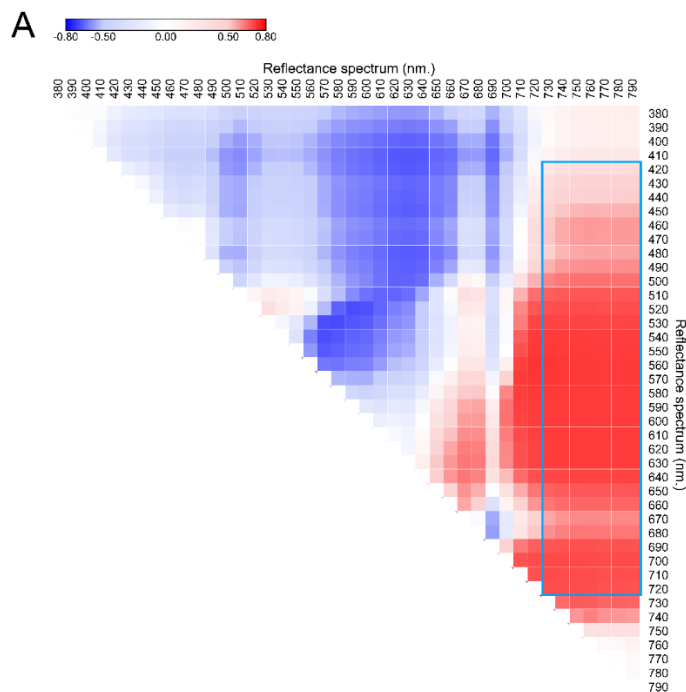

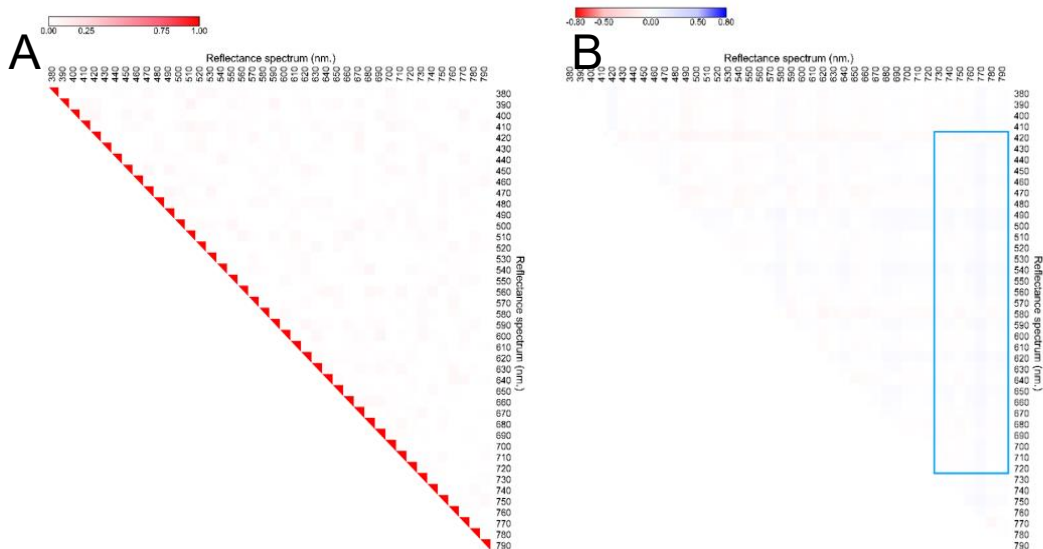**Figure B2** Full matrix correlation between NSR indices and Pi content.

Figure B3 Matrix correlation between its reflectance wavelength (A) and matrix correlation between NSR indices and Pi content (B) of randomly generated data.
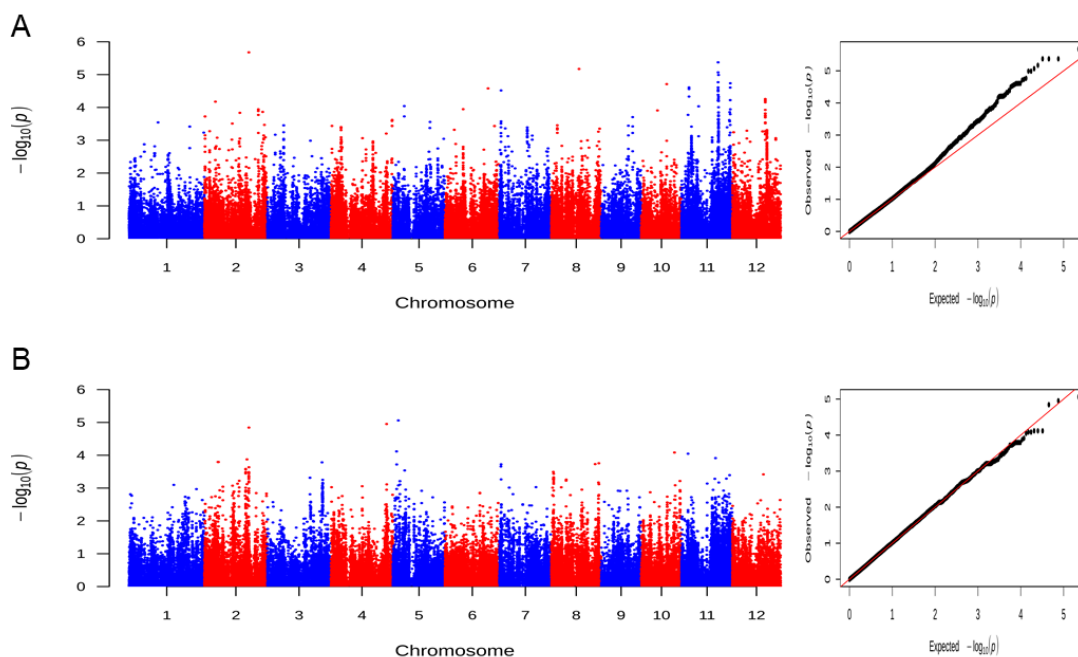

Figure B4 Manhattan plot and Q-Q plot based on GWAS of Pi content measured from leaves grown under sufficient (A) and middle-deficient treatment (B). For Manhattan plots, the x-axis represents SNP positions across the entire rice genome by chromosome, and the y-axis is the -log10 p-value of each SNP.
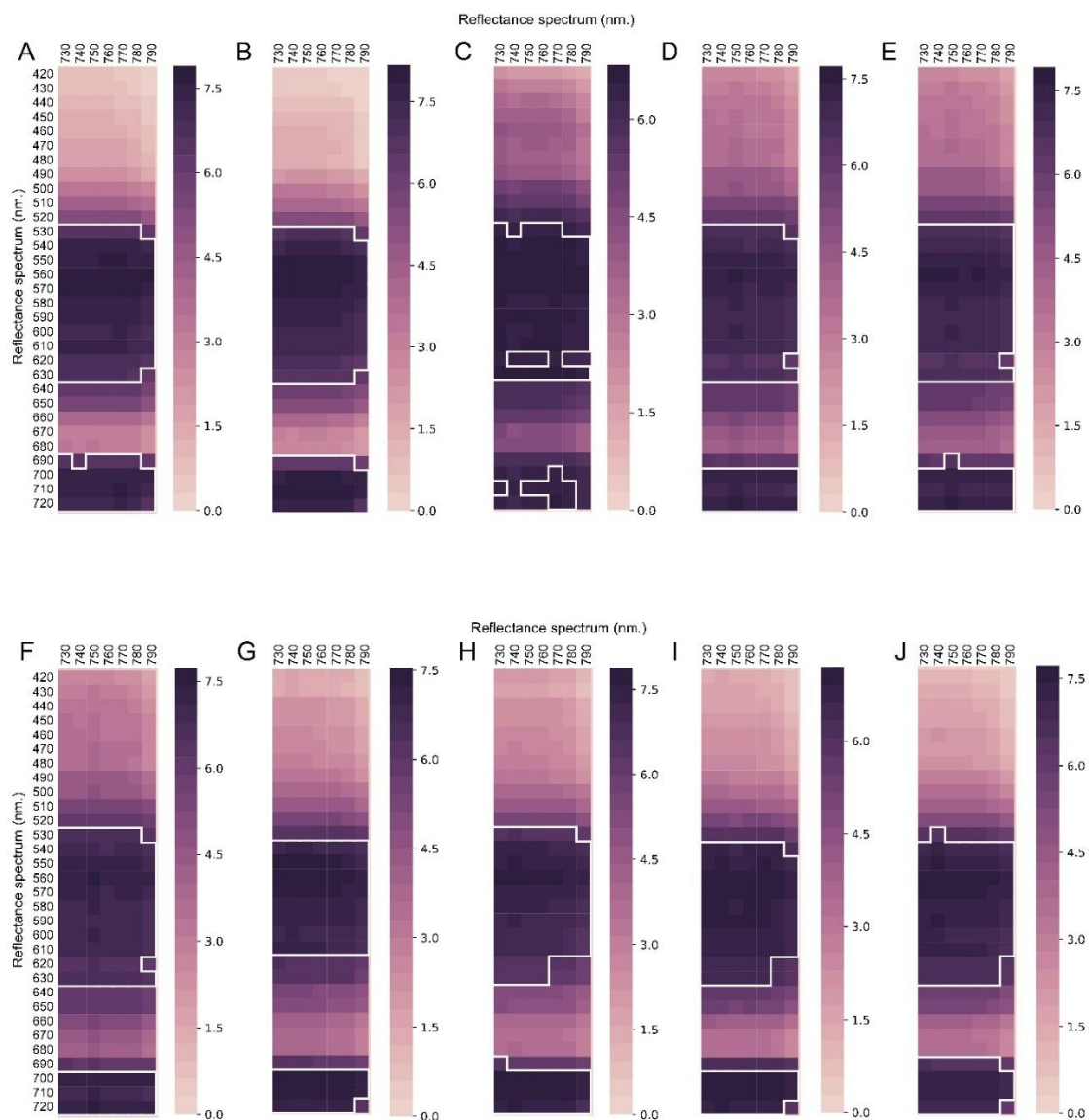
Figure B5 Heat map represents the significant SNPs located in ten candidate genes, including LOC_Os02g02670 (A), LOC_Os02g02690 (B), LOC_Os03g43730 (C), LOC_Os06g13650 (D), LOC_Os06g13670 (E), LOC_Os06g13680 (F), LOC_Os08g15230 (G), LOC_Os08g15330 (H), LOC_Os11g35320 (I), LOC_Os11g42300 (J). The surrounding white line indicated passed significant threshold line at -log(P-value) ≥ 6.35.

Appendix C

Detail of hyperspectral detective device and general vegetative indices

Table C1 Technical specification of PolyPen RP400 UVIS (PSI, 2018)

Spectrum measurement	
Spectral range	380 nm - 790 nm (RP 410 UVIS) 640 nm - 1050 nm (RP 410 NIR)
Spectral response half width	8 nm
Spectral Straylight	-30 dB
Scanning Speed	About 100 ms
Dynamic Range	High gain: 1:4300 Low gain: 1:13000
Size of Aperture	7 mm
Light source	
Type	Xenon incandescent lamp
Spectral range	380-1050 nm
Data storage and transfer	
Internal memory capacity	Up to 16 Mbit
Internal data logging	Up to 4,000 measurements
Data transfer	USB cable
PC software	SpectraPen 1.1 (Windows 7 and higher)
Battery	
Type	Li-Ion rechargeable battery
Capacity	2600 mAh
Max. charging current	0.5 A
Charging	Via USB port - PC, power bank, USB charger, etc.
Battery life	48 hours typical with full operation Low battery indicator
Other	
Sample holder	Mechanical leaf-clip
Display	Touchscreen 240 x 320 pixel; 65535 colors
Built in GPS module	Ultra-high sensitivity down to -165dBm High accuracy of <1.5 m in 50% of trials
Size	150 x 75 x 40 mm
Weight	300 g
Operating conditions	Temperature: 0 to +55 °C Relative humidity: 0 to 95 % (non-condensing)
Storage conditions	Temperature: -10 to +60 °C Relative humidity: 0 to 95 % (non-condensing)
Warranty	1 year parts and labor

Table C2 Detail of general vegetative spectral reflectance indices (PSI, 2018)

Spectral reflectance index	Abbreviation	Formula
Normalized Difference Vegetation Index	NDVI	(R[780nm]-R[630nm])/ (R[780nm]+R[630nm])
Simple Ratio Index	SR	R[780nm]/R[630nm]
Modified Chlorophyll Absorption Ratio Index 1	MCARI1	1.2*(2.5*(R[780nm]-R[670nm])-1.3*(R[780nm]-R[550nm]))
Optimized Soil-Adjusted Vegetation Index	OSAVI	(1+0.16)*(R[780nm]-R[670nm])/ (R[780nm]+R[670nm]+0.16)
Greenness Index	G	R[554nm]/R[677nm]
Modified Chlorophyll Absorption Ratio Index	MCARI	((R[700nm]-R[670nm])-0.2*(R[700nm]-R[550nm]))* (R[700nm]/R[670nm])
Transformed CAR Index	TCARI	3*((R[700nm]-R[670nm])-0.2*(R[700nm]+R[550nm])* (R[700nm]/R[670nm]))
Triangular Vegetation Index	TVI	0.5*(120*(R[750nm]-R[550nm])-200*(R[670nm]-R[550nm]))
Zarco-Tejada & Miller Index	ZMI	R[750nm]/R[710nm]
Simple Ratio Pigment Index	SPRI	R[430nm]/R[680nm]
Normalized Phaeophytinization Index	NPQI	(R[415nm]-R[435nm])/ (R[415nm]+R[435nm])
Photochemical Reflectance Index	PRI	(R[531nm]-R[570nm]) /(R[531nm]+R[570nm])
Normalized Pigment Chlorophyll Index	NPCI	(R[680nm]-R[430nm])/ (R[680nm]+R[430nm])
Carter Indices 1	Ctr1	R[695nm]/R[420nm]
Carter Indices 2	Ctr2	R[695nm]/R[760nm]
Lichtenthaler Indices 1	Lic1	(R[780nm]-R[680nm])/ (R[780nm]+R[680nm])
Lichtenthaler Indices 2	Lic2	R[440nm]/R[690nm]
Structure Intensive Pigment Index	SIPI	(R[780nm]-R[450nm])/ (R[780nm]+R[650nm])
Gitelson and Merzlyak Indices 1	GM1	R[750nm]/R[550nm]
Gitelson and Merzlyak Indices 2	GM2	R[750nm]/R[700nm]
Anthocyanin Reflectance Index 1	ARI1	1/R[550nm]-1/R[700nm]
Anthocyanin Reflectance Index 2	ARI2	R[790nm]*(1/R[550nm]-1/R[700nm])
Caroteniod Reflectance Index 1	CRI1	1/R[510nm]-1/R[550nm]
Caroteniod Reflectance Index 2	CRI2	1/R[510nm]-1/R[700nm]

Appendix D

Standard curve

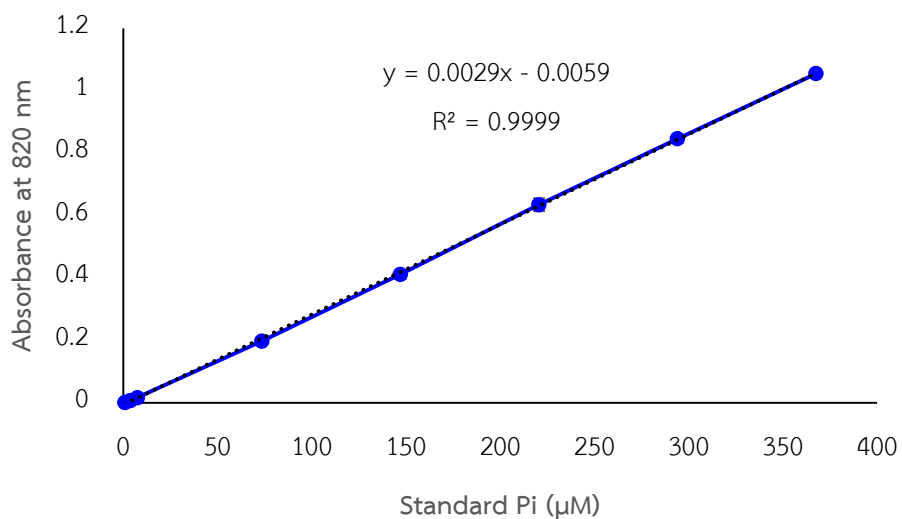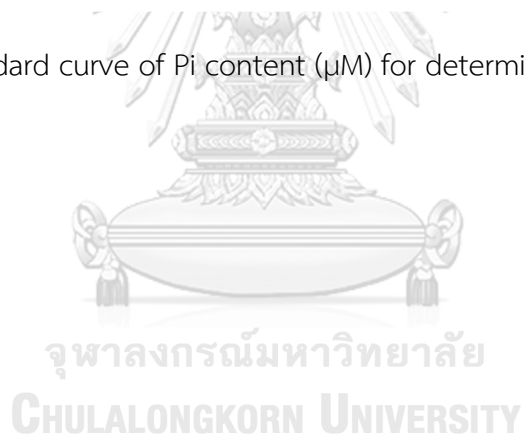$$y = 0.0029x - 0.0059$$

$$R^2 = 0.9999$$

Figure D1 Standard curve of Pi content (μM) for determining the leaf Pi content

Appendix E

Rice growing protocol

1. Seeds were sterilized using commercial bleach (2% sodium hypochlorite) for 10 minutes, then washed with distilled water three times, and continuously soaked the seeds in water for two days under dark condition.

2. Soaked seeds were floated on a plastic net in half-strength Yoshida solution for two days under dark condition.

3. Then the light was given to the seedling for four days.

Eight-day- old seedlings were pre-cultured for the next step
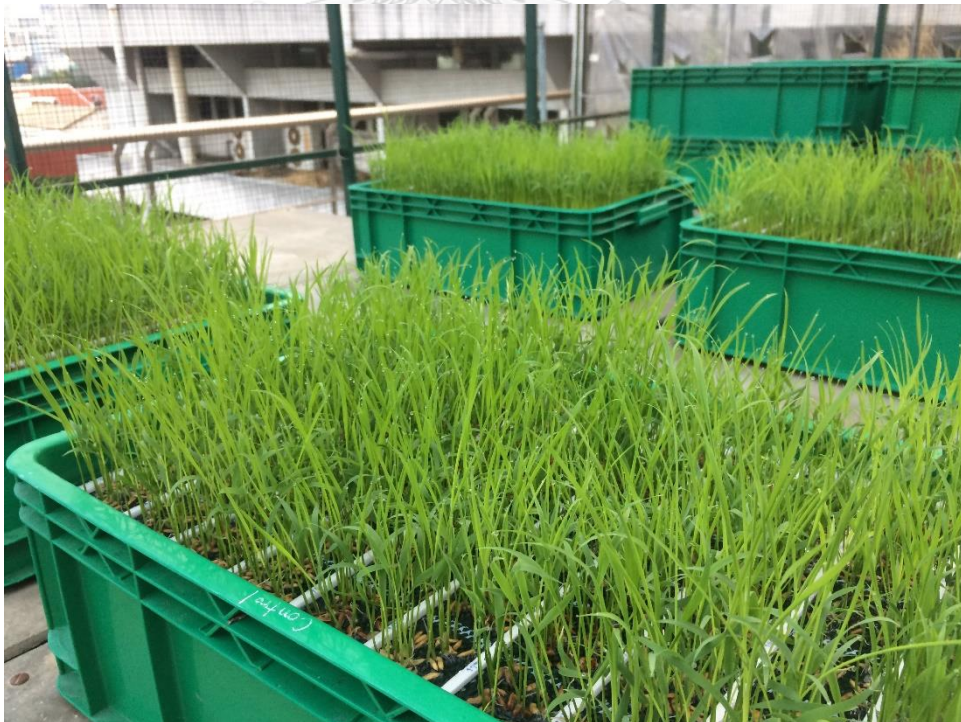
4. The seed endosperm was cut from the seedlings to remove the phosphorus storage resource, and the seedlings were transferred to full-strength Yoshida solution with different P concentrations for 16 days.

จุฬาลงกรณ์มหาวิทยาลัย

CHULALONGKORN UNIVERSITY

After 16 days, the treated rice can be harvested for any observation.

* This experiment was performed by using 80 L containers, which include 219 rice plants. The nutrient solution was renewed every four days and adjusted pH at 5.8 every two days.

VITA

NAME   Sompop Pinit

DATE OF BIRTH   6 June 1991

PLACE OF BIRTH   Phitsanulok

INSTITUTIONS ATTENDED   Bachelor of Science in Biology (2nd Class Honor) from the
                         Department of Biology, Faculty of Science, Naresuan
                         University (2015)
                         Bachelor of Education major in Biology (1st Class Honor)
                         from the Department of Education, Faculty of Education,
                         Naresuan University (2015)

HOME ADDRESS   9/2, Village No.3, Noenkum, Bangkrathum, Phitsanulok,
                         65210 THAILAND

PUBLICATION   Pinit, S., S. Chadchawan, and J. Chaiwanon. 2020. A
                         simple high-throughput protocol for the extraction and
                         quantification of inorganic phosphate in rice leaves.
                         Applications in Plant Sciences 8(10): e11395.
                         DOI:10.1002/aps3.11395.

AWARD RECEIVED   He was supported by the Royal Golden Jubilee Ph.D.
                         Scholarship Grant (RGJ-Ph.D.) of Thailand Research Fund
                         (TRF) to study for the degree of Doctor of Philosophy in
                         Biotechnology Program, Faculty of Science, Chulalongkorn
                         University.